SECURITY CLASSIFICATION OF THIS PAGE (When Data Entered)

AD-A196 704

REPORT DOCUMENTATION PAGE	READ INSTRUCTIONS BEFORE COMPLETING FORM		
1. REPORT NUMBER AFIT/CI/NR 88-159	2. GOVT ACCESSION NO.	3. RECIPIENT'S CATALOG NUMBER	
4. TITLE (and Subtitle) MEASURING ATMOSPHERIC FREE RADICALS USING CHEMICAL AMPLIFICATION		5. TYPE OF REPORT & PERIOD COVERED MS THESIS	
		6. PERFORMING ORG. REPORT NUMBER	
7. AUTHOR(s) BERNARD TONGJOO GHIM		8. CONTRACT OR GRANT NUMBER(s)	
9. PERFORMING ORGANIZATION NAME AND ADDRESS AFIT STUDENT AT: UNIVERSITY OF DENVER		10. PROGRAM ELEMENT, PROJECT, TASK AREA & WORK UNIT NUMBERS	
11. CONTROLLING OFFICE NAME AND ADDRESS		12. REPORT DATE 1988	
		13. NUMBER OF PAGES 156	
14. MONITORING AGENCY NAME & ADDRESS(If different from Controlling Office) AFIT/NR Wright-Patterson AFB OH 45433-6583		15. SECURITY CLASS. (of this report) UNCLASSIFIED	
		15a. DECLASSIFICATION/DOWNGRADING SCHEDULE	

16. DISTRIBUTION STATEMENT (of this Report)

DISTRIBUTED UNLIMITED: APPROVED FOR PUBLIC RELEASE

17. DISTRIBUTION STATEMENT (of the abstract entered in Block 20, if different from Report)

SAME AS REPORT

18. SUPPLEMENTARY NOTES

Approved for Public Release: IAW AFR 190-1
LYNN E. WOLAVER
Dean for Research and Professional Development   22 July 88
Air Force Institute of Technology
Wright-Patterson AFB OH 45433-6583

19. KEY WORDS (Continue on reverse side if necessary and identify by block number)

20. ABSTRACT (Continue on reverse side if necessary and identify by block number)

ATTACHED

DD FORM 1473   EDITION OF 1 NOV 65 IS OBSOLETE
1 JAN 73

UNCLASSIFIED

SECURITY CLASSIFICATION OF THIS PAGE (When Data Entered)

Measuring Atmospheric Free Radicals

Using Chemical Amplification

A Thesis

Presented to

the Faculty of Natural Sciences

University of Denver

In Partial Fulfillment

of the Requirements for the Degree

Master of Science

---

by

Barnard Tongjoo Ghim

May 1988

Measuring Atmospheric Free Radicals
Using Chemical Amplification

Abstract

Atmospheric free radicals play an important role in nearly all atmospheric cycles. The focus of this research was to continue characterizing the PEroxy Radical measurement by Chemical Amplification (PERCA) method first investigated by Cantrell [1983, 1984], then Buhr [1986]. Experiments proved the original model of the PERCA method developed by Cantrell was too simple. New instrument modifications have insured optimum performance for peroxy radical measurement in clean, dry environments.

The instrument is currently calibrated under laboratory conditions by observing the decay of HO_2 radicals in a formaldehyde photolysis system. The reported chain lengths of 600 are in reasonable agreement with previously reported methods. These, higher €

Field experiments revealed strong interferences to the PERCA system. The system's performance deteriates rapidly in dirty air due to interferences from zero-modulation and pernitric acid formation. The signal deteriation in high humidity has been characterized, but the cause is still uncertain. A new reactor design injecting clean, dry air to dilute the sampled air may reduce all three interferences. In addition, Peroxylacyl nitrate (PAN) was not an interference at room temperature, and SO_2 has been shown to carry the PERCA chain reaction, but is a poor substitute for CO.

GRADUATE STUDIES

AT

THE UNIVERSITY OF DENVER

Upon the recommendation of the chairperson
of the Department of Chemistry this thesis
is hereby accepted in partial fulfillment
of the requirements for the degree of

Master of Science

_____
Professor in charge of thesis

_____
Dean of Graduate Studies

_____
Date

TABLE OF CONTENTS

iii

LIST OF TABLES

LIST OF FIGURES

ACKNOWLEGEMENTS

Chapter I

Introduction

Free radicals are critical to a study of the atmosphere because of the important roles they play in the oxidation cycles of many trace species. Atmospheric free radicals of particular interest are the odd hydrogen free radicals. Since the importance of odd hydrogen radicals (hydroxyl, OH, and perhydroxyl, HO_2) to smog chemistry was recognized [**Weinstock et al.**, 1969; **Heicklen et al.**, 1969], our understanding of the significance of these species continues to grow. The role of odd hydrogen radicals in atmospheric cycles in the clean troposphere has been elucidated [**Crutzen**, 1971; **Levy**, 1971; **Molina and Rowland**, 1974] adding to the importance of these atmospheric constituents. It is recognized that the oxidation cycles of NO_x, SO_x, and hydrocarbons are all dependent on the odd hydrogen radicals. HO_2 oxidizes NO to NO_2 and is the major homogenous source of H_2O_2 in a clean atmosphere [**Cantrell et al.**, 1984], and OH plays a major role in the loss mechanisms of many trace species including CO, CH_4, C_2H_4, H_2, CH_3Cl, CH_3CCl_3, CH_3Br, H_2S, and SO_2 [**Logan et al.**, 1981]. Recently, the OH radical has been determined as the dominant loss mechanism for isoprene and monoterpenes at Niwot Ridge [**Trainer et al.**, 1987]. Various models have been developed [**Logan et al.**,

1

1981; **Hov and Isaksen**, 1979; **Thompson and Cicerone**, 1986] to describe the effect of the radicals on atmospheric photochemistry based on known parameters. To validate such models, and gain a clearer understanding of the relationship of odd hydrogen radicals in the atmosphere, accurate measurements are needed. This work will relate the background and the latest research conducted on the PEroxy Radical measurement by Chemical Amplification (PERCA) instrument developed by this group to measure ambient atmospheric free radicals.

Odd Hydrogen Chemistry

The major source of odd hydrogen radicals is from the photolysis of ozone to $O(^1D)$ and O_2 by near 300nm radiation. The $O(^1D)$ combines with H_2O to produce two OH radicals [**Levy**, 1971, 1972]. The OH radical, with a 24 hour mean concentration in the range (0.3-3) x 10^6 molecules/cm^3 [**Hewitt and Harrison**, 1984], is very reactive and has a chemical lifetime of less than a second. It is converted to other odd hydrogen species in reactions with methane or carbon monoxide as in the following reactions:

$$CO + OH \rightarrow CO_2 + H\cdot$$

$$H\cdot + O_2 + M \rightarrow HO_2 + M$$
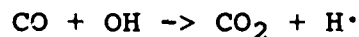
In addition to ozone photolysis, OH can be regenerated by many reactions involving HO_2 and H_2O_2 such as $HO_2 + NO \rightarrow NO_2 + OH$. The HO_2 radical has a calculated average chemical lifetime of 100 seconds and has a calculated global average

concentration of 2×10^8 molecules/cm^3. Although the importance of HO_2 in gas-phase tropospheric chemistry is recognized, the aqueous-phase reaction $HO_2 + H^+ \rightarrow H_2O_2^+$ could represent a major sink of gas-phase free radicals as well as an important source of H_2O_2 in cloud water [Schwartz, 1984]. The importance of H_2O_2 is that it appears to be a principal species responsible for aqueous-phase atmospheric oxidation of SO_2, and hence a major, and sometimes limiting precursor for acid rain [Calvert et al., 1984].

Figure 1 shows the results from a model calculation of the mean concentrations of the odd hydrogen radicals throughout the day and reveals the diurnal variations of the odd hydrogen radicals [Logan et al., 1981]. The odd hydrogen free radicals are involved in important atmospheric cycles including the atmospheric oxidation of methane as illustrated in Figure 2 [Logan et al., 1981]. Figure 3 shows the major chemical reactions affecting odd hydrogen in the troposphere [Buhr, 1986]. The OH molecule interacts with many trace atmospheric molecules, and the close relationship of OH and HO_2 are apparent throughout the various cycles.

The odd hydrogen radical chemistry is complex, and the odd hydrogen chemistry is still not fully understood. It is not certain why some reaction rates involving odd hydrogen radicals vary with temperature, pressure, and humidity. One
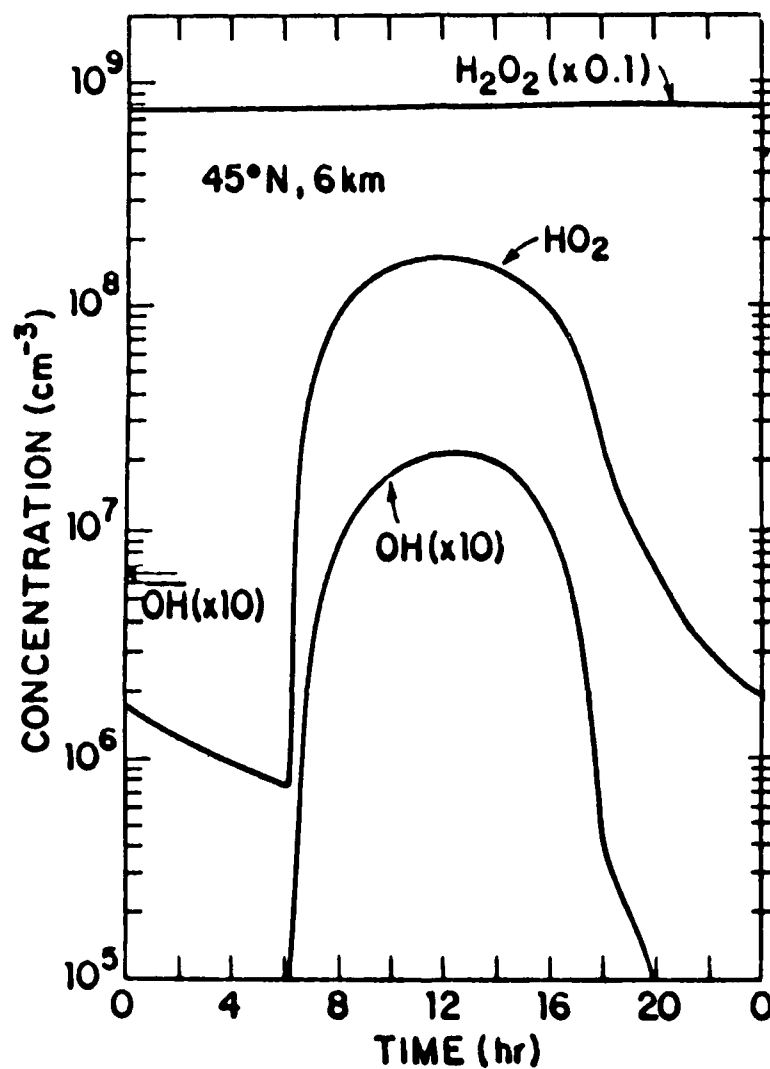
Figure 1. Modelled average mean values of odd hydrogen species free radicals emphasizing the expected diurnal variations in OH and HO_2 radicals [Logan et al., 1981].
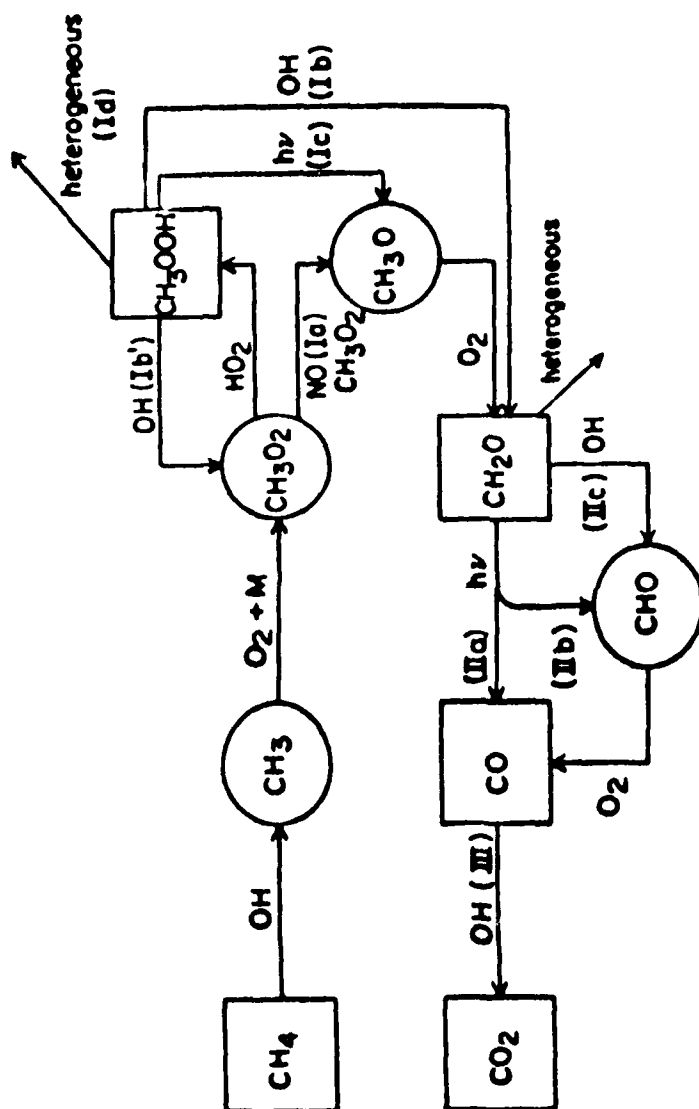
Figure 2. Modelled methane and carbon monoxide oxidation cycle [Logan et al., 1981].
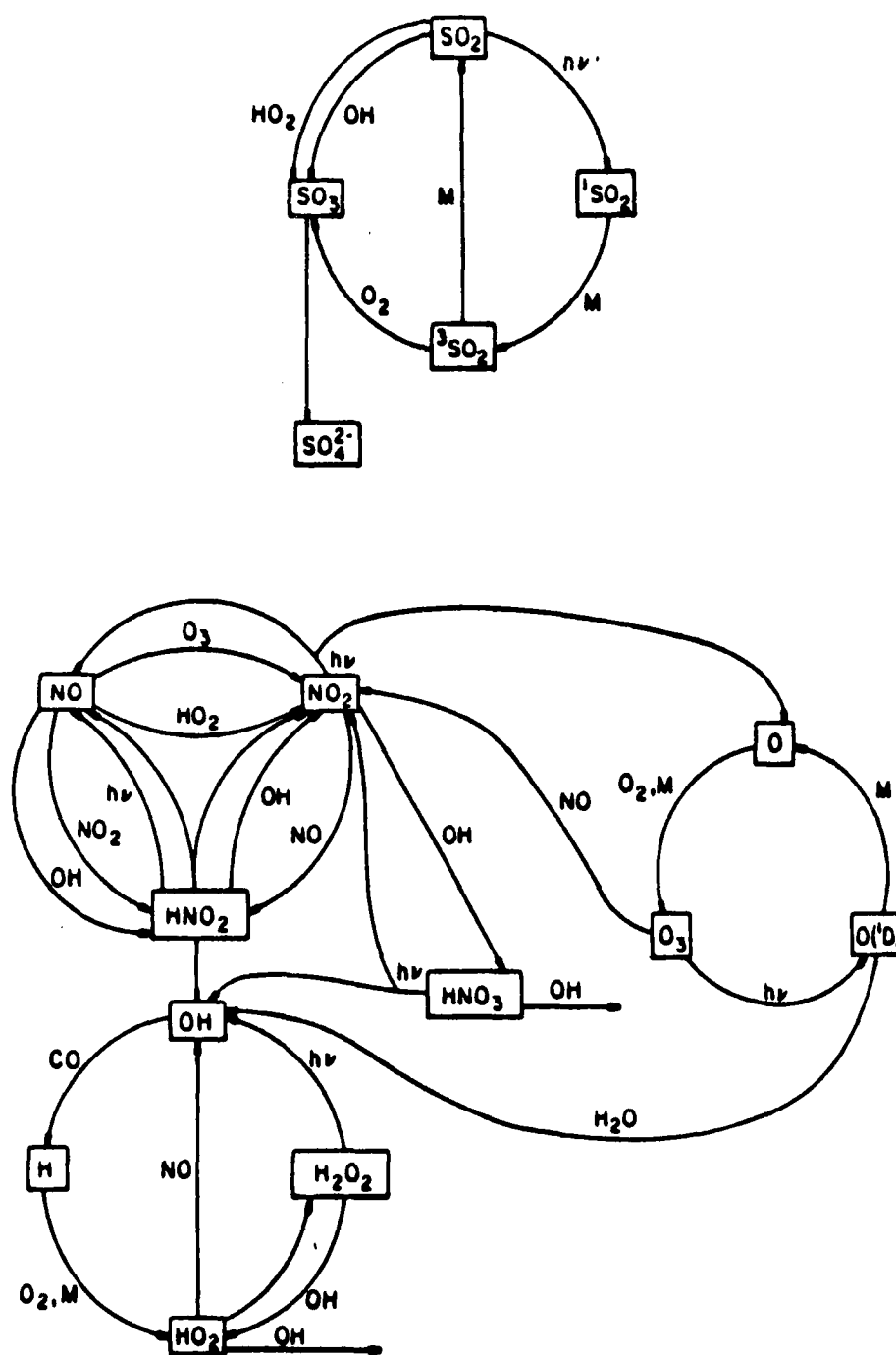
Figure 3. Partial atmospheric cycles involving odd hydrogen species free radicals. Emphasis has been placed on the acid forming oxidation of SO_2 and NO_2 [Buhr, 1986].

reaction which has received considerable study is the second order recombination of HO_2 with itself to form H_2O_2 and oxygen. The reaction rate constant is reported to be $(2.2 \times 10^{-13} \exp(620/T) + 1.9 \times 10^{-33}[M] \exp(980/T)) (1 + 1.4 \times 10^{-21}[H_2O] \exp(2200/T))$ cm^3 molecule^{-1} s^{-1} where M is air over the temperature, pressure, and humidity conditions found in the atmosphere from ground level through the mesosphere [**Kircher and Sander**, 1984]. This rate constant shows a dependence on pressure, temperature, as well as the humidity. The combination of CO and OH to form CO_2 and H has a pressure dependent reaction rate [**Demore et al.**, 1985; **Hynes et al.**, 1986], and the formation of HO_2NO_2 through the termolecular reaction $NO_2 + HO_2 + M \rightarrow HO_2NO_2 + M$ is enhanced by the presence of water vapor [**Sander and Peterson**, 1984]. Continuing research will hopefully elucidate the mechanisms of such reactions and bring a better understanding to odd hydrogen chemistry.

Measurements of Ambient Free Radicals

The importance of free radicals in atmospheric chemistry is well recognized and many methods are being attempted to measure free radical concentrations in the atmosphere. Unfortunately, free radical concentrations have proven hard to measure, and attempts to measure them have met with varying success. Since the OH radical is so prevalent in atmospheric chemistry, much of the effort has been directed toward measuring the OH radical. The direct

methods currently being used to measure OH in the atmosphere consist of Laser-Induced Fluorescence (LIF), high-resolution spectroscopy, long-path absorption, ^{14}CO oxidation, and spin-trapping. Other indirect measurements of OH are made through measuring other atmospheric trace constituents and using modelling and mixing data to estimate OH concentrations.

Of the methods to measure OH concentrations, LIF is the method gaining the most attention. LIF instruments have taken balloon [Heaps and McGee, 1983; Heaps et al., 1982, 1985], air-borne [D.D. Davis et al., 1976, 1979; L.I. Davis et al., 1985, 1987; Wang and Davis, 1974; Wang et al., 1981], and in-situ [Bradshaw et al., 1984; Hard et al., 1979, 1980, 1984, 1986; Rogers et al., 1985; Wang et al., 1975] measurements of OH in the stratosphere and troposphere. LIF involves the tuning of narrow-band UV lasers to one or more of the OH radical electronic absorption lines and detecting fluorescence from its first excited electronic state. The most noted difficulty for this method has been the uncertainty of the ozone/water interference [D.D. Davis et al., 1981a, 1981b, Ortgies et al., 1980]. The effect of the self-generated OH radicals caused by the intense laser radiation dissociating ambient ozone to O_2 and $O(^1D)$, and the $O(^1D)$ subsequently combining with water vapor to form OH radicals is still yet uncertain. Other problems with the LIF method have been the difficulty

in calibration, the complexity of the equipment, and cost of programs. Despite the difficulties, LIF has been the most used method in reporting OH measurements.

A precursor to LIF was resonance fluorescence used by Anderson, [1976] to measure OH in the stratosphere. A resonance lamp generating light in the 308nm region was used to excite fluorescence from atmospheric hydroxyl radicals at the same wavelength. The balloon mounted UV source and detector were raised and sampled while being lowered through the atmosphere. By measuring the difference in fluorescence signal from ambient air and chemically seeded air which had all OH removed, the concentration of OH was determined. The instrument was limited by interference from Rayleigh scattering of the source at lower altitudes and by sunlight scattering into the flow pipe, but did make some successful measurements.

High-resolution spectroscopy [Burnett and Burnett, 1981, 1982, 1983] involves measuring the vertical abundance of atmospheric hydroxyl using a Pepsios spectrometer to observe the resonant absorption of sunlight by OH molecules in the 308nm region. This is a non-calibrated method and observes the relative overall OH concentrations. The method presents interesting studies of seasonal and diurnal patterns of OH in comparison to other species, but is lacking in actual quantitative capabilities for determining OH concentrations.

Long-path UV laser absorption [Hagele et al., 1984; Hubler et al., 1984; Perner et al., 1976] estimates OH radical concentration through absorption of laser radiation of 308nm along a 3-10km pathlength. This method provides an absolute measure of OH concentration, but currently lacks adequate sensitivity to measure ambient OH concentrations due to interference from ambient turbulence, absorption by other atmospheric constituents, and stray sunlight. Reported measurements from this method have been very close to the detection limit of the instrument.

The ^{14}CO radiochemical technique to measure OH [Campbell et al., 1979] involves ^{14}C labelled CO being oxidized to CO_2 through the reaction of $CO + OH \rightarrow CO_2 + H$ in a $100dm^3$ teflon bag and the labelled CO_2 measured. The estimated precision of this method is plus or minus 40% with wall effects being the greatest source of error [Campbell et al., 1980].

The last direct method to measure OH concentrations is spin-trapping with determination by Electron Spin Resonance (ESR) and Gas Chromatography/Mass Spectrometry (GC/MS) [Watanabe et al., 1982]. Ambient OH is spin trapped in a alpha-4-pyridyl-N-tert-butylnitrone alpha-1-oxide (4POBN) impregnated sheet on an aircraft platform. The OH and 4POBN form a stable adduct and amount of adduct is determined by GC/MS. The sensitivity of the method is reported to be 0.2 x 10^6 OH/cm^3, but the overall precision of the method is

suspect. Our group's attempt to duplicate this work found insurmountable interference problems in the method [Buhr, 1986]. No publications after the 1982 paper have been observed on the method from the original authors.

The indirect methods to measure OH concentrations include measuring ground level ^{14}CO and ^{12}CO concentrations [Volz et al., 1981], and tropospheric distribution of methyl chloroform and other halocarbons [Singh, 1977a, 1977b] to derive mean OH concentrations. These measurements used various models to relate the findings and the relationships imposed by the models may be inaccurate.

Although HO_2 does not react with as many species as OH, HO_2 and other radical measurements are important because of the close relationship shared by these species. Measuring HO_2 may be easier due to the higher concentration of HO_2 and the understood relationships between HO_2 and OH in atmospheric chemistry would help validate and bring further understanding to the current atmospheric models. Methods to measure HO_2 include millimeter-wave spectroscopy, matrix isolation with Electron Paramagnetic Resonance (EPR), resonance fluorescence, and an LIF method called Fluorescence Assay with Gas Expansion (FAGE). Total peroxy free radical measurements are made with the technique of PEroxy Radical measurement by Chemical Amplification (PERCA).

One of the latest methods introduced to measure HO_2 concentrations is measurement by millimeter-wave spectroscopy [**De Zafra et al., 1984**]. Millimeter spectroscopy employs a sensitive mm-wave receiver to obtain spectroscopic line profiles of three rotational emission lines in the vicinity of 265.8 GHz. The shape of the rotational transition line due to pressure-broadening was deconvoluted to give information about vertical distribution. The accuracy of the method is uncertain due to the calculated yet unmeasured pressure-broadening coefficient of HO_2 used to decipher the data. The method is also limited to measurements in the stratosphere and cannot be adapted for use in the troposphere because the line widths become too broad.

HO_2 measurement by using matrix isolation with ESR spectroscopy [**Helten et al., 1984; Mihelcic et al., 1978**] consists of trapping HO_2 in a cold trap, followed by laboratory analysis to measure the presence of HO_2. This technique is limited because it yields a time averaged single data point for the entire sampling process, and although EPR has been a successful technique for identifying free radicals in the laboratory, the EPR spectra for NO_2 is similar to the EPR spectra for HO_2 causing a calibration error estimated to be a factor of three in stratospheric measurements. This interference apparently limits the usefulness of this method in the troposphere.

Resonance fluorescence has also been used to measure HO_2 [**Anderson et al.**, 1981] by converting ambient HO_2 to OH through the fast bimolecular reaction $HO_2 + NO \rightarrow OH + NO_2$ and measuring the OH concentration as previously outlined for the resonance fluorescence method. This method is successful in the upper atmosphere, but suffers quenching by oxygen in the lower atmosphere.

Fluorescence Assay with Gas Expansion (FAGE) uses LIF to measure HO_2 by converting HO_2 molecules to OH through reaction with NO and measuring the real time OH concentration [**Hard et al.**, 1984]. FAGE tries to reduce many of the problems associated with LIF measurements of OH by reducing the pressure at the LIF measurement region, and chemical modulation of the signal, but adds to the general complexity of the LIF method.

Considerable effort has been expended to measure ambient atmospheric free radical concentrations. All the methods outlined above have merits and drawbacks. Problems associated with the LIF, and ^{14}CO method have caused recent intercomparisons between different measurement methods for OH radicals to be extremely difficult and inconclusive [**Hoell et al.**, 1984; **Gregory et al.**, 1985; **Beck et al.**, 1987]. The most presently believable real time tropospheric OH measurements are the latest work by the FAGE LIF method [**Hard et al.**, 1986].

A compact, simple in design, real time instrument would be a welcome method in this field. The last technique to measure total peroxy free radicals is the PEroxy Radical measurement by Chemical Amplification (PERCA) method [**Cantrell et al., 1984**]. PERCA meets the needs outlined above. PERCA measures total free radicals (RO_x) on a real time basis by converting injected NO to NO_2 through the following chain reaction with CO:

$$HO_2 + NO \rightarrow NO_2 + OH \tag{1}$$

$$OH + CO \rightarrow CO_2 + H \tag{2}$$

$$H + O_2 \xrightarrow{M} HO_2 \tag{3}$$

Due to its higher concentration in the atmosphere, HO_2 is the principal species initiating the chain reaction at step 1. OH can also intiate the chain reaction by entering the chain reaction at step 2. Other free radicals can initiate the chain reaction by substituting for HO_2 in step 1 and oxidizing NO to NO_2 and creating an OH radical. The resultant NO_2 is measured with a state of the art, compact, and relatively inexpensive, luminol NO_2 detector. By measuring the total RO_x, various models could be validated, and odd hydrogen radical concentrations could be discerned through measurement of atmospheric conditions and known relationships. The remainder of this thesis describes the PERCA instrument, experiments done to optimize the instrument, interferences and calibration methods for the PERCA instrument, and field studies using PERCA.

Chapter II

PERCA

PEroxy Radical detection by Chemical Amplification (PERCA) was first investigated by Christopher Cantrell [**Cantrell and Stedman**, 1982; **Cantrell et al.**, 1984, **Cantrell**, 1983] and further developed by Martin Buhr [**Buhr**, 1986]. The PERCA technique involves injecting a steady stream of NO (3-5 ppmv) and alternating balanced flows of either CO or N_2 (10% by volume) into a reactor to mix with the ambient air. The NO is oxidized to NO_2 in the reaction $HO_2 + NO \rightarrow NO_2 + OH$. The resulting NO_2 is quantified by measuring the light produced by reacting the NO_2 with luminol solution. When CO is added to the reactor, the CO reacts with the OH created by the first reaction and creates another HO_2 molecule and CO_2 through the following reactions:

$$OH + CO \rightarrow CO_2 + H$$

$$H + O_2 + M \rightarrow HO_2 + M$$
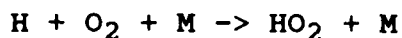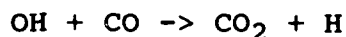
The newly created HO_2 molecule then reacts with another NO molecule continuing the chain reaction.

The reactions thought to be important in terminating the chain reaction are $HO_2 + HO_2 \rightarrow H_2O_2 + O_2$ and $HO + NO + M \rightarrow HONO + M$ [**Buhr**, 1986]. Another potentially important

15

termination step may be the termolecular reaction HO_2 + NO_2 + M -> HO_2NO_2 + M to be discussed later in this chapter.

N_2 is alternated with CO to show a background signal with no chain reaction taking place. In the original theory, the background signal is expected to consist of the weighted sum of the signals of ambient NO_2, PeroxyAcyl Nitrates (PAN), and O_3 [Buhr, 1986]. The theory is inadequate since a field study (to be discussed in a later chapter) conducted in polluted Southern California air yielded a background signal of 1.4 ppm relative to NO_2. Only 60% of the background could be accounted for by the known species above.

Each hydroperoxy or hydroxyl radical entering the system during the CO cycle should produce a number of NO_2 molecules defined by the chain length. Figure 4 shows Cantrell's model of chain lengths based on known involved reactions. It is important to note that Cantrell's model neglected wall losses and is a model for the chain length and not for NO_2 signal. This disfunction is because of the instrument's depressed sensitivity to NO_2 with added NO. The actual number for the chain length has been determined for the present system to be approximately 600 under laboratory conditions. The value is lower than predicted by Cantrell's model, but not unreasonable, considering that the assumptions of instantaneous mixing, plug flow, and no
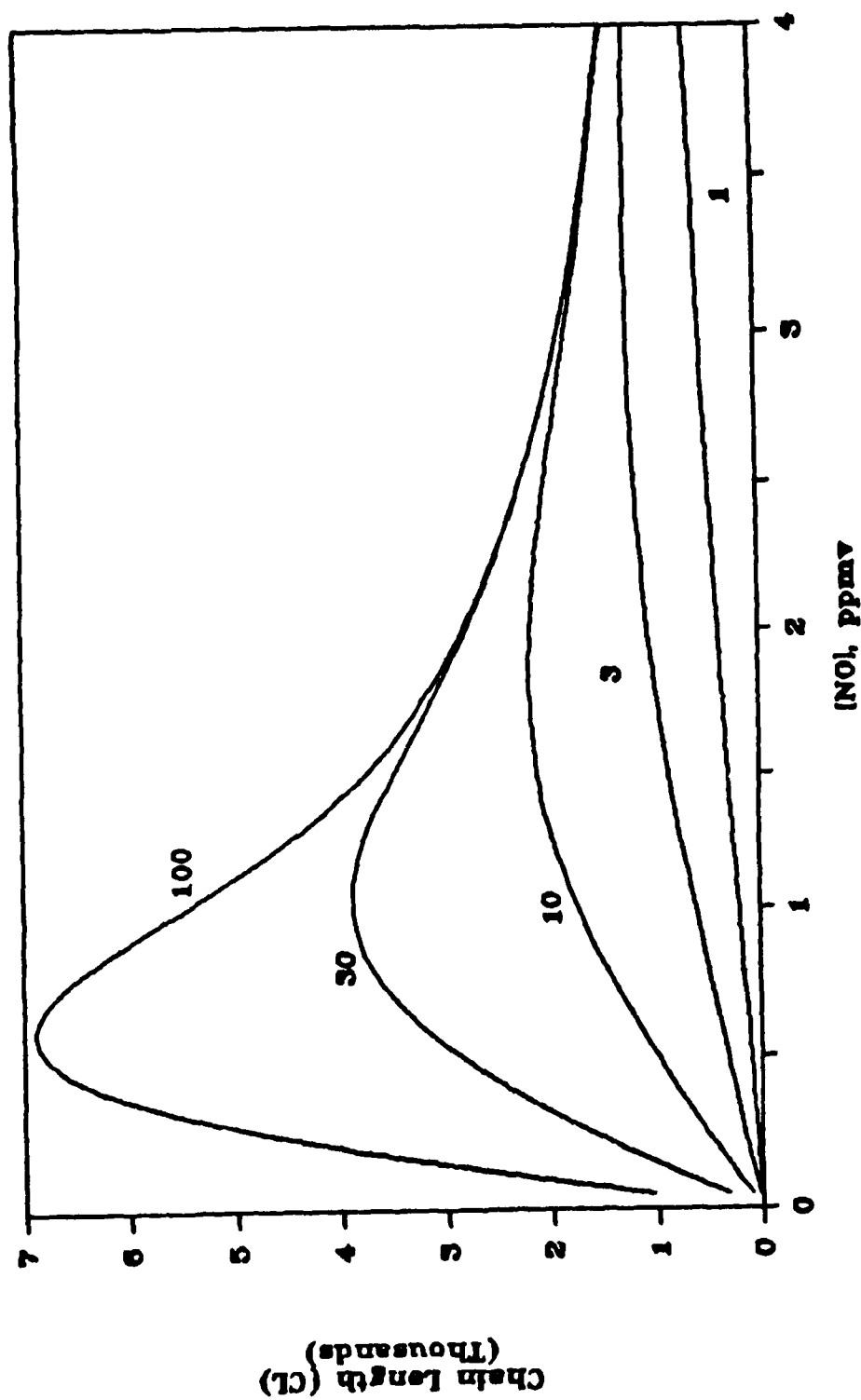
Figure 4. Cantrell's model for chain length vs [NO]. Shown are the reaction times of 1, 3, 10, 30, and 100 seconds. Wall reactions, depressed NO_2 sensitivity with added NO, and pernitric acid formation were ignored.

surface reactions used in Cantrell's model all would tend to overestimate the predicted chain length.

Pernitric Acid Formation

Under certain conditions, pernitric acid formation through the reaction $HO_2 + NO_2 + M \rightarrow HO_2NO_2 + M$ may be the limiting reaction in the PERCA method. Studies by Sander and Peterson [1984] have reported the water vapor enhanced termolecular reaction rate constant for forming pernitric acid to be 1.0×10^{-30} cm^6 molecule^{-2} second^{-1}. The dissociation rate constant of pernitric acid is reported to be 5.2×10^{-6} exp($-19900/RT$) cm^3 mol^{-1} s^{-1} [Sander and Peterson, 1984] which gives an average lifetime of over five hours at room temperature and one atmosphere pressure. This makes the dissociation of pernitric acid irrelevant in the time frame of the PERCA method. The chain propagation reaction of $NO + HO_2 \rightarrow NO_2 + OH$, critical to the PERCA method, has a bimolecular reaction rate constant of 8.7×10^{-12} cm^3 molecule^{-1} second^{-1}. Figure 5 shows a plot of the log of the ratio of the propagation reaction rate of $HO_2 + NO$ divided by rate of $HO_2 + NO_2 + M$ to form pernitric acid, as a function of increasing concentration of NO_2.

In clean dry air with less than 2ppbv NO_2, it is reasonable to assume that HONO formation and wall losses are the limiting factors in the PERCA chain reaction. At less than 2ppbv concentrations of NO_2, the formation rate of NO_2 and OH is more than 800 times faster than the formation rate

Log Rate Ratios vs. [NO2]

Rate NO2/Rate HO2NO2
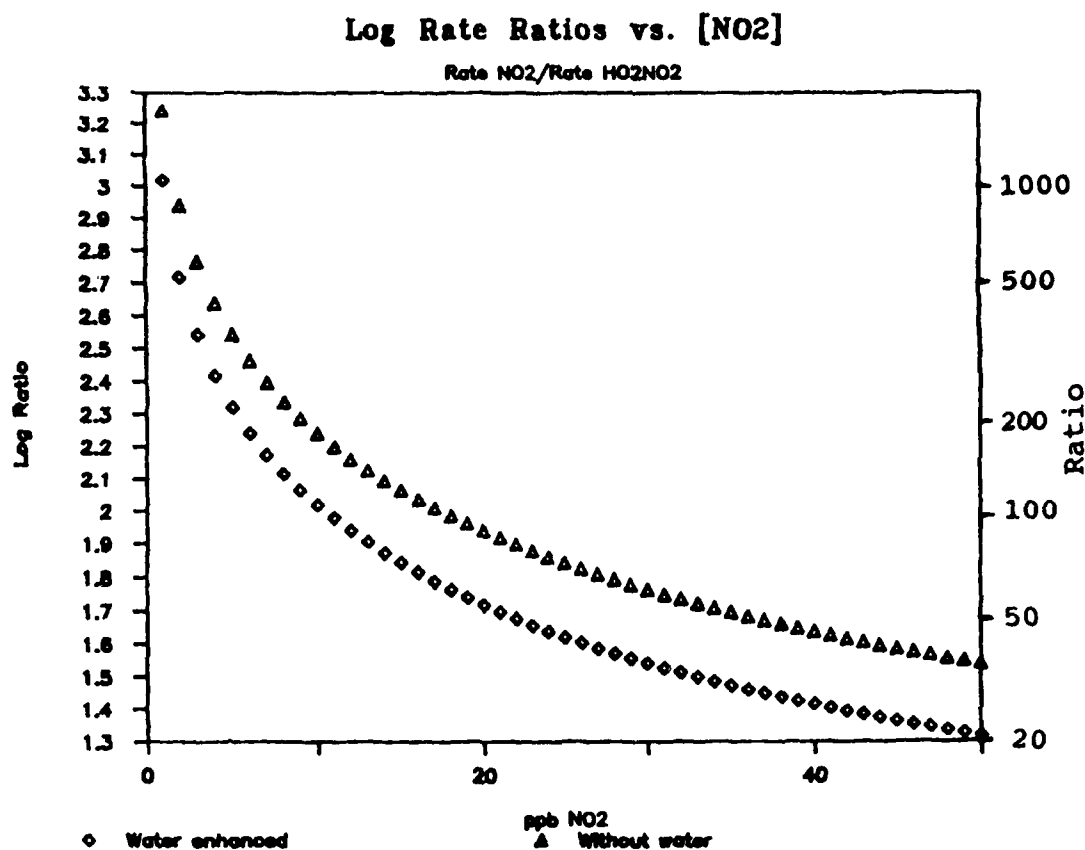
Figure 5. Comparison of the formation rates between the competing reactions NO + HO_2 -> NO_2 + OH, and HO_2 + NO_2 + M -> HO_2NO_2 + M with increasing concentration of NO_2. Plotted is the log ratios using the formation rate of NO_2 divided by the water enhanced and dry formation rates of pernitric acid.

of pernitric acid.   Other factors besides the formation of pernitric acid limit the chemical amplification capabilities of the PERCA instrument in clean dry air.

In dirtier air with higher NO_2 concentrations, HO_2NO_2 formation may become an important sink for HO_2 molecules in the PERCA reactor chamber, limiting the chain length.   In wet air containing 10ppbv of NO_2, the reaction forming NO_2 and OH is only 100 times faster than the formation rate of pernitric acid.   In a recent field study in California, 40ppbv concentrations of NO_2 common in the Los Angeles basin air, could have limited the chain length to the low 20s. The ability of the NO_2 forming reaction to outperform the formation of pernitric acid rapidly deteriorates as ambient NO_2 levels increase, and severely limits the use of the PERCA instrument as currently configured in polluted environments.

Pernitric acid formation may also interfere in calibrations of the PERCA method.   Calibration of the PERCA instrument is often done with NO_2 signals of 100 ppbs or higher.   At each successive chain propagation inside the reactor creating NO_2, the pernitric acid formation rate increases.   At some point, the resultant increase of pernitric acid formation may compete sucessfully for HO_2 radicals limiting the chain length.   The calibrated chain length in the lab with higher radical densities and subsequent higher NO_2 readings may be less than the actual

chain lengths possible in clean air with lower free radical densities. The extent of such an interference from pernitric acid formation is uncertain and requires experimental investigation.

The Instrument

The chemical amplifier instrument consists of two parts. The first is the reaction chamber which provides for reagent gas addition and NO_2 production from chain reaction and other sources. The second is the NO_2 detector. Figure 6 shows a diagram of the entire PERCA system.

The stainless steel reactor is shown in Figure 7. The reactor adds the reagent gases to the ambient air stream through a series of small radial grooves located behind the reactor inlet allowing for even mixing. The inlet is a 1/2" long 1/4" od stainless steel tube with an attached female Swagelok fitting and allows for a tight seal when sampling from bags during calibration. The chamber volume of 250 ml allows for a reaction time of 5 seconds at a total flow of 3 slpm. The entire chamber including the inlet is coated with halocarbon wax to reduce wall losses.

The luminol instrument described by Wendel et al. [1983] detects NO_2 in the system by the photodetection of the chemiluminescent reaction between NO_2 and luminol (3-aminophthalhydrazide). The detector shown in Figure 8, with associated electronics, is able to detect ppt levels of NO_2 and has a response frequency of approximately one Hertz (1

PEroxy Radical measurement by Chemical Amplification (PERCA)
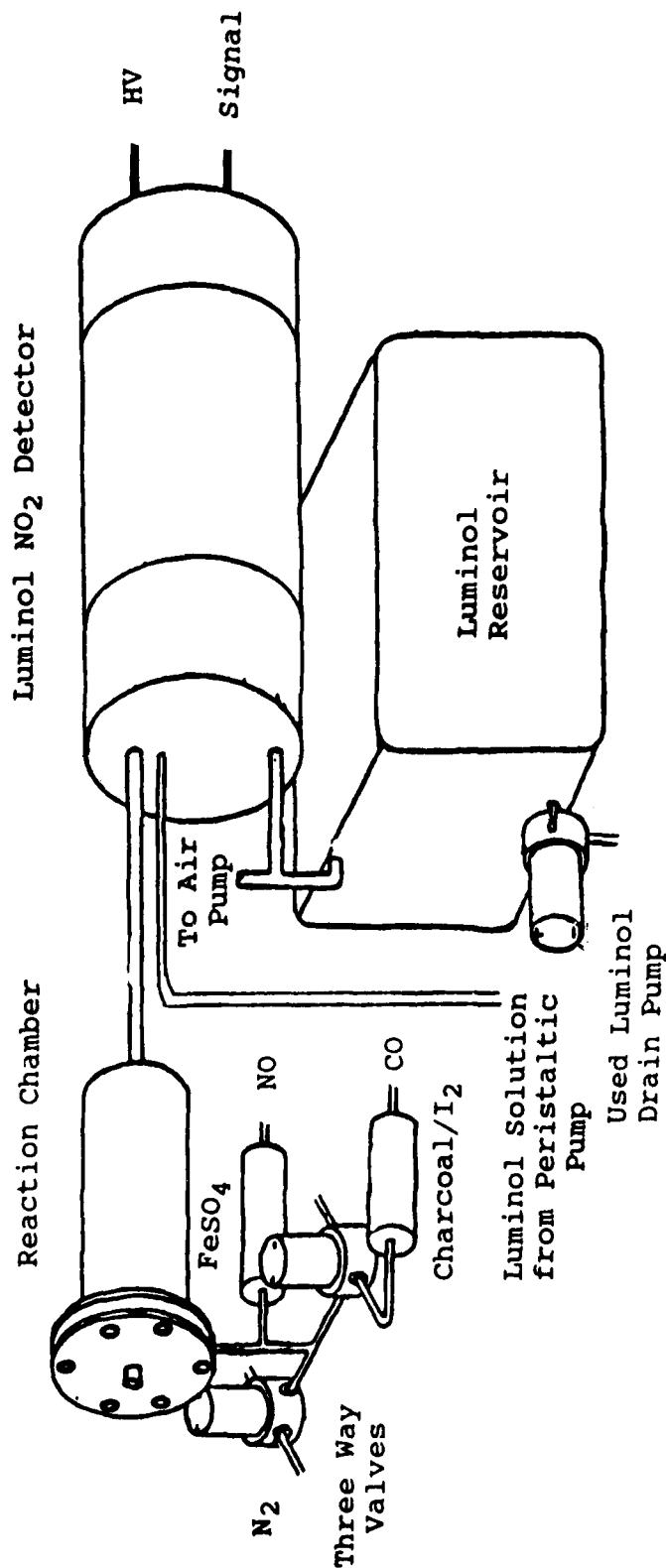
Figure 6. Schematic of the PERCA method. The NO_2 producing chain reaction takes place in the stainless steel reactor, and the resultant NO_2 is measured with the luminol based NO_2 detector.
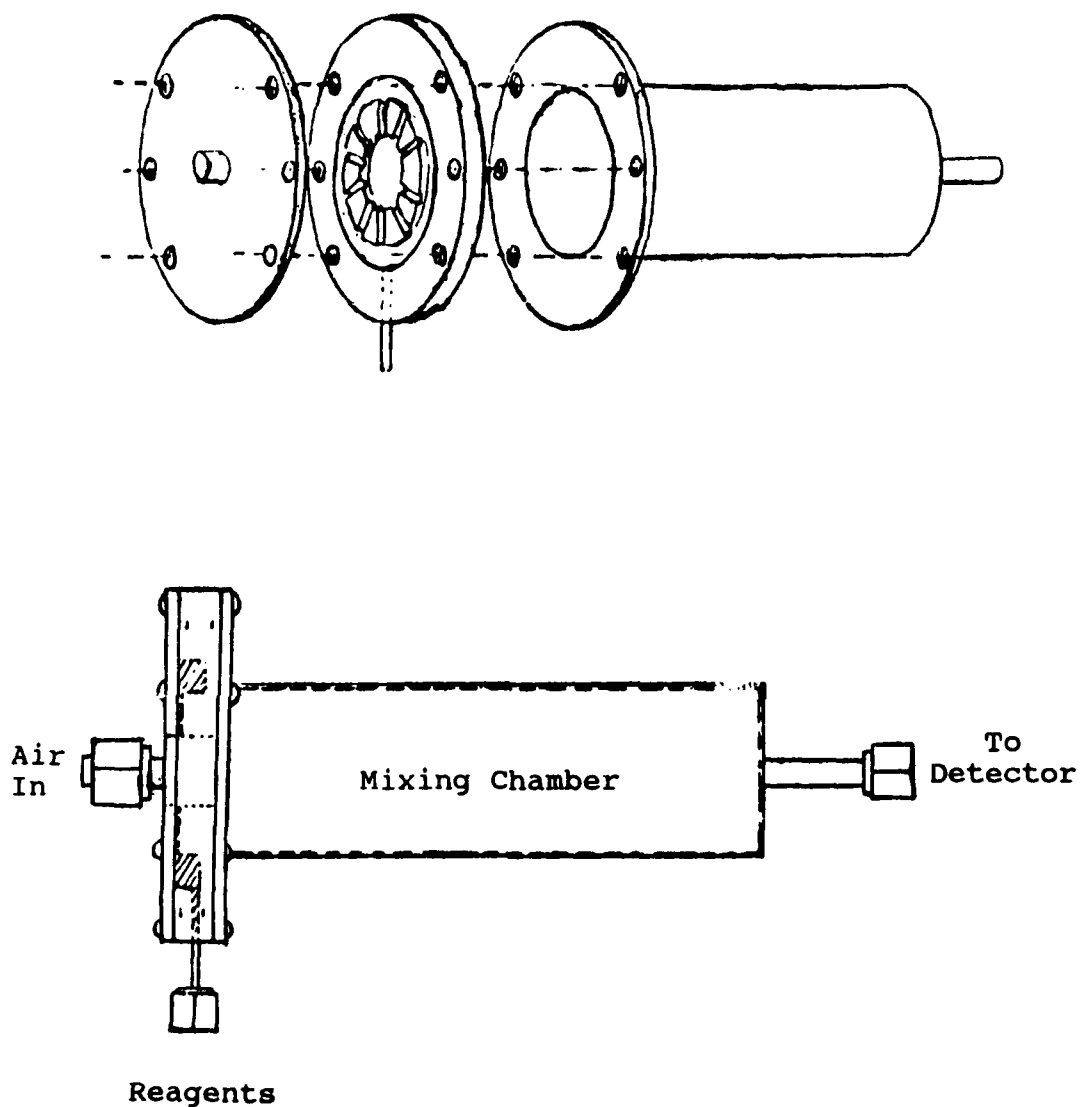
Figure 7. Stainless steel reaction chamber coated with halocarbon wax. The reagent gases enter the plenum and are added to the incoming air through 10 radical grooves. The volume of the chamber is 250ml, allowing for a 5 sec. reaction time at a total flow of 2 L/min.
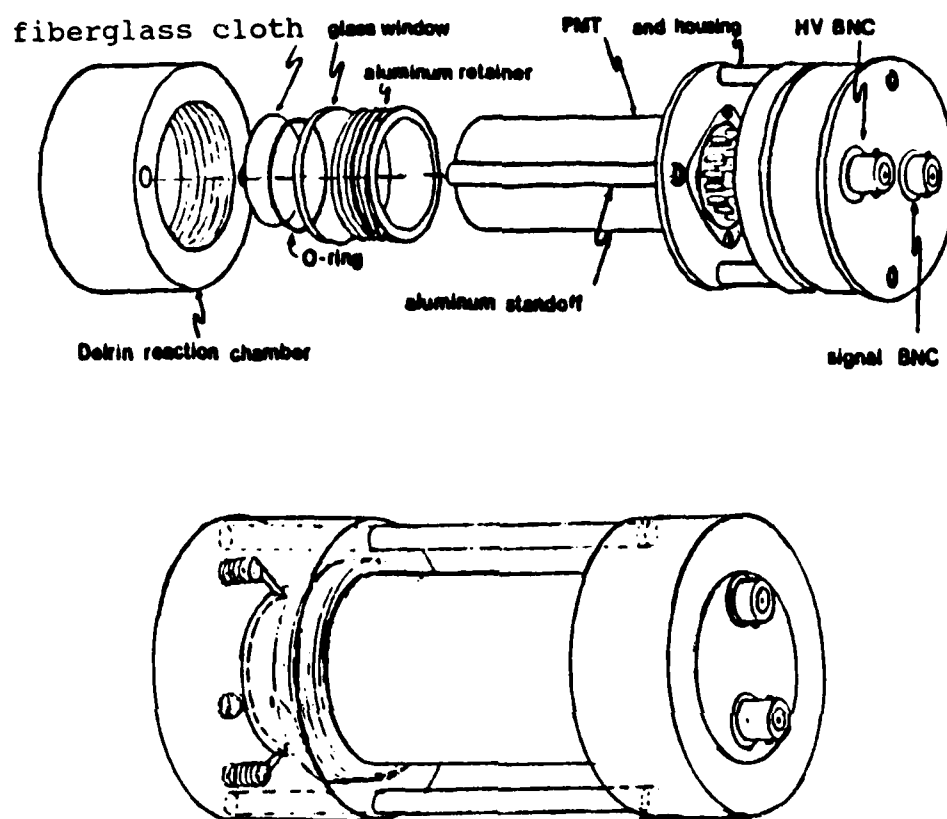
Figure 8. Luminol based nitrogen dioxide detection cell. The NO_2 is detected by observing the chemiluminescent reaction between NO_2 and the luminol solution at the gas/liquid interface on the fiberglass cloth.

s^{-1}). The detector is operated by flowing luminol solution (0.5 ml/min) over a fiberglass cloth which is held on the back wall of the detection cell. The luminol solution is pumped through, in a one-time through fashion, by a peristaltic pump. The gas mixture from the pre-reactor is passed between the fiberglass cloth and a glass window that seals the cell from the PhotoMulitiplier Tube (PMT) (RCA 4507). The blue chemiluminescence occurring at the gas-liquid surface is measured and the photocurrent amplified. The instrument provides a linear response to NO_2 from 1 ppb to a range of 4 magnitudes above. The detection limit of the instrument is highly dependent on the noise produced zero-modulation to be discussed later.

Data acquisition is accomplished with both analog processing using a strip chart recorder and digital processing using an IBM PC with a Tecmar I/O interface. Appendix A lists the program used to collect the data. The Tecmar I/O interface is the Lab Tender model using 8-bits to digitize the signal range from -10 volts to +10 volts. An 8-bit word provides 256 increments to code from -10 to +10 volts giving a 0.08 volt resolution. The electrometer of the NO_2 detector is capable of output from 0 to 15 volts dc. When using the computer to collect the data, the settings on the electrometer must be set to amplify the signal as much as possible without exceeding the 10 volt limit of the computer system. The analog meter on the instrument, rebuilt

from a McMillian Electronics Corporation (MEC) ozone detector, reads 0-1 volt full scale, and has a tendency to peg full scale when using the computer. Placing a resistor in series to make the meter read 0-10 volts should solve the problem. The current system is adequate to collect data, but switching the data acquisition system to a twelve bit board would enhance the resolution capabilities of the computer data acquisition system sixteen times, making it a more flexible system.

The Reagents

The reagent gases used in the PERCA system are: carbon monoxide, CP grade (Linde); nitrogen, CP grade (Linde); and nitric oxide in nitrogen (1250 ppmv, made in aluminum cylinders from high purity nitric oxide and nitrogen). The carbon monoxide is passed through an activated-charcoal/ iodine trap to remove metal carbonyl compounds, principally $Ni(CO)_4$ and $Fe(CO)_6$ [Buhr, 1986]. The filter is mainly activated charcoal (DARCO, HD-3000 grade) with a few crystals of I_2 (Fisher) to remove the metal carbonyls. The I_2 crystals must be positioned so that the CO will pass through the charcoal after contacting the iodine. The nitric oxide is passed through dry $FeSO_4$ to reduce any NO_2 formed in the cylinder back to NO. Copper, instead of teflon, should be used to carry the nitric oxide to prevent the inward diffusion of O_2. The diffusion of O_2 leads to formation of NO_2 in the NO supply lines.

The reagent gas flows are controlled with Tylan mass flow controllers. Electronic mass flow controllers are the only method with the monitoring control required to balance the CO and N_2 flow. Unbalanced flows can increase zero-modulation discussed later in the text. Two three-way valves (General model #1-43-900) housed in an aluminum box with the reactor chamber previously described, gates the entry of the carbon monoxide and nitrogen into the reaction chamber. CO and N_2 pressures must be balanced because unbalanced pressures between CO and N_2 can cause spiking in the instrument signal when the gases are switched through the valves. Normal pressures for NO, CO and N_2 to the Tylan flow controllers are 25 psi.

The luminol solution is an aqueous, sulfite buffered, pH 12 mixture optimized for response to NO_2 [Wendel, 1985]. The dry reagents (Baker Analyzed) are used without further purification with the possible exception of luminol. Depending on the individual batch of luminol, further purification of luminol through recrystallization in an alkaline aqueous solution may be required for adequate sensitivity to NO_2.

Chapter III

Optimizing the Instrument

In developing a model for the chemistry of the instrument, Cantrell assumed instantaneous mixing, plug flow, and no wall losses. The model suggested increasing chain lengths for increased reaction time [**Cantrell**, 1983]. These assumptions provided a basis to work from, but gave a model that was too simplistic. The assumptions were tested in efforts to define what was needed to optimize the instrument. This effort included investigating different reaction chamber designs, finding optimum reagent concentrations, minimizing zero-modulation, and incorporating the latest changes into the luminol detector.

Reaction Volume and Chain length

To test if the model was correct in assuming higher chain lengths for higher reaction times, different adjustable volume reactors were tried for their effect on a steady radical signal flow generated by chlorine photolysis (Figure 9). HO_2 radicals are produced in this flow tube system by the following mechanism:

Cl_2 + hv (320nm) --> 2 Cl·

Cl + H_2 --> HCl + H·

H + O_2 + M --> HO_2 + M

29
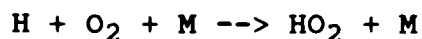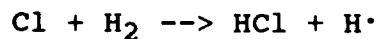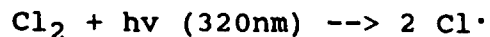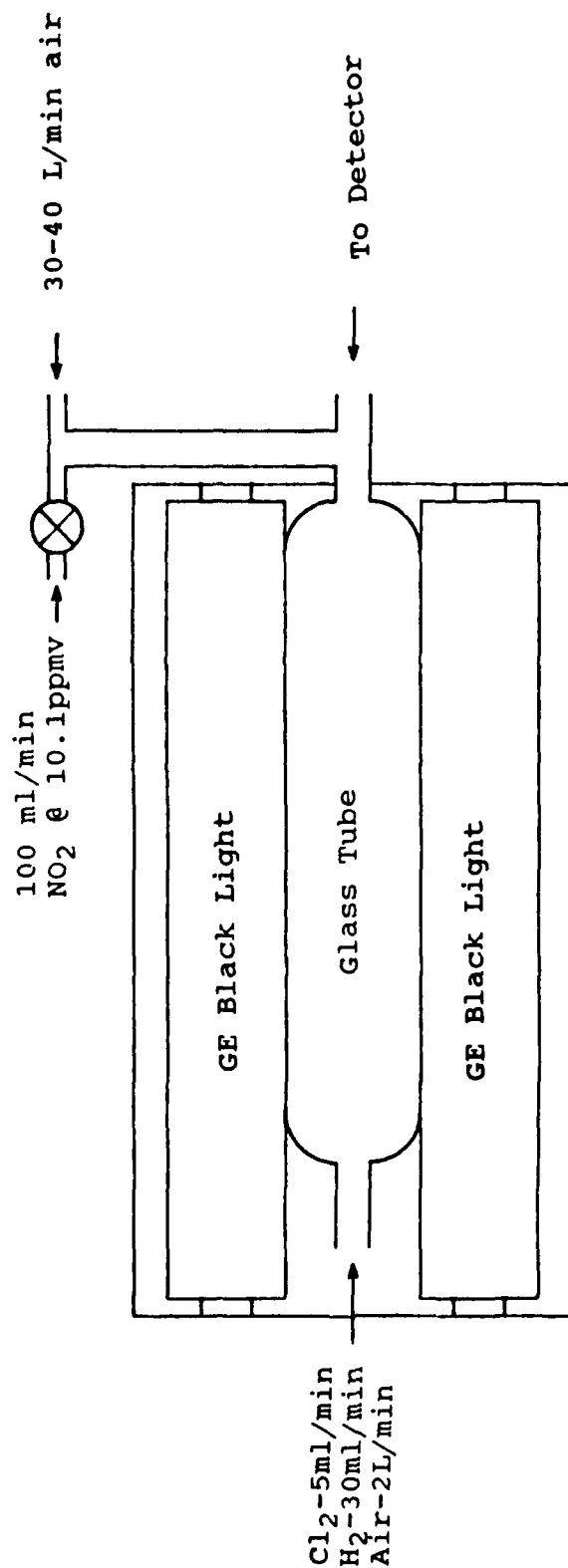
Figure 9. Steady radical source using chlorine photolysis. HO_2 radicals are generated in this apparatus by using GE black lights to provide near 300nm radiation to excite the entering chlorine. The created chlorine radicals react with the hydrogen and create hydrogen radicals which combine with oxygen to form HO_2 radicals. The final flow is diluted with a large air flow, and NO_2 calibrations are accomplished by injecting NO_2 into the large diluent air flow.

An example of the actual steady signal characteristic of the chlorine photolysis system is shown in Figure 10.

The first attempt used an adjustable volume reactor consisting of two inch diameter by five inch long teflon tubes that could be screwed together to adjust the volume. The reagent gases were injected through 1/8 inch diameter teflon tube as shown in Figure 11. By adding teflon tube sections as required, it was hoped that an optimum volume could be found. Adding a second teflon tube failed to increase the signal received from just one section. The optimum volume for the first adjustable volume reactor was achieved using only the first 5 inch section. An adjustable volume reactor with a smaller volume was needed.

The second adjustable volume reactor shown in Figure 12 consisted of a 23 1/2" by 3/4" outer diameter (od) teflon tube and a 1/8" teflon tube injector. The reaction volume was adjusted by moving the 1/8" teflon tubing inside the larger tube. The raw data in Figure 13 shows the signal decreasing after two inches. The signal decrease was unexpected and could be due to the new teflon absorbing NO_2. Since at zero distance, the signal is almost zero, the effect of the tubing connected to the reaction chamber is assumed to be negligible. The total volume of reaction was 5.5 cm^3 with a reaction time of about .2 seconds at an intake flow of 2L/min. To confirm the findings, a shorter adjustable volume reactor was tried.

31
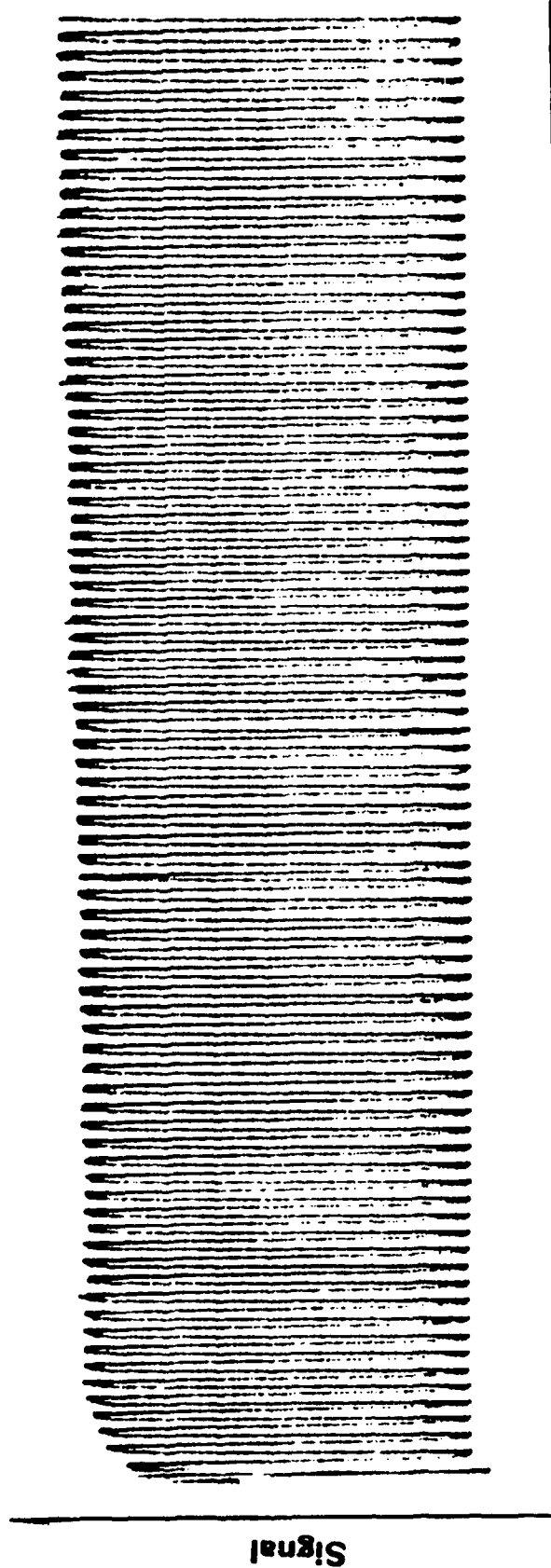
Figure 10. Sample steady signal from chlorine photolysis radical source shown in figure 9. The source dependably produces a constant signal. The PERCA instrument was set to cycle once every minute. Each peak represents a one minute passage in time.
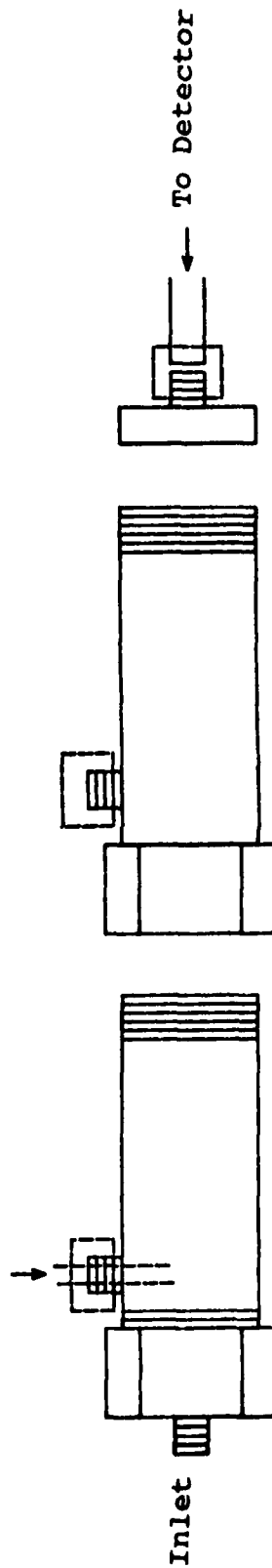
Figure 11. Teflon adjustable section reactor. Cantrell's assumption
that higher chain lengths were possible with increased reaction times
was tested by checking the radical signal with one then two 5 inch long
2 inch diameter teflon sectioned reactor chambers. The addition of the
second section failed to increase signal.

Reagent
Gases

To Detector

Intake
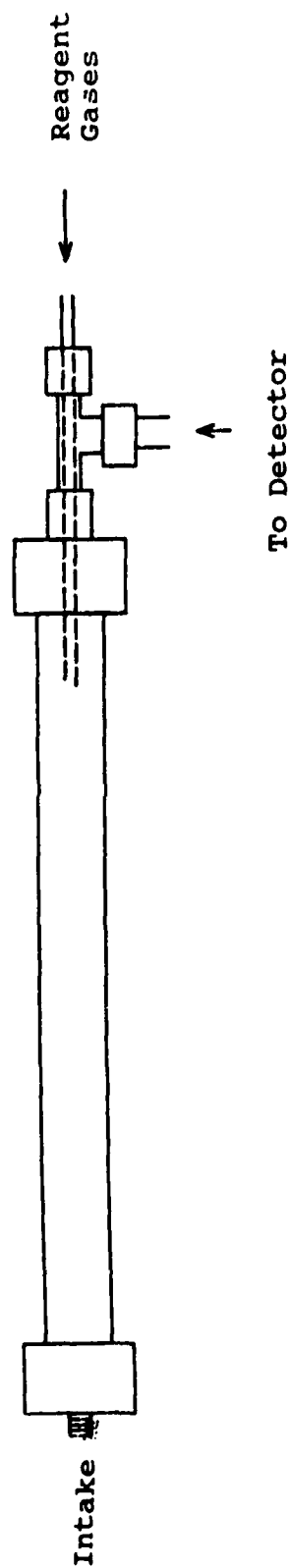
Figure 12. Adjustable Volume Reactor. To find the optimum reaction time, the reagent gases were injected through a 1/8" od teflon tube at various intervals inside the 3/4" od teflon tube. The optimum time was found to be less than .2 seconds.
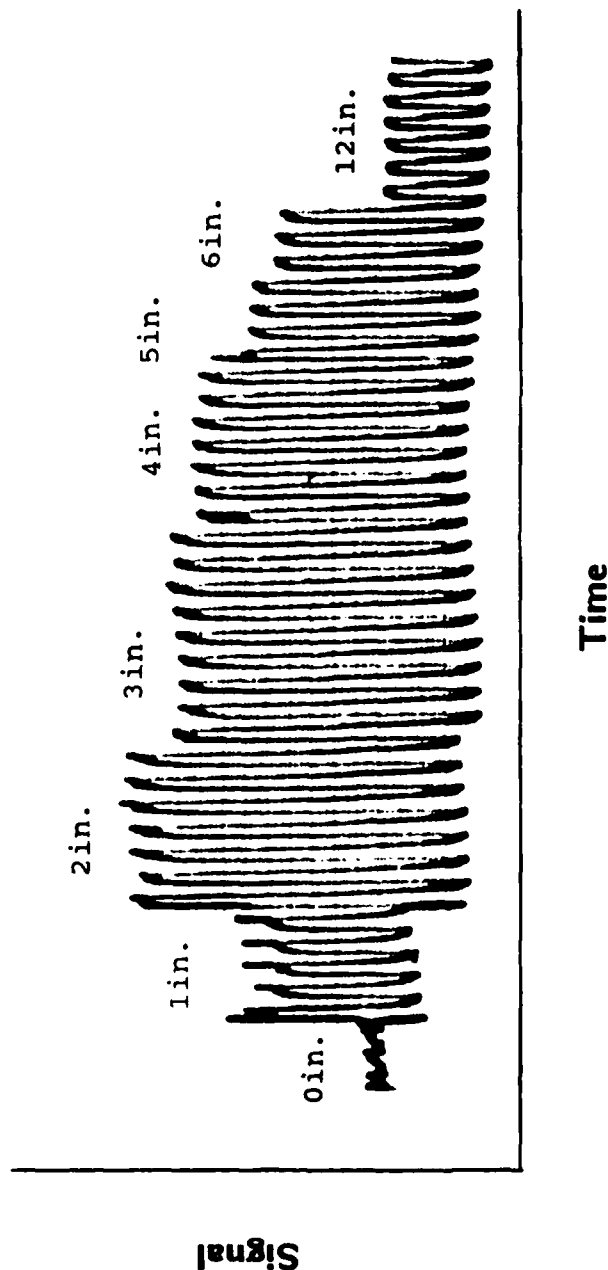
Figure 13. Actual recorded signal generated by injecting reagent gases at different intervals in the adjustable volume reaction chamber. The PERCA instrument was cycled once every minute. The reason for the decrease in signal may be due to the new teflon absorbing the NO_2.

The third reactor was configured just as the second reactor except that the reactor was now only 7 1/2" long of the same diameter teflon. The optimum volume occurred again at the 2 inch injection mark, but the radical signal was stronger, presumably due to less radical or NO_2 loss on the reactor wall surfaces. The conversion of NO to NO_2 apparently requires little reaction time and increased residence time in a reactor does not seem to give gains in performance, despite the predictions of the model in Figure 4.

Reducing Wall Losses

Wall reactions and mixing play an important part in determining chain length. Buhr developed a stainless steel reactor to provide for better mixing and suggested coating the reactor with halocarbon to reduce wall losses. To study to effect of wall losses, various materials and reactor configurations were examined for their effect on a steady radical flow generated by chlorine photolysis (Figure 9).

To test different surfaces for radical losses, 1/4" od Swagelok Tees of brass, stainless steel, stainless steel coated with halocarbon wax (Halocarbon Products Corp. 82 Burlews Court, Hackensack, NJ 07601), polypropylene, translucent teflon, and polyvinyl chloride were screwed on to the Swagelok fitting located on the front of the stainless steel reactor chamber and the effect on signal observed. This directly affected the density of the

radicals prior to mixing with the reagent gases in the reactor. Results in Figure 14 show the most signal loss was caused by brass followed closely by stainless steel. Translucent teflon, polypropylene, and polyvinyl chloride surprisingly performed the same. The least losses occurred with the stainless steel coated with halocarbon.

The original reactor was stainless steel, the second worst offender in terms of radical losses, so different reactor designs were tried. The first was a regular teflon Swagelok Tee as the reactor. The reagent gases (NO, CO, and N_2) were injected into the main stream and the 3 foot long by 1/4" od teflon line to the luminol instrument became the reactor. This configuration gave approximately 20% of the signal attained on the chlorine photolysis radical source under the same conditions using the stainless steel reactor.

To reduce production costs from the stainless steel reactor, a simple polypropylene bottle reactor was tried (Figure 15). It provided 80% of the signal achievable by using the uncoated stainless steel reactor. Although the reactor design is simpler and less expensive to implement, the plastic bottle did not improve on the original stainless steel reactor design.

The next effort was to compare the original teflon adjustable volume reactor (with one section) and coated stainless steel reactor chambers. The advantage of the stainless steel reactor is the superior mixing of the

Signal Reduction by Various Materials

Normalized (No T attached = 100%)
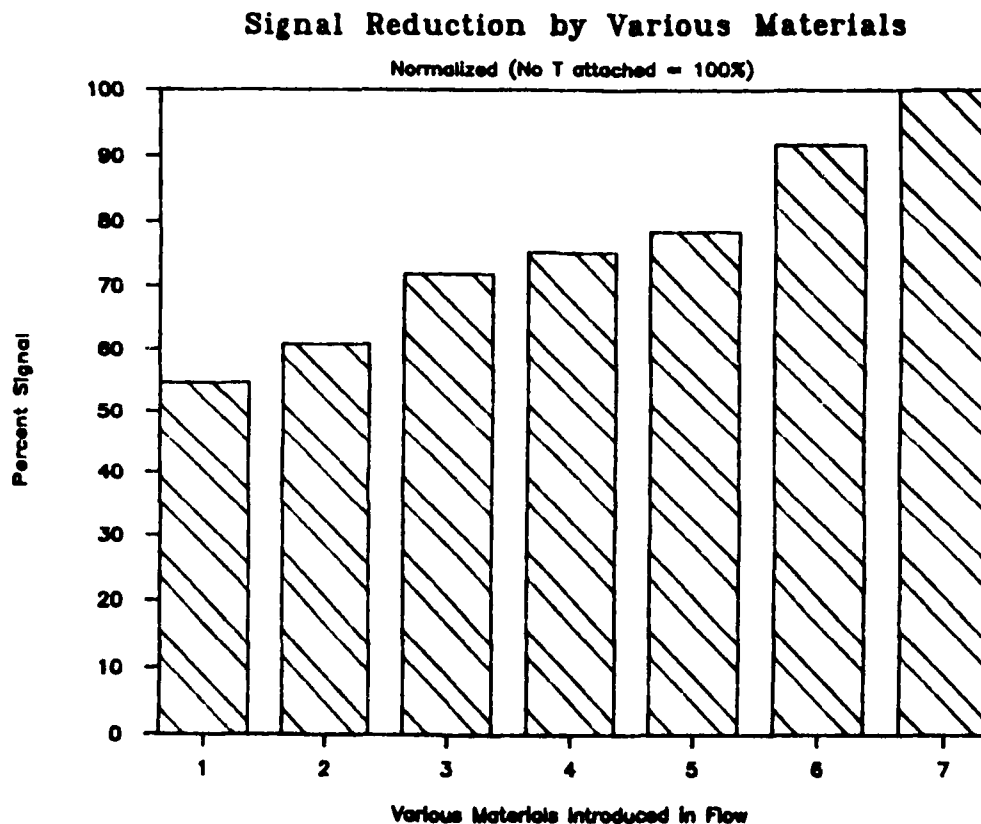
Figure 14. Materials comparison. The potential for radical losses on different surfaces was compared by observing the change in signal after attaching Swagelok Tees of different materials in front of the reactor chamber. The materials were: (1) brass; (2) stainless steel; (3) translucent plastic; (4) teflon; (5) polypropylene; (6) stainless steel coated with halocarbon wax; and (7) no Tee attached.
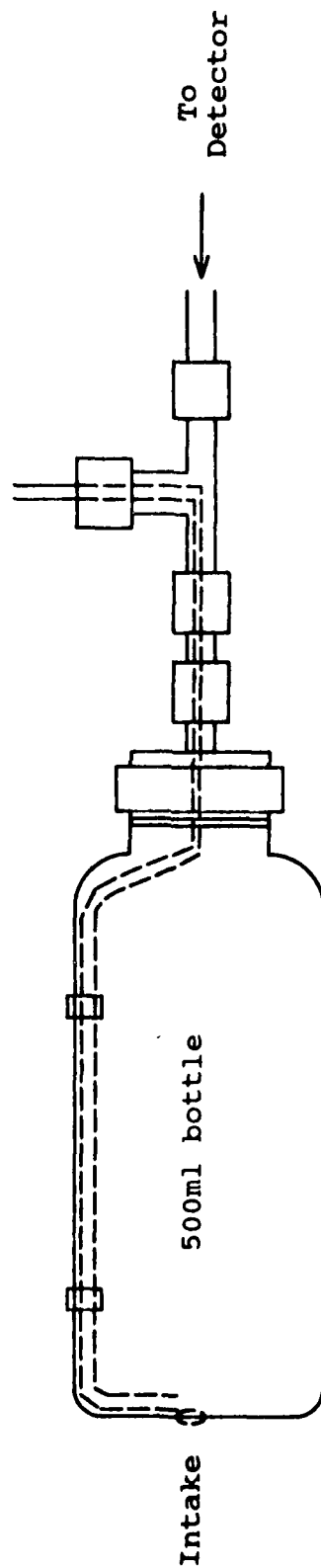
Figure 15. Polypropylene bottle reaction chamber. To lower production costs, a reactor made from a polypropylene bottle was tried. Although a very inexpensive design, it failed to provide enough signal.

reagent gases, so wall coatings were tried to decrease wall losses, yet continue using the mixing characteristics of the stainless steel reactor. Although the volume studies indicate the stainless steel chamber volume of 250ml may be more volume than required, the extra volume is not a major problem. The signal from the steady radical density chlorine photolysis source was observed for the stainless steel chamber. The signal from the same source was recorded for the original teflon adjustable volume reactor (Figure 11) with only the first section being used. The coatings were then tried.

The first coating tried was a 10% phosphoric acid solution shown in studies to reduce loss of radicals to wall reactions [Clark et al., 1966]. The stainless steel chamber was cleaned with Alconox, rinsed in deionized water, and wiped dry. The 10% H_3PO_4 solution was drawn into the reaction chamber by suction, allowed to drop out by gravity, and the chamber allowed to dry in a vertical position to allow the excess solution to drip out. The coating was allowed to dry overnight. Sampling the chlorine photolysis radical generator with the same settings, the phosphoric acid coating improved the signal by 60% over the plain stainless steel.

The next coating tried was halocarbon wax (Halocarbon Products Corp.). It has been used in HO_2 studies showing a reduction of HO_2 losses on walls [Kircher and Sander, 1984].

The stainless steel reactor was cleaned as before and coated with halocarbon wax by heating the reactor chamber and sliding small chunks of wax around the chamber. After the wax had been applied to all surfaces, the chamber was placed in a vertical position and heated. Excess wax was dripped out and the chamber rotated slowly on its side until the wax hardened to ensure an even coating. Coating the chamber with halocarbon wax improved the signal by 300% over the plain stainless steel reactor and outperformed the teflon reactor. The results are shown in Figure 16. The results prove surface chemistry and mixing characteristics, left out of Cantrell's model are important.

Wall cleanliness is another factor in wall losses. Figure 17 shows a plot of the chain lengths using the formaldehyde decay method. After each time of the two times the reaction chamber was recoated with halocarbon wax, the chain length calculation increased to approximately the same level. The exact effects of wall contamination as a function of instrument running time is worth study to determine the necessity of recoating under different environmental conditions. A constant, and preferably calibrated field radical source would assist greatly in determining the need to recoat the reaction chamber. This, however, is not currently available.
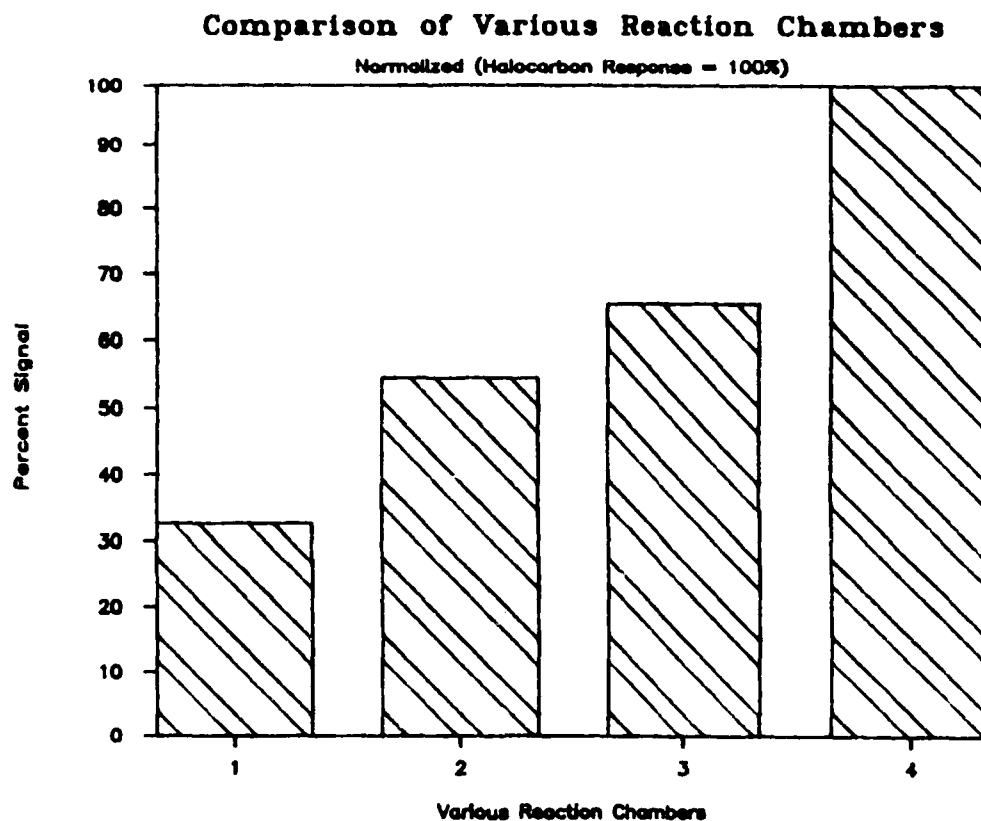
Figure 16. Comparison of reaction chambers. The signals recorded by different reactor chamber configurations were compared. The chambers were: (1) stainless steel chamber with no coating; (2) stainless steel chamber with H_3PO_4 coating; (3) adjustable section teflon chamber with one section; and (4) stainless steel chamber coated with halocarbon wax.
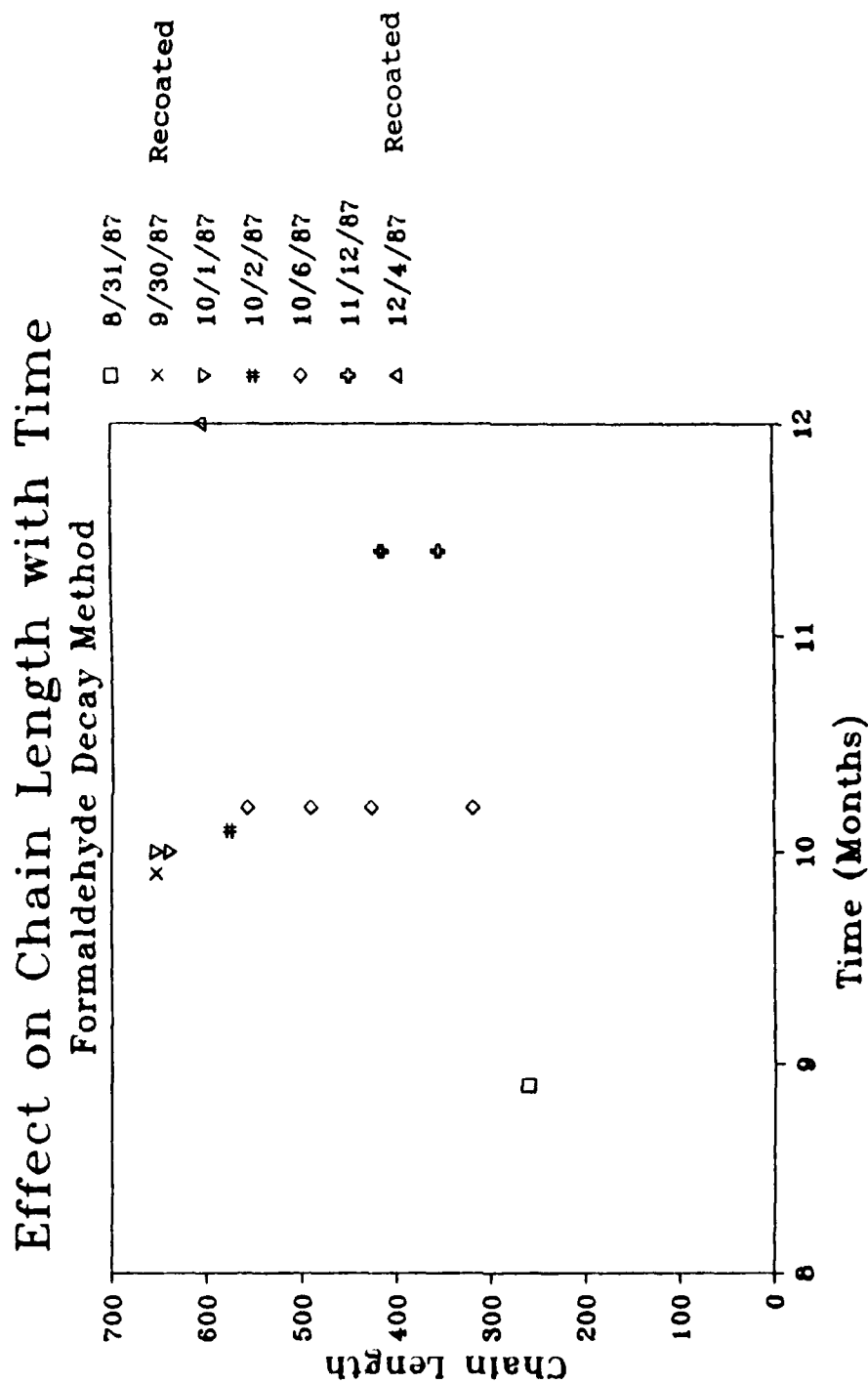
Figure 17. The effects of wall contamination. The performance of the PERCA instrument were regained after recoating the reaction chamber with halocarbon wax.

Zero-modulation

The phenomena referred to as "zero-modulation" is the presence of a modulation signal when we believe there are no radicals present to be measured. Zero-modulation is often made worse by a flow imbalance between the CO and N_2 channels. Prior instruments using stainless steel frits to control the gas flows had problems with zero-modulation and were unreliable. Also, any difference in pressure and flow rates can cause spiking, as well as a false positive signal, when the solenoids are activated switching the reagent gas flows. This false positive signal zero-modulation shows definite correlation to the background signal of the instrument and rises proportionally with the background signal. This is evidenced by injecting different calibration amounts of NO_2 from a calibration gas cylinder into a clean stream of air being sampled by the instrument. This effect is shown in Figure 18. Zero-modulation has made it difficult to quantify the detection limit of the instrument. In clean air (less than 1 ppb NO_2), the instrument easily detects a change of 1 ppb of signal relative to NO_2, but as the background signal levels increase, so does the zero-modulation noise. This zero-modulation can be effectively reduced to less than 10% of the background signal with careful attention to flow rates and pressures between the CO and N_2 channels and may be, in part, a true signal for radicals since our clean air source
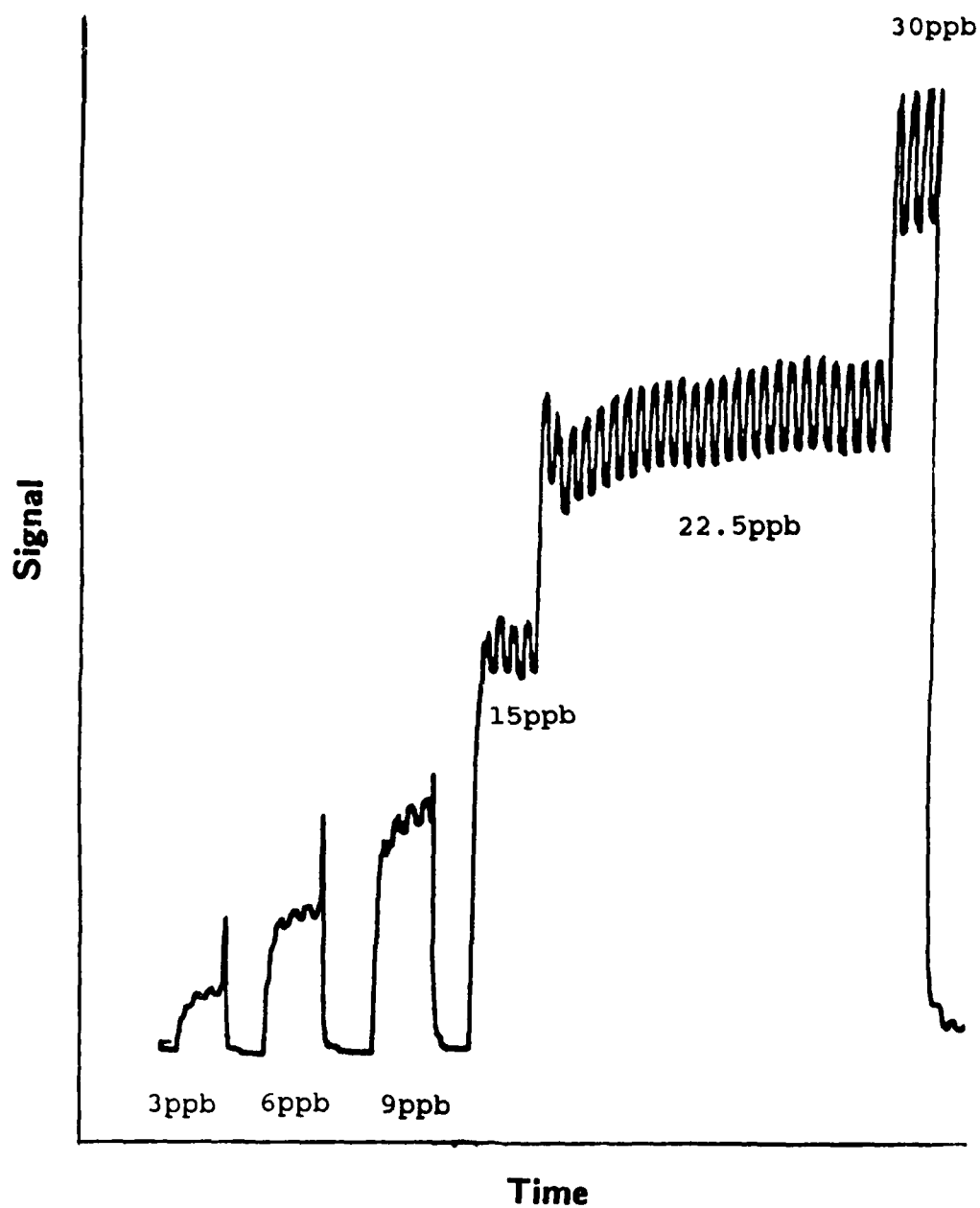
Figure 18. Zero-modulation. The effect of zero-modulation is shown by injecting different concentrations of NO_2 into the reaction chamber.

may indeed be not so clean. Since NO_2 absorbs light, experiments were conducted in the light and in complete darkness. The resulting zero-modulations were no different for the two different conditions.

A possible cause of zero-modulation is the formation of pernitric acid through the reaction:

$$NO_2 + HO_2 + M \rightarrow HO_2NO_2 + M$$
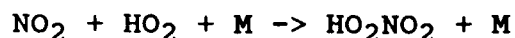
Since pernitric acid is very sticky, pernitric acid could form, stick to the reactor walls, leech off, and finally dissociate at its own leisure causing, zero-modulation.

Reagent Gas Concentrations and Chain Length

In addition to balancing the reagent gas flows, the concentrations of reagent gases in the reaction chamber are important for the proper performance of the instrument. NO is important not only as the reagent gas to be converted to NO_2 in the reaction $NO + HO_2 \rightarrow NO_2 + OH$, and the resultant NO_2 to be detected by the luminol instrument, but NO also has a direct effect on the sensitivity of the luminol instrument to NO_2.

NO inhibits the response of the luminol instrument to NO_2. Cantrell's model proposed that the NO_2 sensitivity followed the equation $S = 1/(1 + A[NO])$. A plot of experimental data and Cantrell's model (Figure 19) shows similarities. However, a comparison of plots of log signal vs. [NO] (Figure 20) and 1/signal vs. [NO] (Figure 21) reveals the decay in sensitivity is closer to being

PERCA Sensitivity

Signal Strength vs. NO Concentration
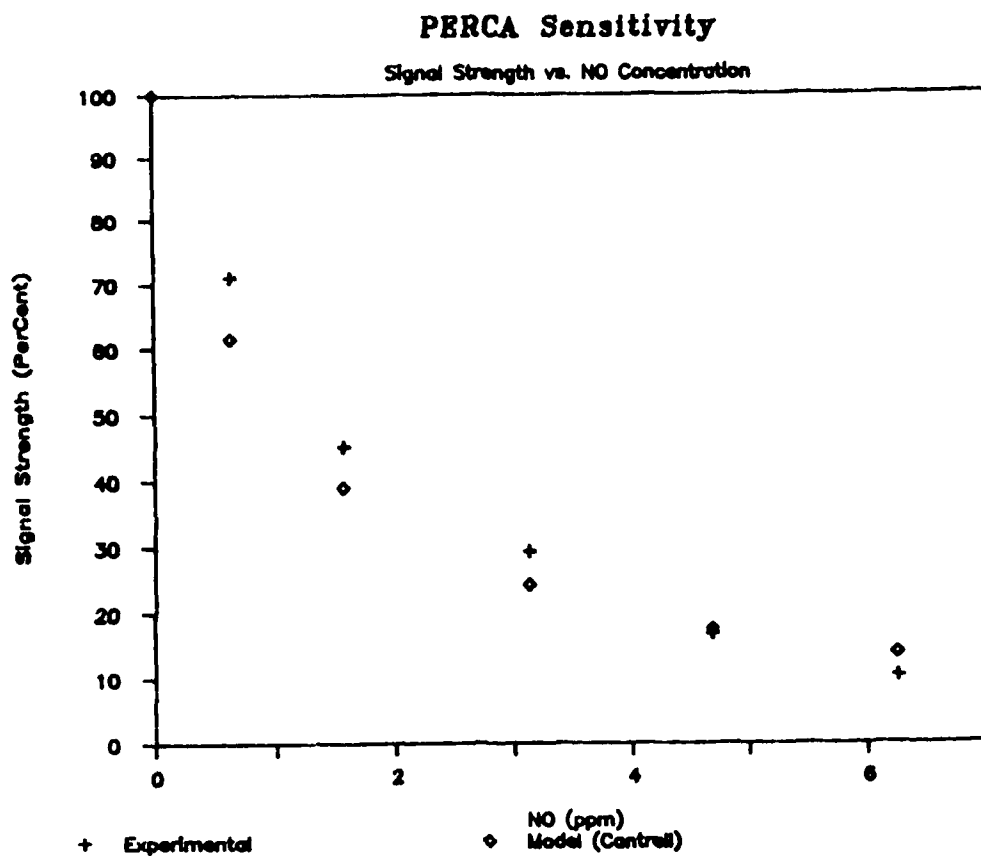
Figure 19.   The change in NO_2 sensitivity of the luminol instrument with added NO.   Both the actual and modelled sensitivity are shown.

PERCA Sensitivity

Log Signal Strength vs. [NO]
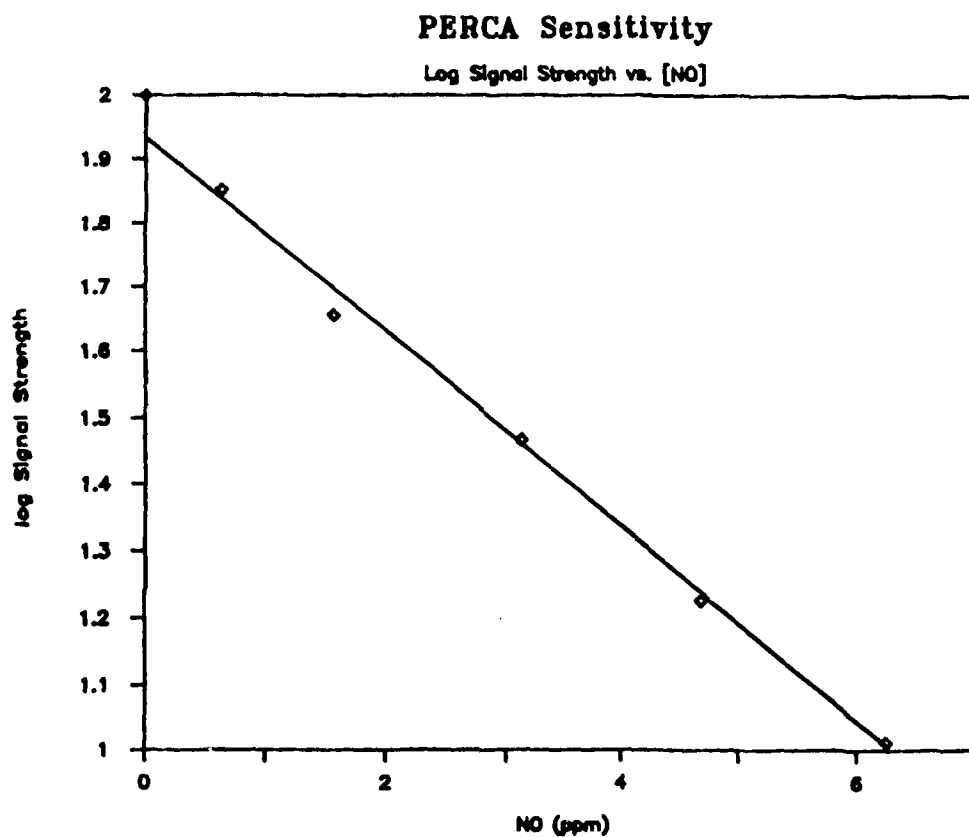
Figure 20. A log plot of the changing NO_2 sensitivity with added NO shows the dependence is exponential.

PERCA Sensitivity

1/Relative Signal Strenth vs. [NO]
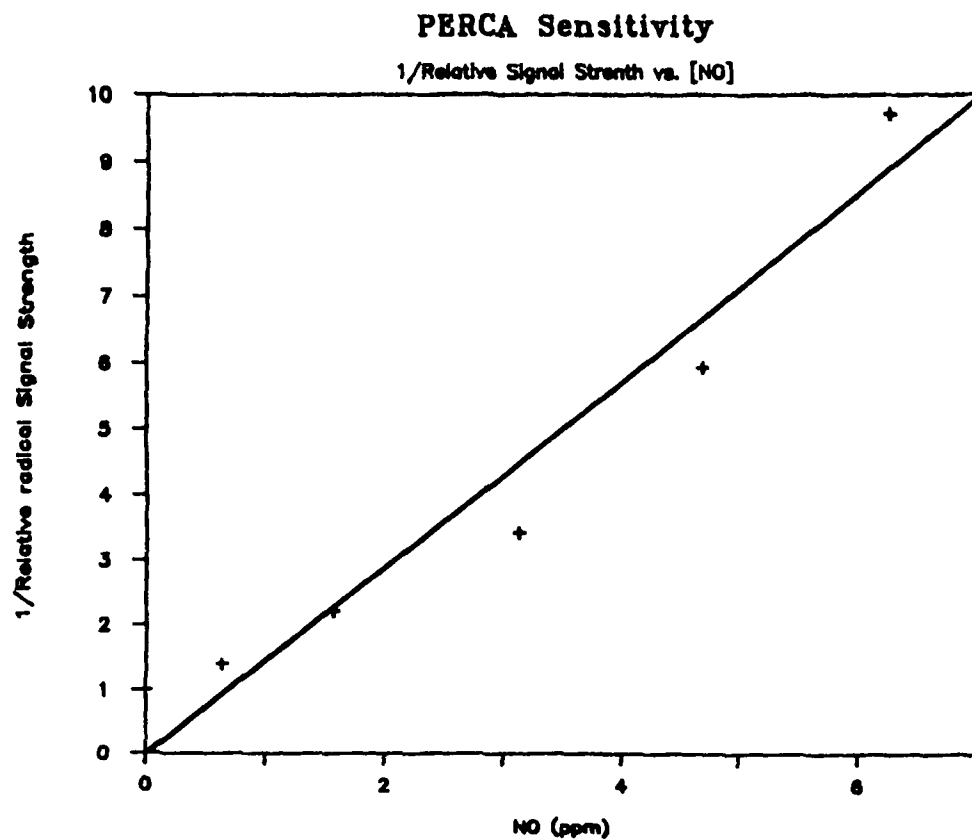
Figure 21. A plot of $1/NO_2$ sensitivity with added NO shows poor fit. Cantrell's model predicts a straight line.

exponential. A curve fitting routine (Asystant, MacMillan Software Company) in the form $Y = \exp(AX - B)$ gave the A value as -0.4 and the B value as 4.6, where Y is the relative signal strength and X is [NO] in ppm. The R^2 was 0.98. Although NO changes the luminol instrument's sensitivity to NO_2, it does not change the linearity of the response of the luminol instrument to NO_2 as shown in Figure 22.

Figure 4 showed Cantrell's model of the estimated chain lengths for various concentrations of NO and reaction times. The optimum NO concentration for a five second reaction time given by the halocarbon wax coated stainless steel reactor can be estimated to around 3 ppm. To insure the maximum chain length, the NO flow was adjusted with the instrument in front of a steady chlorine photolysis radical source (Figure 9) to observe the change in signal with changing NO concentrations. Figure 23 shows the raw data. The curve in Figure 24 rises to a peak and then decreases. The optimum signal occurred at NO concentrations of 3.5 ppm to 4.5 ppm. The same signal strength at 3.5 ppm and 4.5 ppm NO concentration means that although the instrument is becoming less sensitive to NO_2 as NO concentration increases from 3.5 to 4.5 ppm, the chain length is increasing to maintain the steady signal by creating more NO_2. At higher than 4.5 ppm concentration, the signal drops off, but the drop in signal may not be steeper than the changing sensitivity to NO_2 due
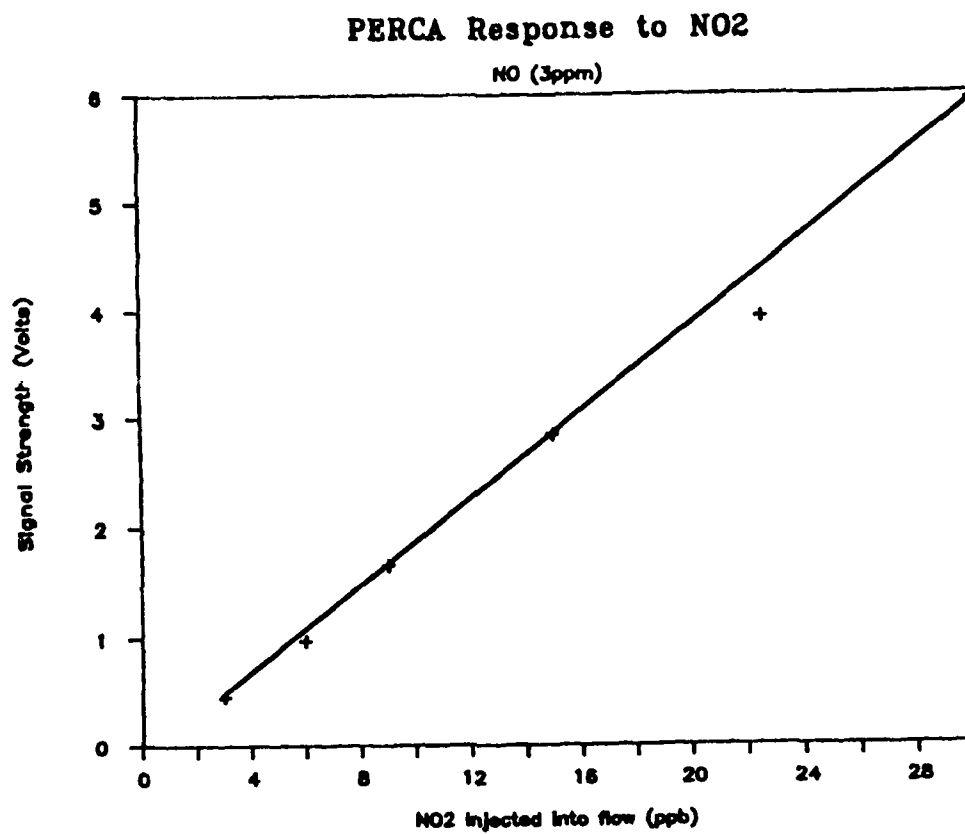
Figure 22. The PERCA's shows a linear response to NO_2 with 3ppm of added NO.
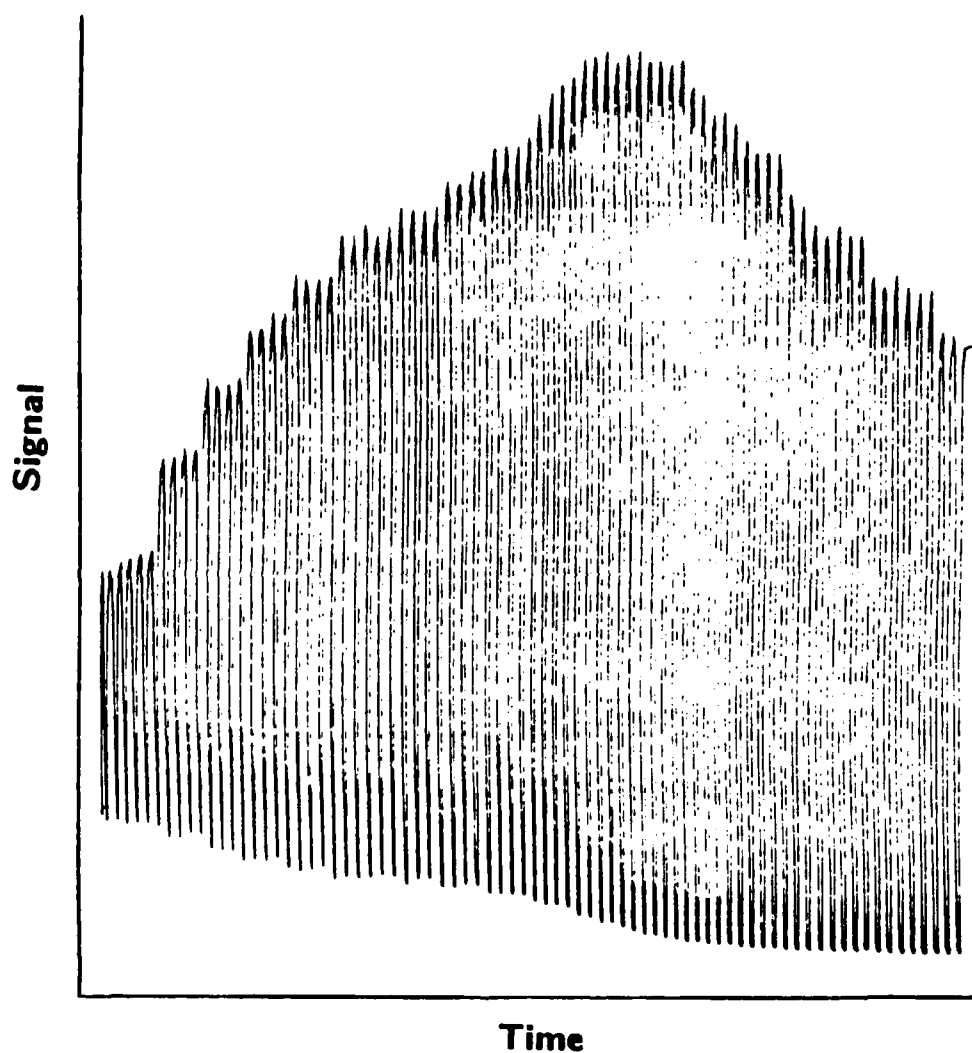
Figure 23. The actual variation in PERCA's response to a steady radical source with added NO. The decreasing baseline shows the depressed response to NO_2 while the increased modulated signal indicates increased chain lengths.

PERCA Sensitivity and NO

Radical Signal Strength vs. NO Conc
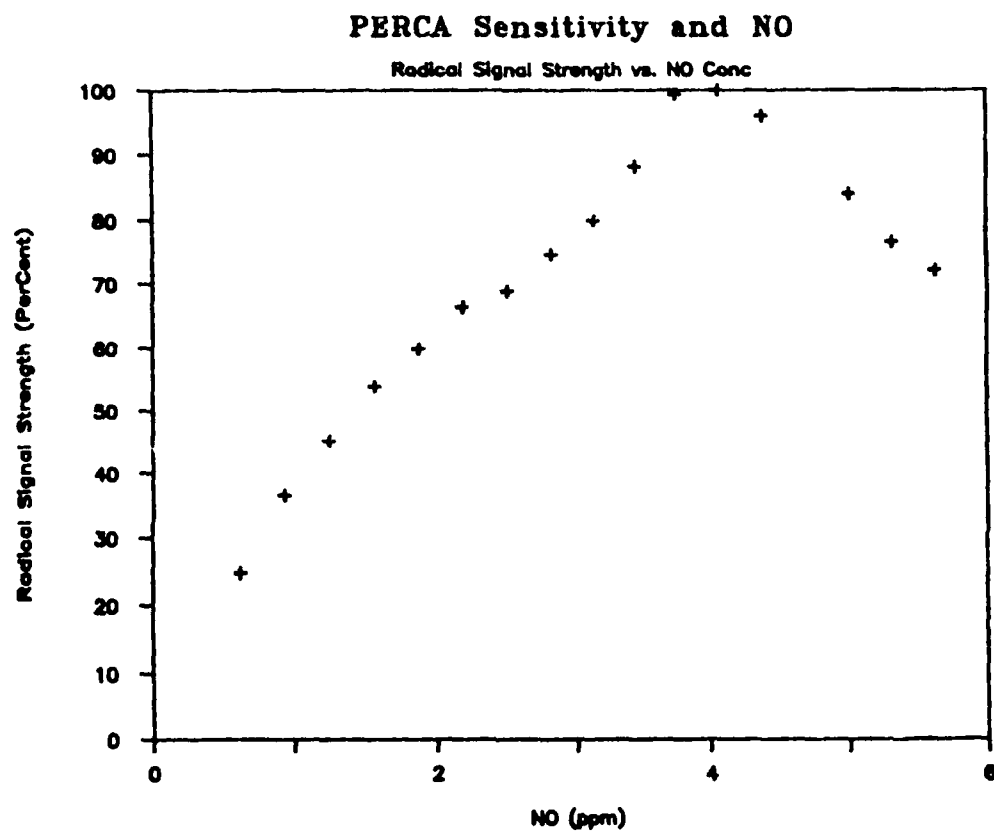
Figure 24. The plotted radical signal from sampling a steady radical source with changing concentrations of added NO. The peak signal is reached at 3.5-4.0 ppm NO.

to NO, thus the chain length may be found at a higher NO concentration than the NO concentration corresponding to the highest NO_2 signal. The optimum NO concentration to produce the highest chain length for this system was found by dividing the radical signal by the changing NO_2 sensitivity as a function of the NO concentration. Figure 25 shows the optimum NO concentration to be 5 ppm for the halocarbon coated stainless steel reactor.

CO is the chain carrier gas in the chemical amplification reaction $CO + OH \rightarrow CO_2 + H\cdot$ and is normally run at 10% (200ml/min) of the intake flow (2L/min). To assure the optimum CO concentration, different CO and balancing N_2 flows were used while monitoring a steady radical flow from the chlorine photolysis radical source. The results in Figure 26 show that changing the CO concentration from 7 to 15% has little effect on the system's performance. As long as there is an adequate amount (at least 7%), the CO concentration inside the halocarbon coated stainless steel reactor does not make a discernable impact.

Other Improvements

PERCA has benefited through improvements made to the luminol based NO_2 detector. Previous models of PERCA recirculated the luminol solution through the detector cell. Luminol can lose up to 30% of its sensitivity to NO_2 when recirculated. The system currently uses one-time through

PERCA Chain Length and NO

Radical Signal/NO2 Sensitivity vs. [NO]
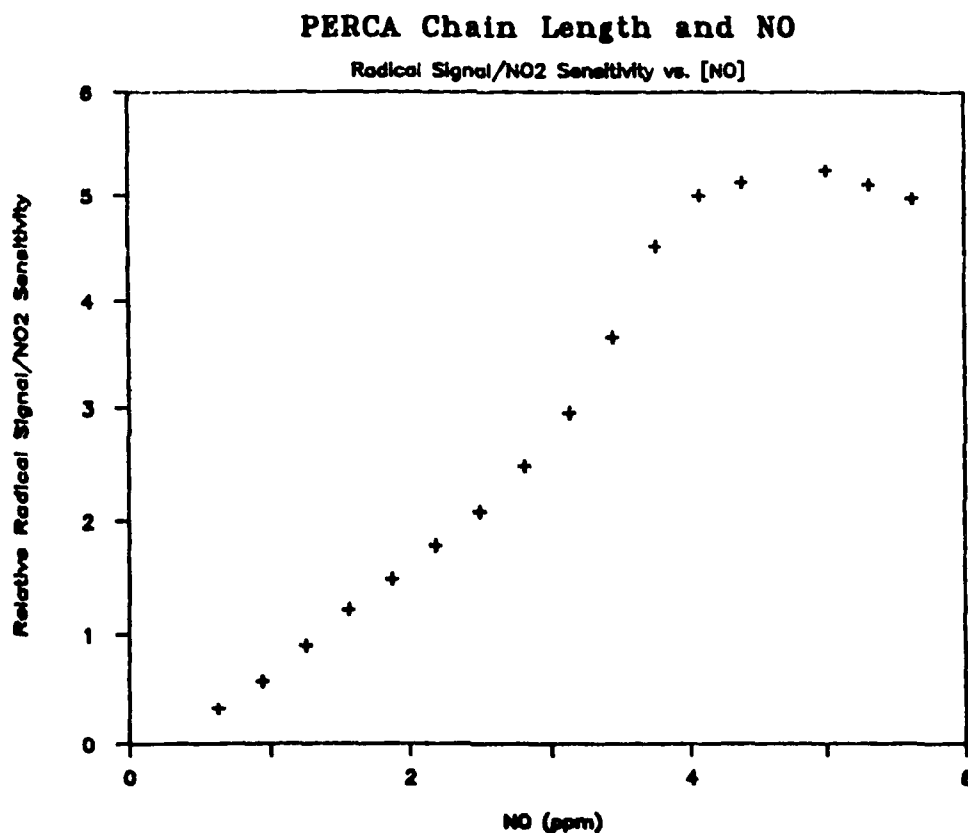
Figure 25. The radical signal divided by the NO_2 sensitivity with changing NO. The optimum chain length is found by dividing the radical signal by the NO_2 sensitivity to find the point where the largest number of NO_2 was produced. This value, 5.0ppm, is higher than the point where the signal is highest.

Radical Signal vs. CO Concentration
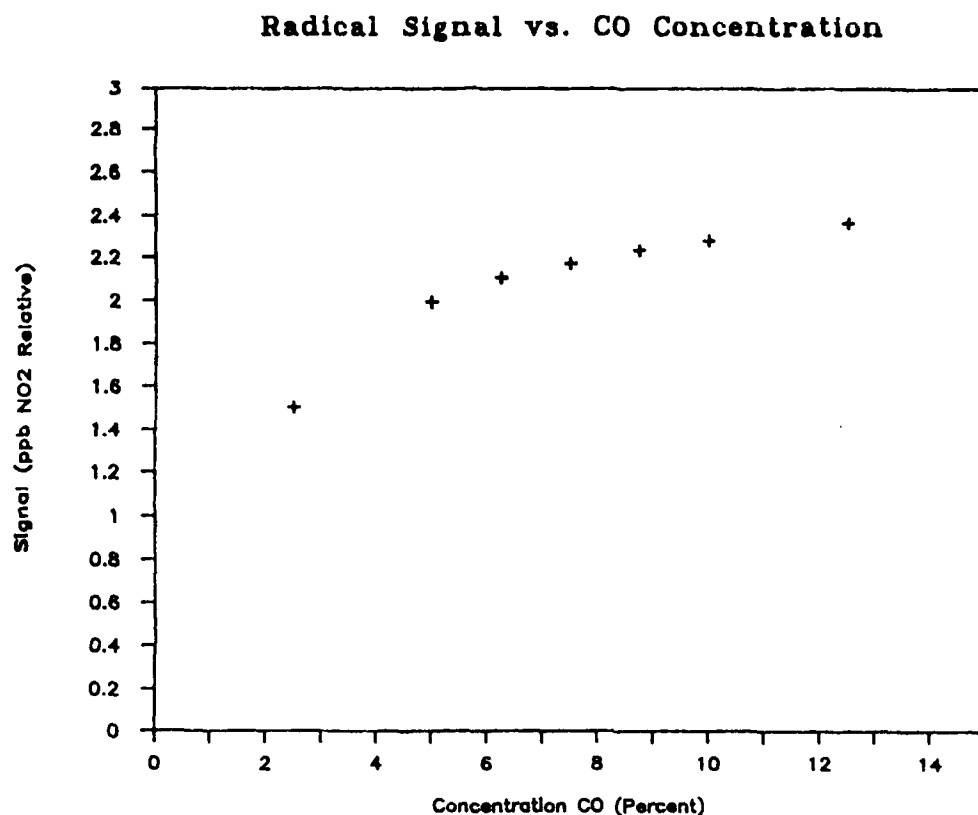
Figure 26.   The change in radical signal
observing a steady radical source with varing
concentrations of CO injected into the
reaction chamber.   The NO concentration was
3ppm.   The study was in agreement with Buhr's
findings [Buhr, 1986].

method for luminol. The linearity of the luminol solution's response to NO_2 which broke at 4 ppb has been improved by using t-butyl alcohol instead of methanol in the luminol solution. The instrument shows a linear response to NO_2 above 1 ppb to 10 ppm, a range of 4 orders of magnitude. The temperature dependent sensitivity of luminol solution has also been solved by Unisearch corporation based in Canada marketing Luminox LMA-3 instruments, a commercial version of our NO_2 detectors. Our laboratory plans to incorporate their temperature compensating circuit in the near future.

Chapter IV

Calibration

The ability to calibrate this instrument and quantify atmospheric free radical measurements would greatly enhance its usefulness. The ability of this instrument in detecting free radicals is undisputed. The chemistry of the involved reactions is well recognized, and when exposed to a known radical source, the PERCA detector responds without fail. Even without quantitative calibration, the instrument is a revealing tool in free radical chemistry. The system is able to distinguish the diurnal cycle of free radicals in clean atmospheres [Buhr, 1986], and can compare relative quantities from varying sources, as well as distinguish changes in free radical concentration from the sources. High resolution spectroscopy has revealed seasonal variations of OH radicals in the atmosphere [Burnett and Burnett, 1984]. PERCA could make similar contributions to the study of atmospheric chemistry even if uncalibrated but constant in chain length. Many different uses for the instrument are possible such as studying the diurnal and seasonal variations in free radical abundance even without definite quantitative calibration, but undoubtedly the PERCA system would be able to contribute much more if it could quantitatively measure atmospheric free radicals.

To calibrate the PERCA method, a two part procedure must be used. The instrument must be calibrated to a known NO_2 source and to a known radical source. Using the numbers provided from the calibrations, the chain length (the factor representing the number of NO_2 molecules produced by the introduction of a free radical) can be determined. With a defined chain length, the concentration of an unknown source of free radicals is determined by measuring the NO_2 signal and dividing it by the chain length.

Various methods have been tried to calibrate the PERCA instrument. All involve using the recombination rate of HO_2 with itself to discern the concentration of the radical source to find the chain length. Cantrell [1983] photolyzed a variety of constituents to produce HO_2 radicals to calibrate the system including H_2O, formaldehyde, Cl_2/H_2, and bottled air. The results of his photolysis methods produced erratic calculated chain lengths varying from 1 to 10,000. The last investigated method by Cantrell, and his most consistent, used air over hot wire in a flow tube which resulted in calculated chain lengths from 810 to 1320. Although it seems to be a very consistent method, it wasn't certain that only HO_2 chemistry was taking place in the flow tube thus making the method suspect. Buhr [1986] photolyzed Cl_2/H_2/air mixtures in a dynamic flow tube system and in a static teflon bag system. He reported chain length from the methods varied from 40 to 1016. Buhr found the static bag

decay method was consistent with figures from 800 to 1016, but prone to contamination. His results from the flow tube method were erratic, with calculated chain length ranging from 40 to 776. With all the calibration methods tried, it is apparent that creating radicals is not the problem, but the difficulty is in knowing the type and amount of radicals produced by the different methods, and eliminating unwanted reactions. The methods investigated for this report were dynamic Cl_2/H_2/air flow tube photolysis, static Cl_2/H_2/air photolysis bag decay, water electrolysis, and static formaldehyde photolysis followed by free radical decay in the dark.

Dynamic Chlorine/Hydrogen/Air Photolysis

The chlorine/hydrogen/air flow tube system was first developed in regard to research for PERCA as a steady source of free radicals. HO_2 radicals are produced in this flow tube system by the following mechanism:

Cl_2 + hv (320nm) --> 2 Cl·

Cl + H_2 --> HCl + H·

H + O_2 + M --> HO_2 + M
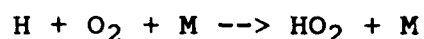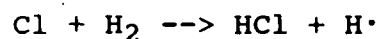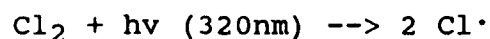
As a steady free radical source, the method currently has no equal and continues to be our method of choice for such applications. Figure 10 showed a sample output from a chlorine/hydrogen/air free radical source.

The calibration for the chain length in the flow tube system is based on the assumption that the chemical pathway inside the flow tube system is as follows:

$$Cl_2 \xrightarrow{\;j\;} 2\ Cl \tag{1}$$

$$Cl\cdot + H_2 \xrightarrow{\;k1\;} HCl + H\cdot \tag{2}$$

$$H\cdot + O_2 \xrightarrow{\;k2\;} HO_2 \tag{3}$$

$$2HO_2 \xrightarrow{\;k3\;} H_2O_2 + O_2 \tag{4}$$
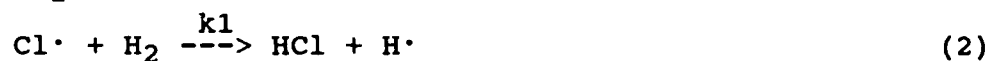
Then the following equations hold true.

$$\frac{d[Cl]}{dt} = 2j[Cl_2] - k_1[Cl\cdot][H_2] = 0 \tag{5}$$

$$\frac{d[H]}{dt} = k_1[Cl\cdot][H_2] - k_2[H\cdot][O_2] = 0 \tag{6}$$

$$\frac{d[HO_2]}{dt} = k_2[H\cdot][O_2] - 2k_3[HO_2]^2 \tag{7}$$

For the initial region when chlorine is injected into the photolysis tube, $2k_3[HO_2]^2$ is assumed negligible. Then

$$\frac{d[HO_2]}{dt} = k_2[H\cdot][O_2] = k_1[Cl\cdot][H_2] = 2j[Cl_2] \tag{8}$$

Integrating terms gives:

$$\text{change in } [HO_2] = 2j[Cl_2] \times \text{change in time} \tag{9}$$

therefore the initial slope in the flow tube equals $2j[Cl_2]$.

For the steady state:

$$\frac{d[HO_2]}{dt} = 0 = 2j[Cl_2] - 2k_3[HO_2]^2 = 0$$

$$[HO_2]^2 = \frac{j[Cl_2]}{k_3} \tag{10}$$

Since the chain length equals $[NO_2]/[HO_2]$, combining the chain length with equation (9) gives:

$$\frac{\text{Change in } ([NO_2]/\text{Chain length})}{\text{Change in time}} = 2j[Cl_2] \tag{11}$$

Substituting chain length into equation (10) gives:

$$CL^2 = \frac{k_3[NO_2]^2}{j[Cl_2]} \qquad (12)$$

Combining equation (9) and (12) gives:

$$\text{Chain Length} = \frac{2k_3[NO_2]^2 \text{ at steady state}}{\text{Initial Slope}} \qquad (13)$$

Calibrations using dynamic chlorine photolysis systems have not been successful. **Cantrell** [1983] abandoned the method due to irreproducible data, and attributed the erratic behavior to an interfering reaction between HO_2 and Cl_2. **Buhr,** [1986] also experienced irreproducible data, but attributed it to poor mixing in the flow tube. Our efforts attempted to reduce the problems suffered by Cantrell and Buhr.

The first chlorine/hydrogen/air dynamic flow tube setup is shown in Figure 27. Additional emphasis was made in cleaning the carrier air and hydrogen prior to reacting it with the injected chlorine to reduce the unwanted reactions in the flow tube. Additional clean up was thought necessary because ambient air without hydrogen flowing into the system created a higher radical signal than when hydrogen was injected into the photolysis system. Having the radical signal initially drop when hydrogen was injected showed that the reaction of chlorine with hydrogen was indeed the dominating reaction when hydrogen was present, but also showed the potential for side reactions. The first phase of clean up was cleaning the carrier air. The carrier air was
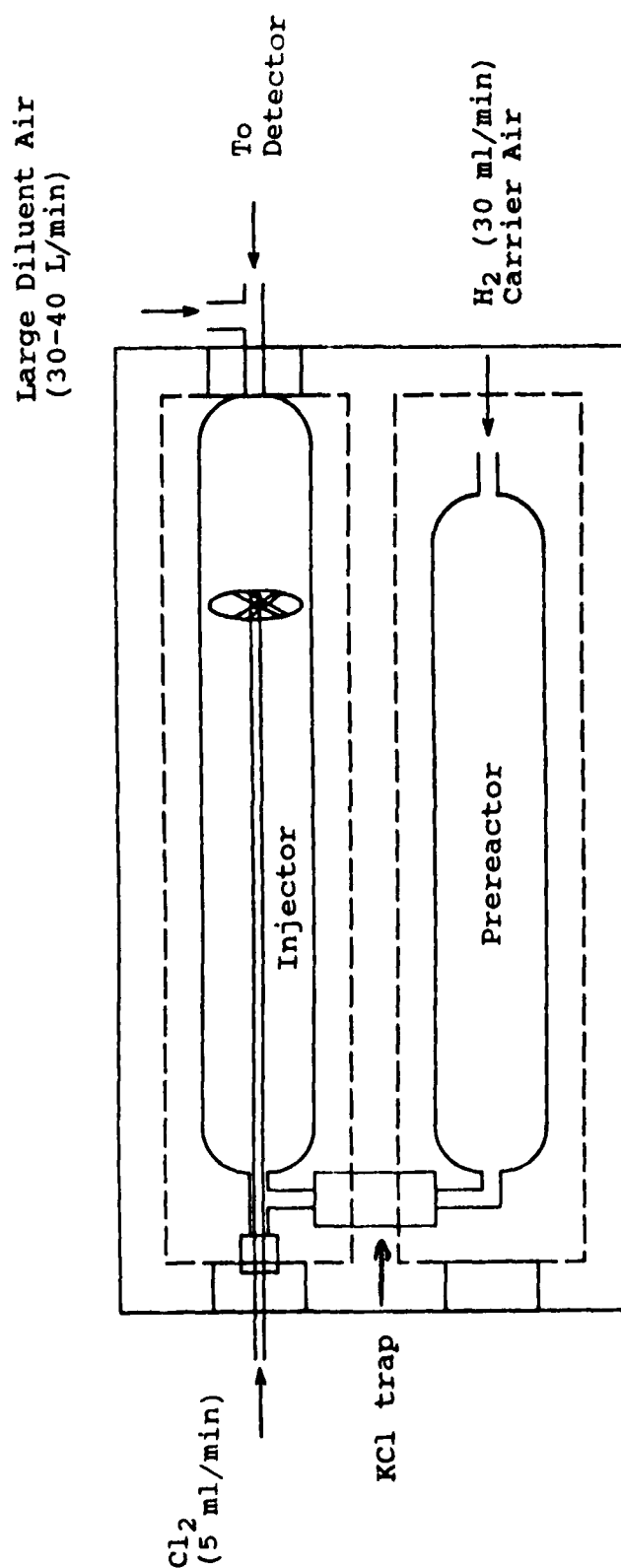
Figure 27. Chlorine photolysis flow tube calibrator with clean up prereactor for the carrier air and hydrogen. The chain length was derived by comparing the slope of the radical signal when injecting the chlorine at different points in the final flow tube with the radical signal at steady state.

passed through activated charcoal to remove hydrocarbons, NO_x, and water, ascarite to remove CO_2, Purafill to remove CO, and finally a heated trap (400 C) containing Pt on Al_2O_3 to further remove hydrocarbons. The second phase involved using a pre-reactor to clean the hydrogen and carrier air. The carrier air normally set at 2 L/min and hydrogen (Linde CP) at 30ml/min was introduced in a premixture flow tube (1 1/2 inch diameter glass) and subjected to photolysis under a bank of two GE black lights rich in 320nm radiation. The air and hydrogen mixture was then passed through a KCl trap to remove radicals [**Baldwin et al.**, 1984] into the main photolysis tube where 0.1% chlorine (Linde) was injected into the stream. Three attempts at calibration yielded chain lengths of 116, 263, and 1920 (Table I). Figure 28 shows the signal in ppb NO_2 relative as the Cl_2 injector was moved to different intervals to calculate intial slope and steady state concentrations. Since the different chain lengths were gained at different carrier air flow settings, the mixing characteristics were suspect. The next efforts were to enhance the mixing characteristics of the flow tube.

To provide better mixing, yet insure a proper steady state signal, the flow tube arrangement in Figure 29 was used. The prereactor scheme was discarded and hydrocarbon free air (Linde) passed through Purafill, Dryrite, and the heated trap was used as the carrier gas. The steady state signal was reached by injecting chlorine in the larger

Table I

Chain length with $Cl_2/H_2/air$ photolysis

==

First Flow Tube

date	SS NO_2 Signal	air flow (liters)	Chain Length
3/18/87	150	2	486
4/2/87	240	2	1920
	166	4	263
	173	6	116

Second Flow Tube

date	SS NO_2 Signal	air flow (liters)	Chain Length
5/1/87	33	2	70
5/11/87	36	2	51
	33	2	68
	66	2	85
5/12/87	60	2	93
6/1/87	132	4	157
8/7/87*	50	2	90
	56	2	90

* flow tube coated with halocarbon wax

Static bag Decay

date	Starting ppb signal (relative to NO_2)	Chain Length
5/26/87	1040	26
	1500	100

==

H2 Calibration

11 may 87
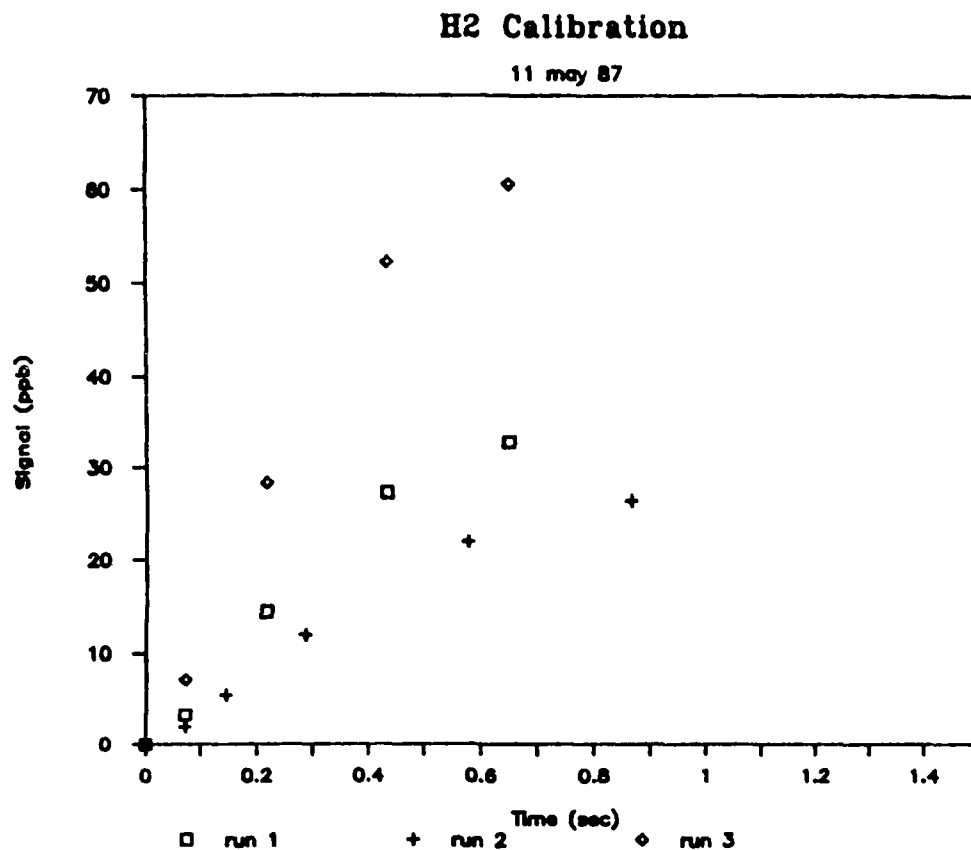
Figure 28. Signal recorded by changing the chlorine injection point in the chlorine flow tube calibrator. The runs were made with the following carrier air flows: (run 1) 2 L/min; (run 2) 4 L/min; and (run 3) 6 L/min.
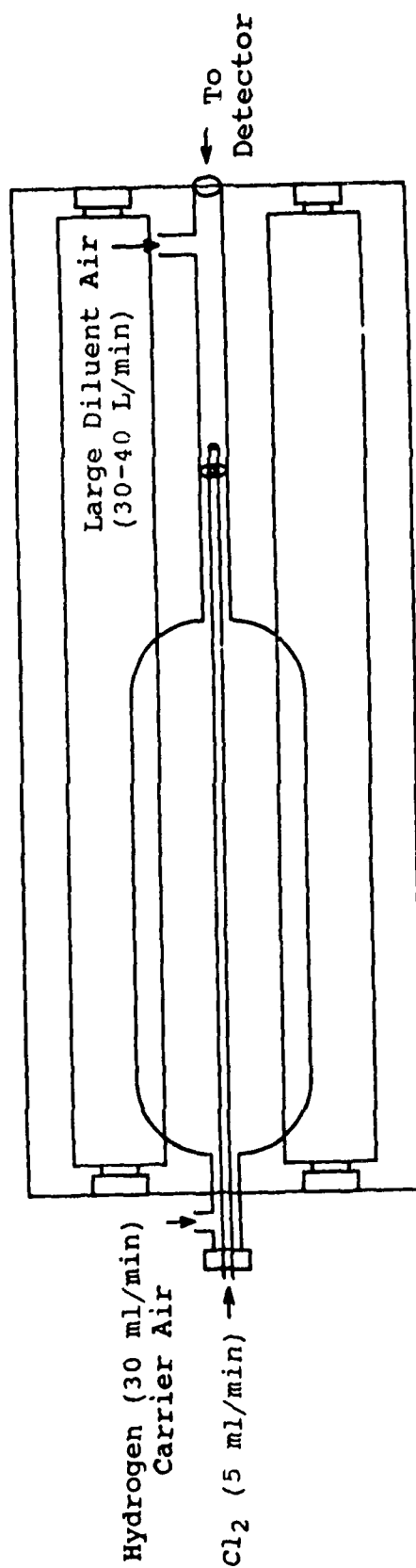
Figure 29. Ballooning chlorine photolysis flow tube calibrator. The different diameter sections emphasized different areas of chlorine photolysis. The larger portion provided a definite steady state signal and the narrower diameter tube provided the initial slope.

portion of the tube, and the initial slope was provided by injecting chlorine at different intervals in the smaller 11 mm od region. The chain lengths provided using this method were fairly consistent ranging from 51 to 157 (Table I). The chain length figures, however, were disappointingly low, so the inner surface of the flow tube was coated with halocarbon wax (Halocarbon Products Corp.) to reduce wall reactions. The chain length figure did not improve and was calculated to be 90.

Our model of the flow tube chemistry shown in equations (1) through (4) may be too simplistic. Other pathways for the direct reaction with HO_2 and Cl exist, and are pressure dependent [Cattell and Cox, 1986]. Also others using the chlorine photolysis method use higher O_2 pressure (>300 torr) to sucessfully compete with the reaction $H + Cl_2 \rightarrow Cl + HCl$, and high H_2 pressures (>100 torr) to prevent $Cl + HO_2 \rightarrow HCl + O_2$ from interfering [Sanders et al., 1982]. Currently the chlorine photolysis flow tube method is not yet perfected. Increasing the O_2 and H_2 pressure in the current flow system may improve its characteristics. Unfortunately, increasing the O_2 and H_2 pressures will cause safety problems due to the 4% explosion limit for H_2 mixture, but a flow tube designed with safety considerations in mind to handle the higher O_2 and H_2 concentrations may prove to be an excellent calibration method for the PERCA method.

Static Chlorine/Hydrogen/Air Photolysis

Since the chlorine photolysis flow tube method of calibration is currently suspect, the chlorine, hydrogen, and air bag photolysis method outlined by Buhr was tried to confirm the results. The radicals were generated in an identical method as in the dynamic flow tube system, but the calibration was done by observing the decay of HO_2 through HO_2 recombination. The decay may be described by the equation:

$$-d[HO_2]/dt = 2k[HO_2]^2$$

where k is the HO_2 recombination rate. Substituting the relationship:

$$[HO_2] = ([NO_2]/ \text{ chain length})$$

into the above equation and integrating gives:

$$1/[NO_2] = [2k/(\text{chain length})] \text{ x change in time}$$

The chain length is found by plotting $1/[NO_2]$ versus time and finding the slope and using the equation:

$$\text{Chain Length} = 2k/slope$$

The principal assumptions are that the radicals are HO_2 and the decay is dominated by the HO_2 recombination to form H_2O_2 and oxygen [Buhr, 1986].

The procedure began by suspending a 500L teflon bag from the ceiling and filling it with a mixture of hydrogen (0.6%), chlorine (10ppmv), and hydrocarbon free air. The gases in the bag were mixed by a small, continuously functioning, fan. The bag was sampled through a half inch

polypropylene Swagelok fitting attatched to the bag wall. Room overhead fluorescent lights were replaced with 4 GE black lights to provide the near 300nm radiation for photolysis. The PERCA detector was set on the CO channel and the black lights turned on until the bag had reached steady state. The lights in the entire room were then turned off and the decay in signal measured on a chart recorder. After the initial decay region (usually 2 minutes), the detector was then turned to the N_2 channel to find the background baseline for determination of the decay rate. All attempts with this method, including attempts using a new bag in case of bag contamination, failed to produce second order decays shown by a comparison plots of 1/signal versus time and log signal versus time in Figure 30. The decay is clearly exponential first order decay. Chain lengths calculated by this method were 25 and 100 (Table I) which were consistent with the latest chlorine photolysis flow tube method, but are highly suspect since the kinetics were incorrect. The same problems which plagued the flow tube method are likely causing non-second order decay in the static chlorine photolysis bag decay method. Another added problem may be that since so much NO is converted to NO_2 in this method, the luminol detector's sensitivity to NO_2 may change during the decay. The changing of NO concentration in the reaction chamber makes the decay curve difficult to interpret with non-linear NO_2

Chlorine Photolysis Bag Decay

Comparison of 1/Signal and log (Signal)
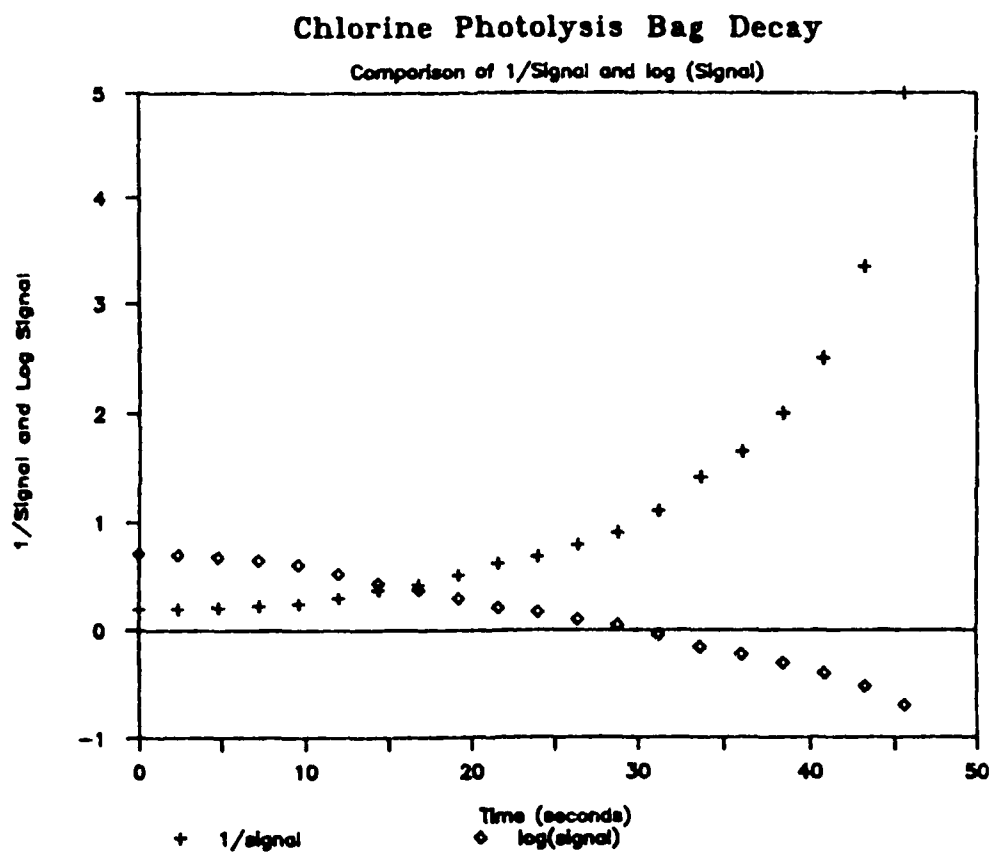
Figure 30. Comparison of 1/signal and log signal from chlorine photolysis bag decay. Neither plot was very straight showing neither first nor second order decays.

response by the luminol detector. Attempts at calibration using this method should use lower radical densities to insure proper response of the luminol detector. Starting steady state NO_2 signals around 100ppbv would be the ideal starting point for the decays.

H_2O Electrolysis

A direct determination of the chain length was tried using H_2O electrolysis by Lars-Johan Jansson of ADA Technologies. Water was electrolyzed in a sealed 100 ml polypropylene bottle equiped with platinum electrodes and two openings fitted for Swagelok fittings. Only 80ml of deionized water was put inside the bottle to allow a small gas capture area above the water. A small amount of NaCl was added as the electrolyte. The hydrogen radical produced by the electrolysis of water should combine with oxygen and become an HO_2 radical. A small flow of air mixed with NO to combine with OH radicals to make NO_2 was passed over the water and then to the luminol based NO_2 detector. Figure 31 describes the system's NO_2 output with no CO amplification and 4L dilution air at various current levels. It is apparent that this system converts NO to NO_2 very well. After a steady stream of NO_2 was detected, CO, the chain carrier was introduced into the air stream. The resulting rise in signal divided by the original signal gave a direct chain length calculation. The numbers provided in the experiment ranged from 46 to 350 for a chain length using

Radical Signal vs. Cell Air Flow
Water Electrolysis Method
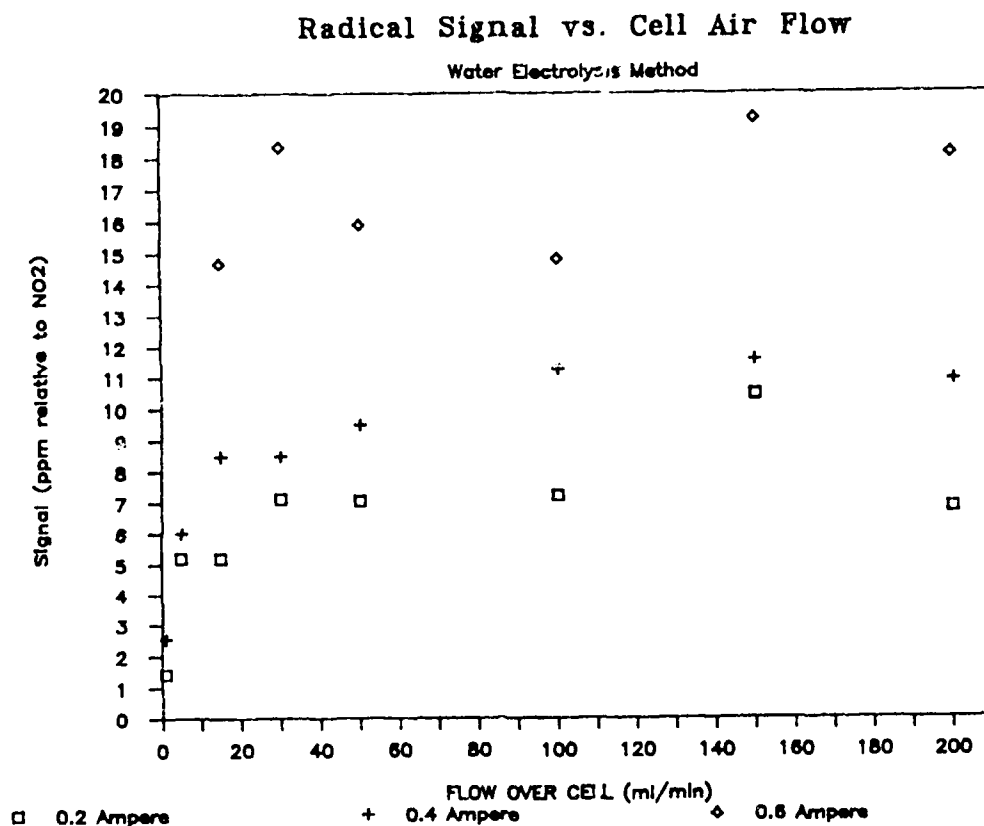
Figure 31. NO_2 signal produced from water electrolysis. Carrier air containing NO was passed over electrolyzed water at different flows and the NO_2 signal detected. This is a direct measurement of the OH radicals produced by the system assuming each OH converts an NO molecule to NO_2.

t h a teflon Swagelok Tee and the stainless steel reactor at different voltage settings (Figure 32). The chain lengths decrease with increasing electrolysis cell voltage possibly because the larger concentrations of radicals take other faster pathways than the CO chain reaction. These experiments showed that the chain length calculated by the chlorine photolysis methods were indeed too low. It is, however, difficult to discern the highest chain length possible with the system since a low concentration of radicals is difficult to produce with this method. Another factor which still has to be resolved with this method is the effect of humidity. The actual perturbation of humidity on the system in this particular calibration was undetermined and required more research, some of which is described later.

Static Formaldehyde Photolysis

The calibration method which showed the most promise was the static formaldehyde photolysis bag decay method. The method was adapted from the HO_2 calibration method used by Dr. Hard and his research group at Portland State University (Portland, Oregon) for their FAGE measurements of HO_2 [Hard et al., 1984]. HO_2 radicals are created in formaldehyde photolysis by the following reactions:

$CH_2O + hv \rightarrow HCO + H$

$H + O_2 + M \rightarrow HO_2 + M$

$HCO + O_2 \rightarrow HO_2 + CO$

Chain Length vs. Volts

Water Electrolysis Method
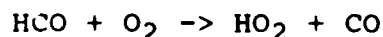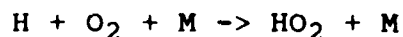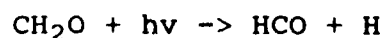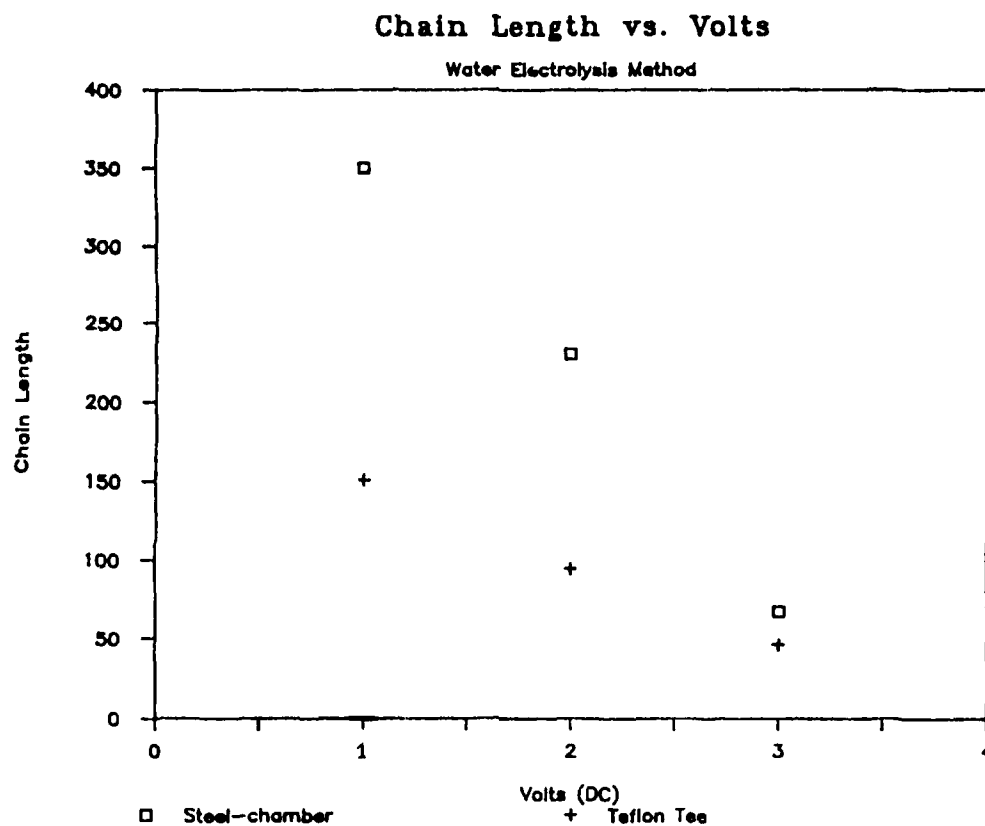
Figure 32. Chain lengths vs. volts. The chain lengths were calculatd by dividing the signal recorded from passing carrier air with NO and CO promoting the chain reaction with the signal recorded from passing carrier air with only NO though the water electrolysis source.

HO_2 radicals have been shown to be a major product of formaldehyde photolysis in the presence of air [**Calvert et al.**, 1972; **Horowitz et al.**, 1978]. The chain length is derived in the same manner as the static $Cl_2/H_2/air$ photolysis bag decay method, by turning out all lights, after a steady signal is observed.

The first formaldehyde photolysis trials attempted to use the same apparatus used in the chlorine/hydrogen/air photolysis bag decays, but no appreciable radical signal was detected. More light was apparently required for formaldehyde photolysis. A setup with more black lights was arranged. The method involved filling a 500L teflon bag with air filtered through activated charcoal, ascarite, and purafil. Then to provide the formaldehyde, 75ml of air was bubbled through formaldehyde (Fisher) 37.7% in aqueous solution with up to 10% methanol as preservative. Absorbances at 280nm were used in a preliminary experiment to quantify the exact concentration, but the effort failed (Appendix B). The mixture was thoroughly mixed with the small fan inside the bag. The bag was then photolyzed using twelve GE black lights in a half shell configuration with the bag suspended above the half shell. The rate of decay was observed as previously discussed in the bag chlorine photolysis method.

Decay profiles were observed leaving the mixing fan operating and not operating. Whether the fan was on or off

made no difference in the decay curves. The formaldehyde decay method consistently produced approximately the same chain lengths (Table II) as long as the initial NO_2 concentration reading of radicals at steady state was above 50 ppb. Below 50 ppb, a plot of $1/[NO_2]$ produces a poor second order decay plot shown in Figure 33. Calibration with steady state NO_2 readings above 50 ppb consistently gave a closer fit shown in Figure 34 giving a second order decay curve. The static formaldehye photolysis bag decay method was further confirmed through a second PERCA instrument (ADA Technologies) sampling the same bag and getting nearly the same consistent results. The disparity between the results may have occurred due to different NO_2 calibration factors between the two instruments.

Possible interferences from the addition of methanol to the luminol instrument's sensitivity to NO_2 were checked and found negligible. Luminol has been shown to increase in sensitivity to NO_2 due to the presence of alcohol [Cantrell, 1983]. Possible changes in sensitivity of the luminol instrument to NO_2, with the addition of the formaldehyde solution in the bag, were checked by first filling the 500L teflon bag with air and a known concentration of NO_2 and checking the luminol instruments response to the present NO_2. Then the formaldehyde solution was added while continuing to monitor the NO_2 signal. The presence of the formaldehyde solution showed no change in the sensitivity of

Table II

Chain Lengths with the Static CH_2O
Photolysis Bag Decays

===

Our PERCA Instrument

date	Starting ppb Signal (relative to NO_2)	Chain Length
8/31/87*	182	261
9/30/87**	480	653
10/1/87	144	653
	182	638
10/2/87	10	12
	16	36
	35	147
	98	576
10/6/87	76	490
	116	557
	116	426
	120	319
11/12/87	49	354
	48	414
	49	415
12/4/87**	112	605

ADA Technologies PERCA Instrument

date	Starting ppb Signal (relative to NO_2)	Chain Length
11/12/87	68	521
	65	499
	94	526

===

*   accomplished after Oregon field trip
**   reaction chamber recoated with halocarbon wax

First run formaldehyde decay — 10/2/87
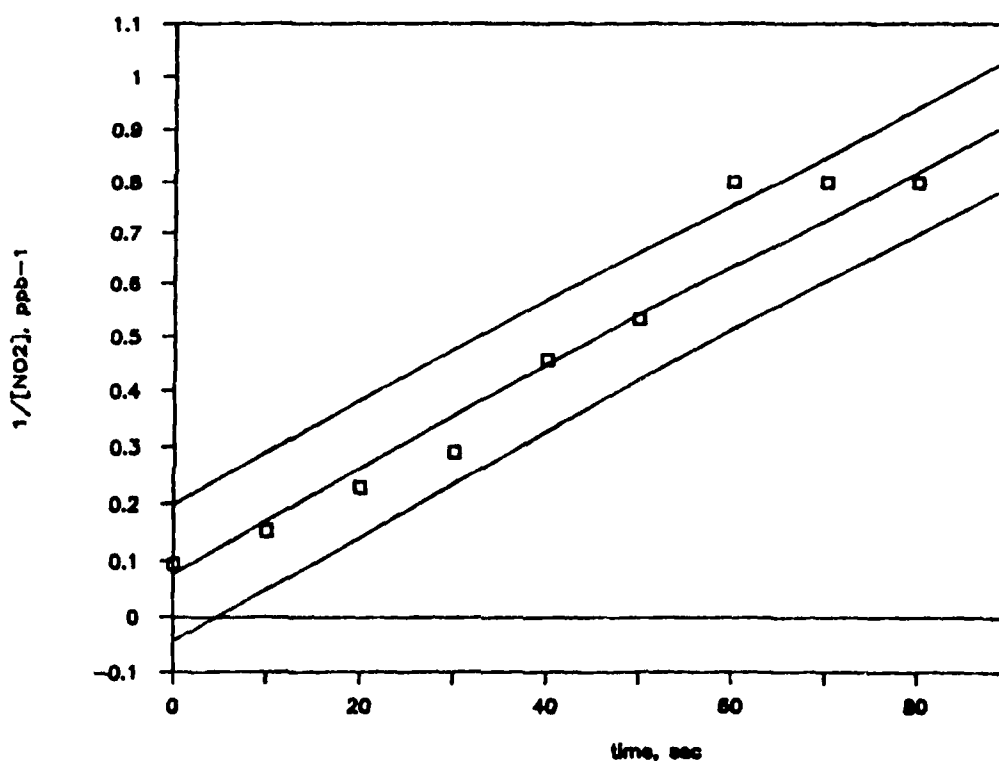
Figure 33. 1/signal of formaldehyde decay vs. time with initial steady state signal <50ppb. The plot of 1/signal with time is linear for a second order decay. Formaldehyde decays with initial starting signals <50ppb relative to NO_2 showed poor second order decay characteristics. The least mean squared line is plotted with the lines on either side representing a range of 1.5 standard deviations.

First run formaldehyde decay — 10/01/87
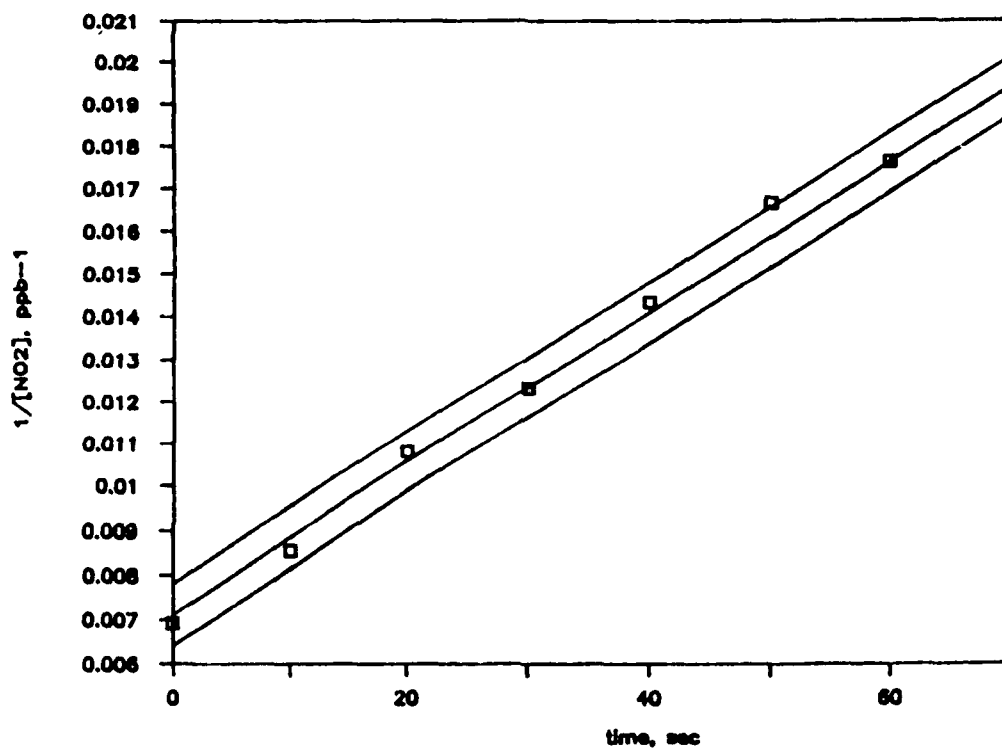
Figure 34. 1/signal of formaldehyde decay with initial steady state signal >50ppb. Formaldehyde decays with initial starting signals >50ppb relative to NO_2 showed good second order decay characteristics. The least mean squared line is plotted with the lines on either side representing a range of 1.5 standard deviations.

the luminol detector. This was expected since we had already introduced t-butyl alcohol in the original luminol solution.

Chapter V

Field Experiments

Two field studies were conducted during the summer of 1987. The first, in June, was to participate in the Southern California Air Quality Study (SCAQS) to determine if the PERCA method would work in polluted tropospheric conditions near Claremont, California. The second was an intercomparison study with the Fluroescence Assay with Gas Expansion (FAGE) method of LIF used at Portland State University conducted on the coast of Oregon. Although the actual data collected during the field trips were disappointing in terms of measuring free radicals, the data pointed out particular areas that required attention.

Southern California Air Quality Study (SCAQS)

We were invited to participate in SCAQS conducted throughout the summer of 1987. SCAQS was an especially appealing program since over 200 investigators from all over the world were participating to provide modelling data on the tropospheric photochemical chemistry as pollution rolled across the Los Angeles area basin. Our group planned to investigate ambient free radicals, PAN, and nitric acid.

The SCAQS plan was to have at least fourteen intensive days. Intensive days were defined as days when the meteorological conditions produced high concentrations of

photochemical smog during which time all participants would take data. The 8 week summer study gained data on a wide range of atmospheric constituents to provide the atmospheric modellers with as much ambient data as possible. A repeat study was scheduled during the winter months with the same motives. We did not attend the winter segment.

There were five sites for the SCAQS studies. Our site was in Claremont, California. Our equipment was set up on a 5 foot high sampling platform on the campuses of Claremont Colleges in a parking lot next to a recently resodded soccer field (figure 35). Since the wind normally blew in from the west, our equipment was set up to sample from the west. Although our group sampled throughout the two weeks we participated, June of 1987 happened to be an unusually clean summer for Claremont. There were only two intensive days during our two week stay, and the program was later postponed for 2 weeks and ended up continuing in August due to the lack of smog in Claremont.

During the two weeks we sampled at Claremont, two major interferences became apparent. They were background and humidity. The background signals during polluted episodes were greater than any past field studies. Over 1 ppm of background relative to NO_2 was noted on the worst pollution day (Figure 36) effectively swamping out any possible radical signal through zero-modulation. It is possible to account for 60 percent of the background due to O_3, NO_2, and
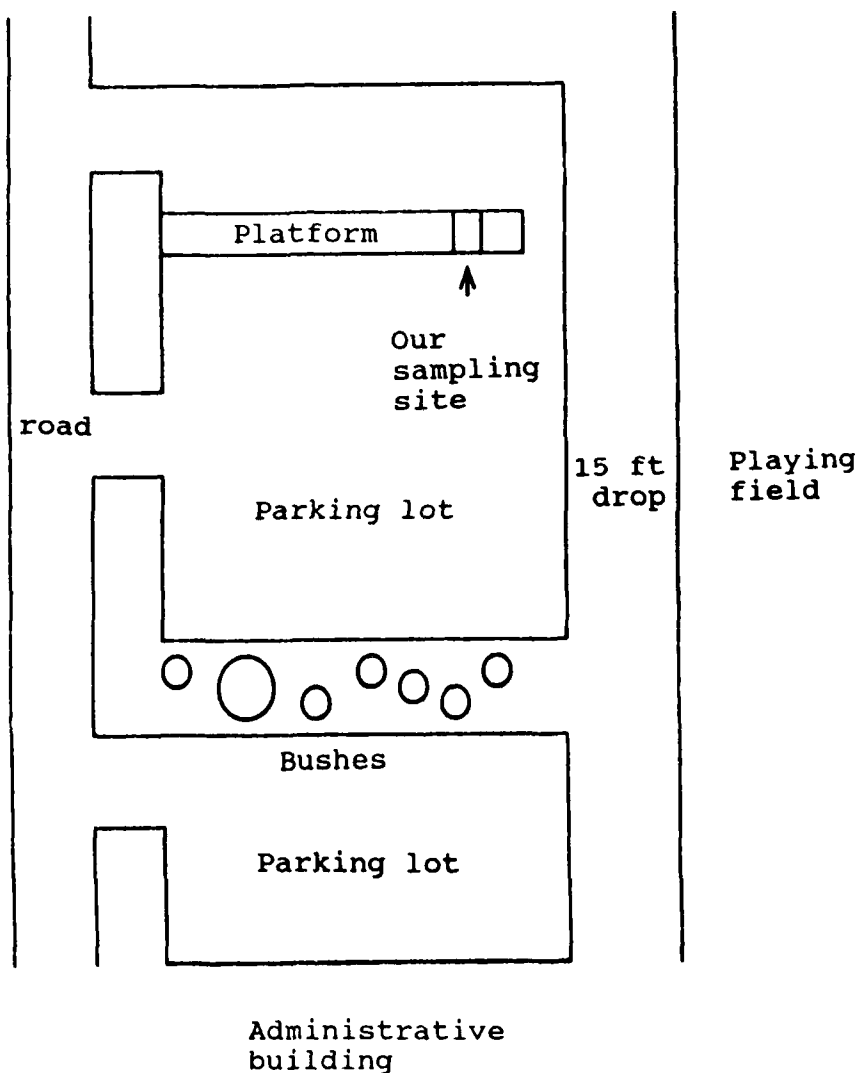
Figure 35. Southern California Air Quality Study (SCAQS) sampling site at Claremont Colleges. The four foot high sampling platform was located in a parking lot north of an administrative building and adjacent to a newly sodded playing field that was spray irrigated regularly.

Background Signal on June 24, 1987
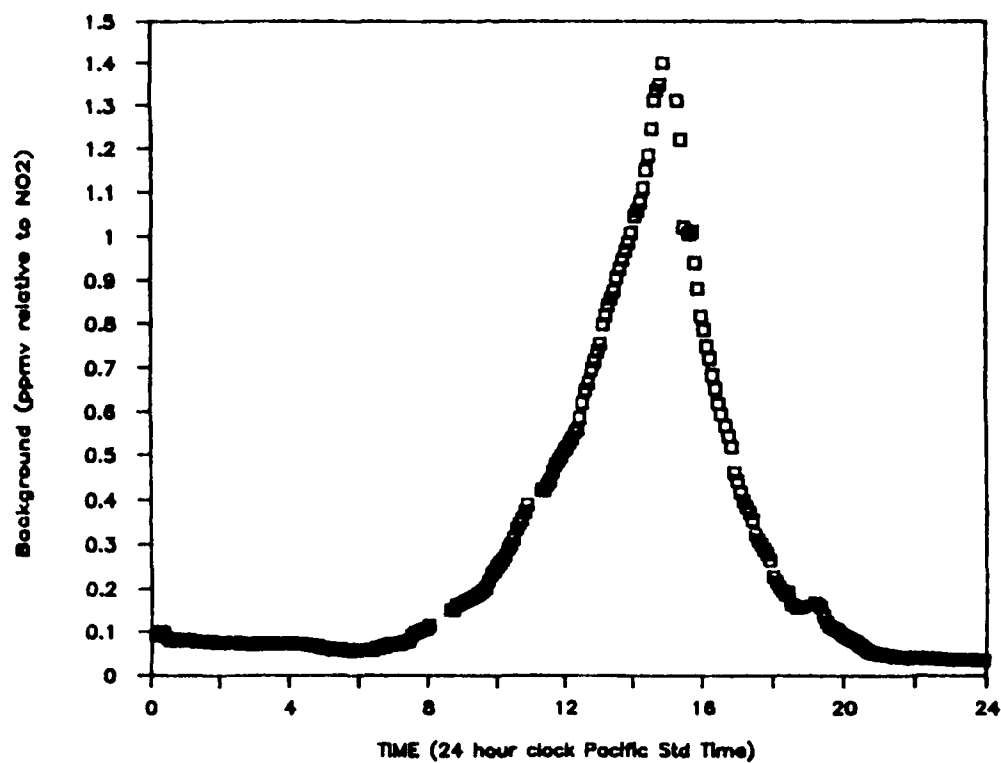
Figure 36.   Background signal relative to NO_2 on June 24, 1987.   The original theory of the background signal being the collective signal of ambient NO_2, PAN, and ozone could only account for 60 percent of the background signal.

PAN present during the episode, but the rest of the background signal cannot be accounted for according to the present knowledge of the instrument. Originally, we thought that it might be a temperature dependent phenomenon. The temperature at times reached above 30° C during the early afternoon when the sun was at its zenith and we thought that the NO present in the system was converting to NO_2 on the stainless steel reactor due to the increased temperature. An experiment was performed to confirm this hypothesis.

While sampling ambient air, the reactor was slowly heated and cooled to see the effect on the background signal level. The reactor was heated from ambient room temperature of 21° C to 34° C. There was no observed increase in background due to the temperature and there was no decrease as the reactor cooled. Another phenomenon is the culprit of the high background signal and will require further research.

Possible explanations for the unaccounted 40% of the background include a dependence of the background signal on the radical signal, and other atmospheric constituents capable of inducing a response in the luminol instrument. The instrument senses radicals by converting NO to NO_2 through a chain reaction that is modulated over a one minute period. In the polluted Claremont air where a lot of free radical species may be present, a dynamic equilibrium of newly produced NO_2 and NO_2 produced in previous CO cycles

occurs in the reaction chamber. The reaction chamber was designed for maximum mixing and not flow-through characteristics. The flow inside the chamber may retain swirling pockets of NO_2 slowly mixing with the new air to create the background signal. This hypothesis is based on the fact that when the UV lights are illuminated on the chlorine photolysis radical source, the radical modulation starts and the background goes up. When the UV light is subsequently turned off, the background goes down. This may account for the large background signals observed in Claremont.

Other atmospheric constituents beside O_3, PAN, and NO_2 that may elicit a response in the luminol detector and subsquently raise the background include SO_2, H_2O_2 and other oxidizers. SO_2 reported later in the text has been shown to carry the chain reaction used in the PERCA method under laboratory conditions at ppbv concentrations, and could be an interfering species in polluted air.

The second plaguing observation was the humidity. The observation platform was next to a newly resodded soccer field and the field was frequently spray irrigated. When the water was sprayed on June 11, 1987 (Figures 37 and 38), the background and radical signals went down with the radical signal becoming erratic during the periods of great changes. The spraying water caused the relative humidity in the area to jump from 30 to 75%, and evaporating droplets of

Background signal on June 11, 1987
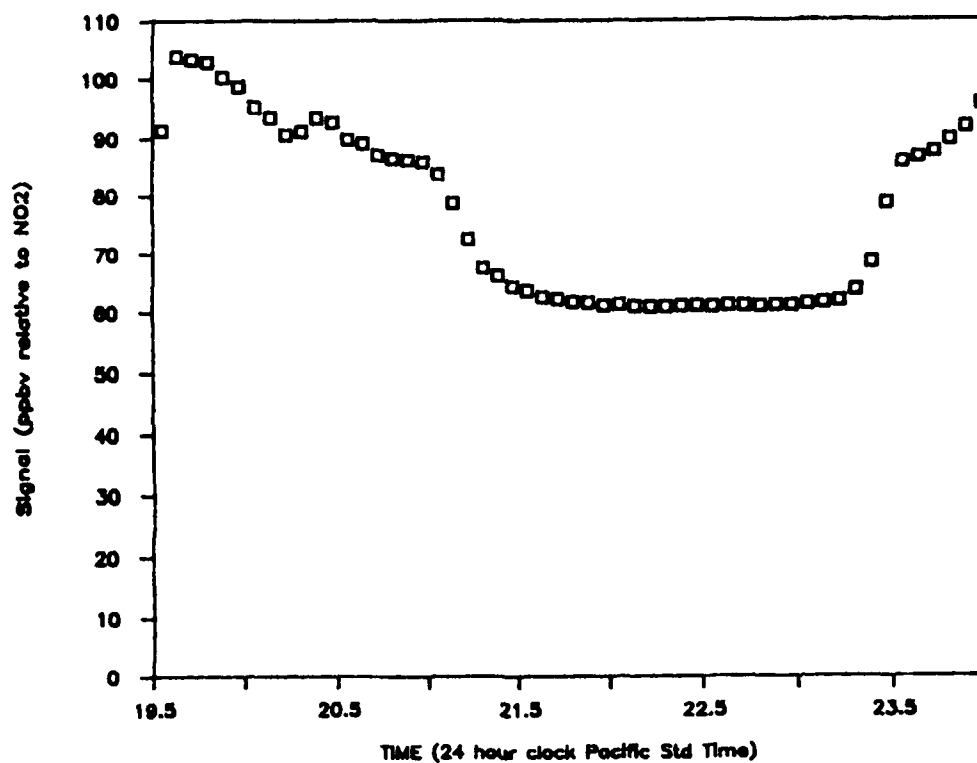
Figure 37. Background signal relative to NO_2 on June 11, 1987 showing the deleterious effect of spray irrigation on the background signal.

ROx signal on June 11, 1987
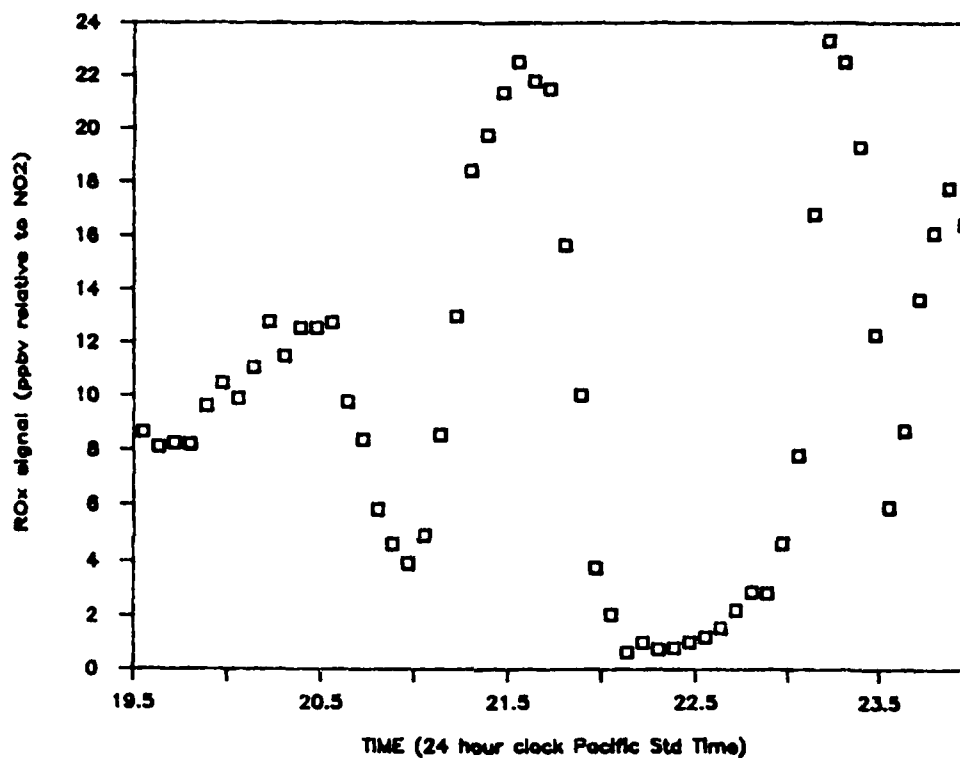
Figure 38. RO_x signal relative to NO_2 on June
11, 1987. The true RO_x concentration could be
calculated by dividing the NO_2 signal by the
chain length.   An exact chain length was
unavailable and the data is reported in NO_2
signal. The spray irrigation between 20-2400
hours produced erratic RO_x signals.

water were also present in the air (The humidity data was received from the GM research van).

Another minor but bothersome factor in the studies was that the luminol solution changed its sensitivity with the temperature. Hourly calibrations from a heated (40° C) permeation NO_2 source for a typical twenty-four hour period are presented in Figure 39. Although the luminol was shaded and covered with alumninum foil, the exposure to the environment and the resulting changing sensitivity made the data harder to interpret.

Portland State University Intercomparison

An intercomparison study between Portland State University's FAGE (Fluorescence Assay with Gas Expansion) method for HO_2 and our instrument was conducted from August 23 to August 27, 1987. The location of the comparison was a site at Lincoln City on the Oregon coast. The site was about 200 feet from the high water mark at the beach on a parking lot at the north side of town. One hundred feet directly north was the Shiloh Inn resort. Both instruments were inside an air conditioned motor home with site power being provided by a city 120V AC hookup. The FAGE instrument's intake was on the roof, and our instrument intake was placed on a three foot high platform on the south side of the motor home with the reactor facing the Pacific ocean (figure 40). Our instrument's reaction chamber was placed inside an aluminum covered cinder block with adequate

variations in calibration of 100ppb NO2
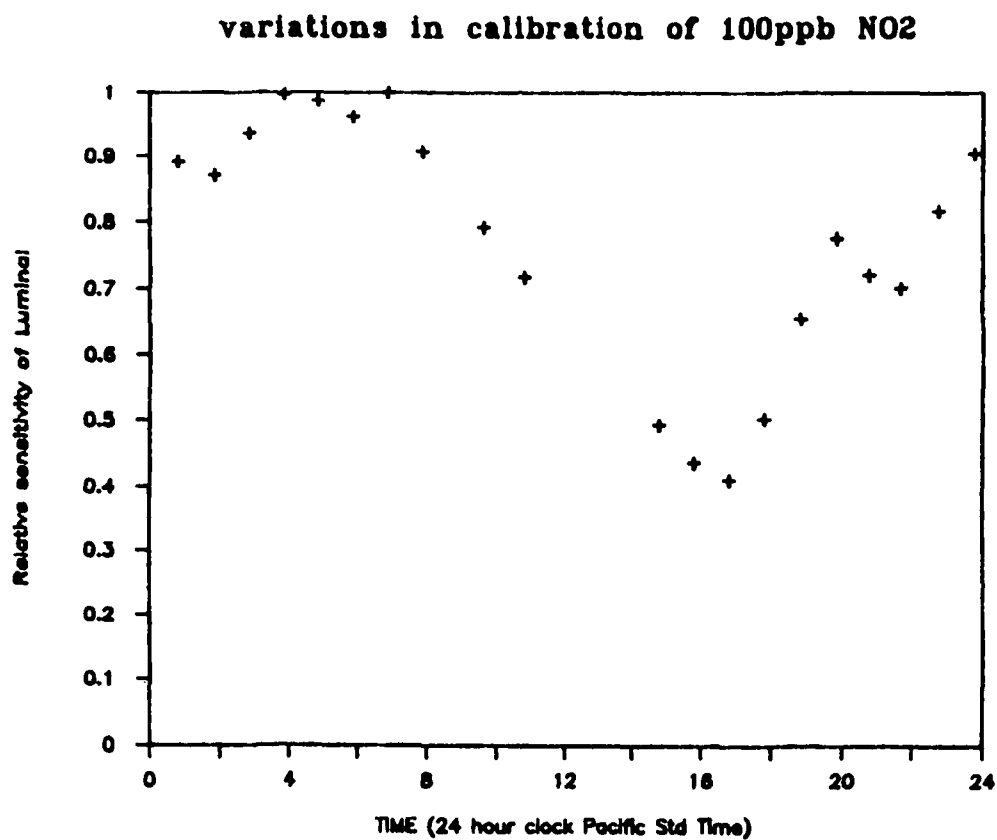
Figure 39. Changing luminol sensitivity to NO$_2$ with temperature. Luminol lost sensitivity to NO$_2$ as temperatures increased, creating a cycling calibration curve.

Beach
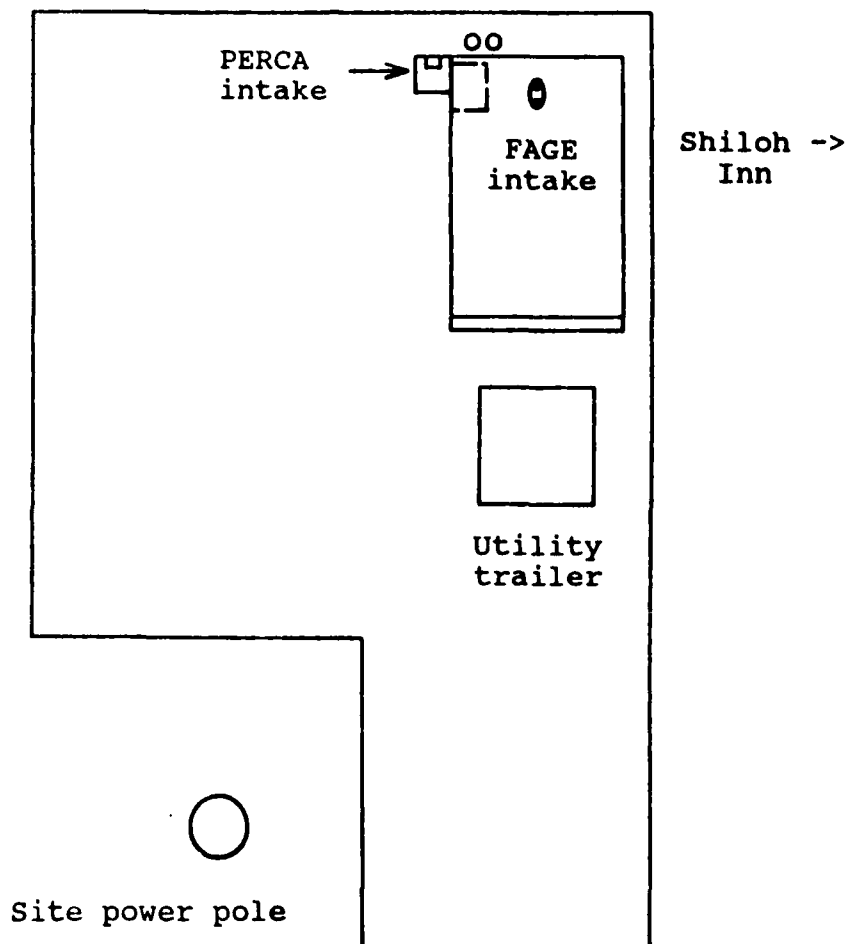
Figure 40. Oregon coast sampling site. The site was a parking lot at the beach in Lincoln city. The instruments were housed in an air-conditioned RV with the PERCA reaction chamber outside by the instrument. The FAGE instrument sampled from the roof while PERCA sampled from the west on a three foot high platform.

room around the chamber to provide ventilation. This arrangement ensured a relatively constant temperature range for the reactor as the wind was constantly blowing. The normal direction of the wind was from the west, but occasionally the wind would shift out from the northwest.

Since the instrument was kept at a constant temperature and the reactor cell also kept at a relatively constant temperature, there were no cyclic swings in the luminol solution's sensitivity to NO_2. The instrument was calibrated for NO_2 with a heated NO_2 permeation source, and data collected.

Critical factors in this study were the humidity and sea salt. Fog was a very common occurance on the Oregon coast. Each time fog appeared, the instrument performed poorly. The data from the August 27, 1987 shown in figure 41 shows poor data from midnight until almost noon. This is because until noon, dense fog was present. Figure 42 shows the day's UV intensity. FAGE also showed small concentrations of HO_2 until the sun appeared, but their data in Figure 43 showed a continual rise while PERCA did not. Humidity also presented the FAGE instrument problems in erratic negative reading in fog, but their instrument registered HO_2 in small concentrations when UV reading went up while our instrument did not work properly until the fog had dissipated.

ROx Signal August 27, 1987

ppt calculated using chain length 261
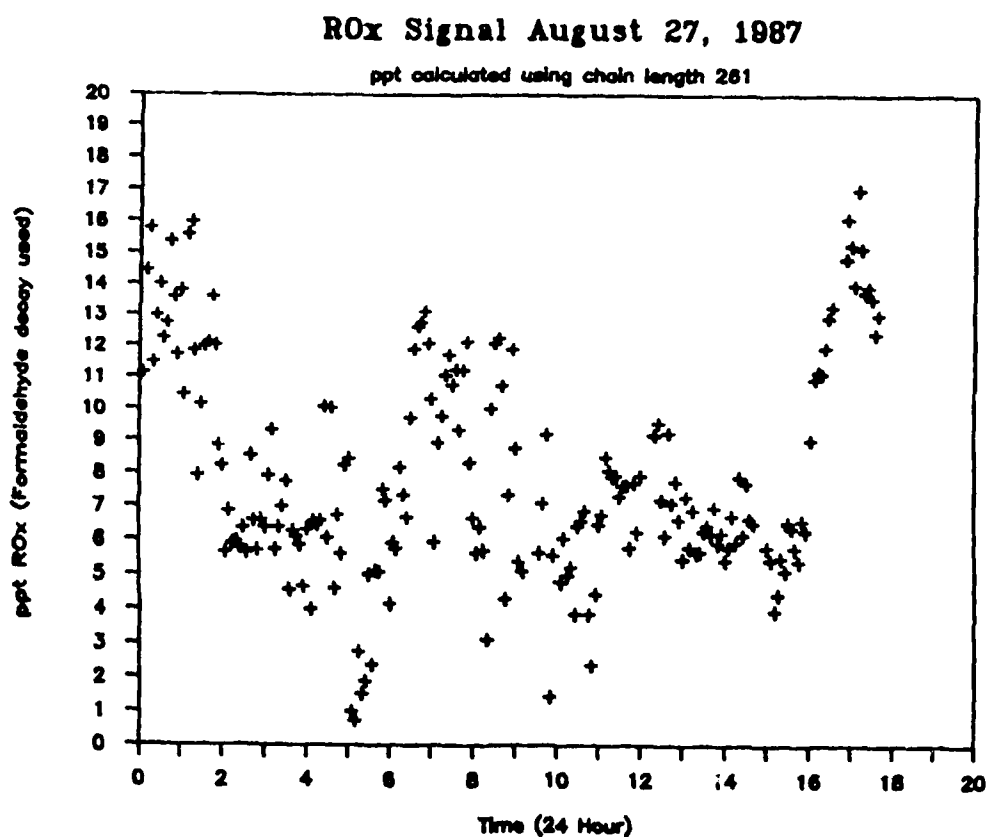
Figure 41. PERCA RO_x data recorded August 27, 1987. Fog was a common occurance on the Oregon coast. On the 27th, the RO_x signal was erratic until the fog dissipated close to noon. The exact reason for the erratic behavior during foggy episodes is uncertain.
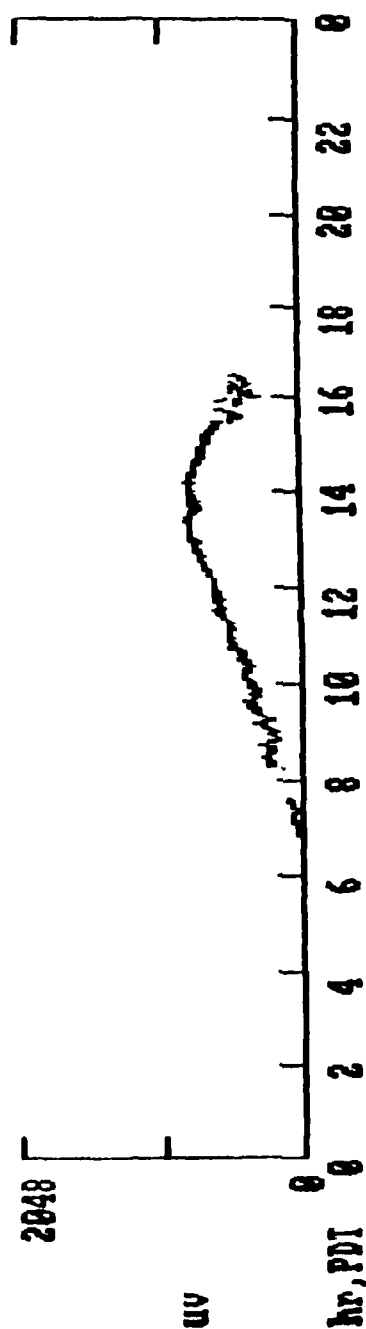
Figure 42. UV intensity on August 27, 1987. UV intensity was recorded by Portland State University's group at the Oregon coast site in Lincoln City. The sun rose at 7 AM and UV intensity increased until around 1300 hours when clouds began to appear. The PSU group's equipment was turned off at 1600 hours.
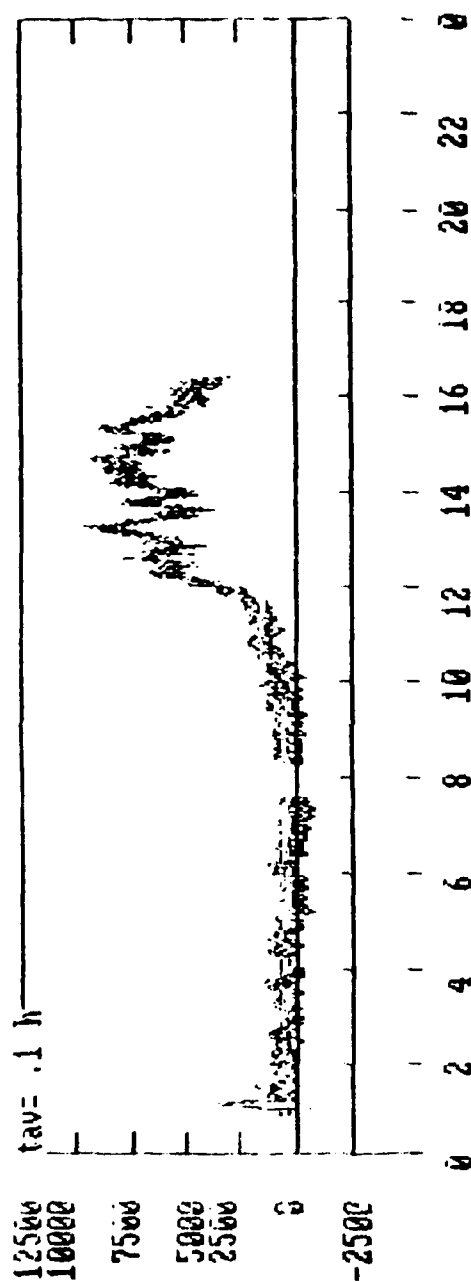
b:AHOX27AU 1101

Figure 43. FAGE HO$_2$ data recorded August 27, 1987. FAGE began detecting HO$_2$ concentrations as soon as the fog began dissipating shortly after 10 AM and reported increasing HO$_2$ concentrations until the clouds began appearing after 1400 hours. High humidity also affects the FAGE equipment. During heavy fog, FAGE reports negative values for HO$_2$ concentrations.

Sea salt was everywhere. There was a fine coating of sea salt on the reaction chamber and this probably meant that there was a coating of sea salt inside the reactor cell. KCl has been used to remove radicals [Baldwin et al., 1984], and since NaCl is likely to have similiar characteristics, the presence of sea salt inside the reactor chamber may have reduced the chain length due to wall reactions. This is probable because the chain length calculated by the static formaldehyde photolysis bag decay method was 261 immediately after returning from Oregon (Table II). After a fresh coating of halocarbon was put on the reactor wall, the static formaldehyde photolysis bag decay method produced chain lengths of over 500 for the same reactor.

Chapter VI

Humidity

Humidity has been a persistent problem for the PERCA system. In periods of high humidity, the system fails to register a signal. Cantrell reported no readings during periods of high humidity and attributed it a change in the atmospheric sinks for the radicals [**Cantrell et al**, 1984]. This effect presented itself again during ambient air sampling in Claremont, California. To determine whether the PERCA system was failing in high humidity, or the radical density actually disappeared in high humidity as suggested by Cantrell, the effects of humidity on the PERCA system were studied.

The first experiment consisted of placing the reaction chamber intake in front of the steady source chlorine photolysis radical generator and varying the humidity of the large diluent air. The humidity of the large diluent flow was varied by passing the diluent air through a variable rheostated steam bath and condenser. The humidity of the final air stream being detected by the PERCA instrument was monitored by a Vaisala HMI 32 with a HMI 31UT humidity and temperature probe. Figure 44 shows the change in radical signal with humidity. The humidity has an inverse effect on the radical signal.

Percent Radical Signal vs. Humidity

Highest signal = 100%
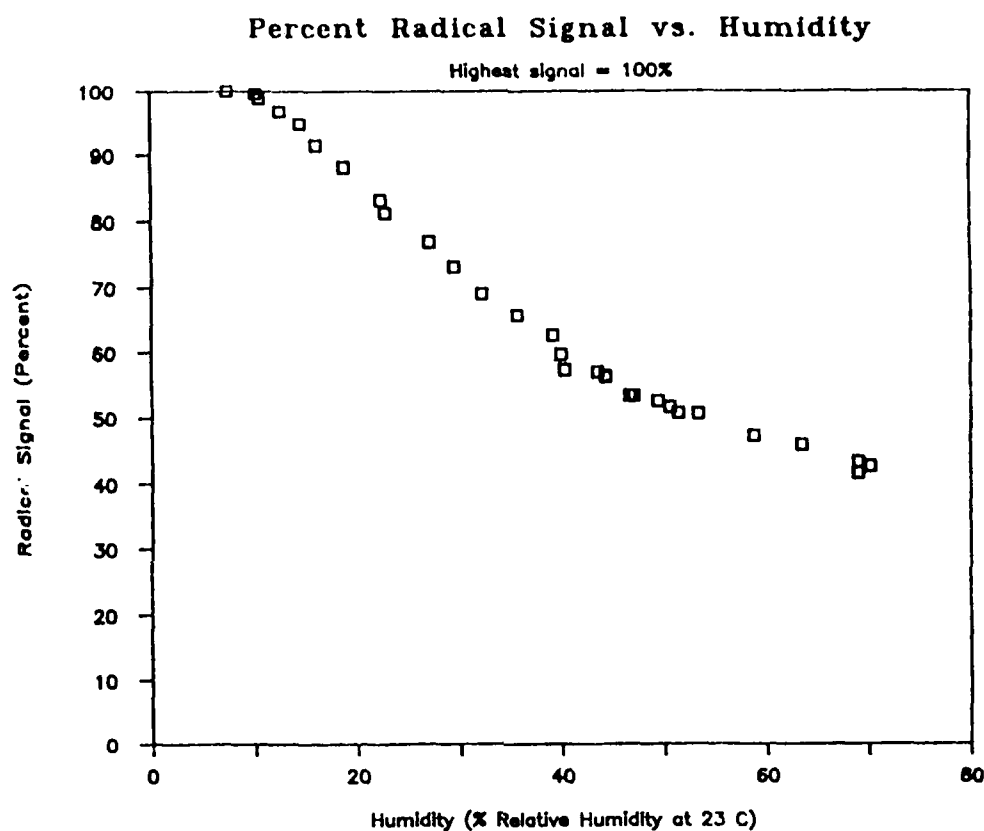
Figure 44. Change in radical signal vs. humidity. The signal from a steady radical was recorded at different humidities by passing the large diluent air flow of the chlorine photolysis radical source through a humidifier. Only 70% saturation at 23° C of the air was possible through this method.

To insure that the water vapor being mixed with the radicals was not changing the radical density, formaldehyde decay calibrations were accomplished at different humidities. Air from the same diluent source previously discussed was used to fill the 500L teflon bag in which the formaldehyde decays were conducted. The humidity and temperature were monitored with the Vaisala humidity and temperature detector with the probe completely enclosed inside the bag. A fan inside the bag circulated the air until the actual decays were being conducted. The results of the bag decays calculated with the humidity dependent reaction rate are shown on Table III. Even taking into account the enhanced recombination rate of HO_2, Figure 45 still confirmed that the instrument performance and not reduction in radical densities were the cause for the drops in signal with humidity.

The cause of the lowered chain lengths and signal are not fully understood. It is possible that the water enhanced termolecular formation of pernitric acid may proceed even faster on the surface of the reaction chamber. Since pernitric acid, like nitric acid, is not expected to elicit a response from the luminol instrument, its formation could explain the decrease in both radical and background signals with increasing humidity.

Table III

Calculated Chain Lengths Using Formaldehyde
Photolysis Bag Decay Method
At Different Humidities
On February 19, 1988

Volume air bubbled through formaldehyde solution	Relative Humidity at 23° C	Starting Signal ppbv	Chain Length
75ml	7%	52	634
75ml	7%	53	591
120ml	30%	31	336
120ml	30%	41	364
180ml	60%	20	99
180ml	60%	26	128

Chain Lengths at different humidities

Formaldehyde Decay Method
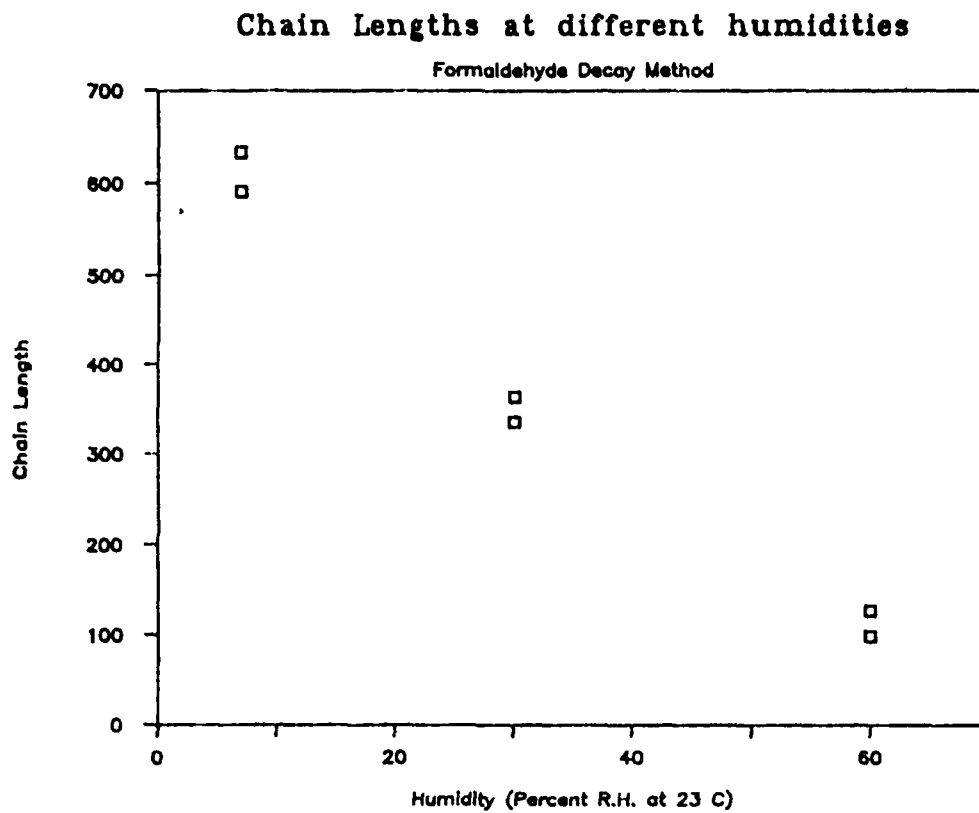
Figure 45. Chain lengths at different humidities. Formaldehyde bag decays were conducted with the bag filled with air at different relative humidities.

Chapter VII

PAN

Cantrell expected peroxyacyl nitrates (PAN), with a chemical formula of $CH_3C(O)O_2NO_2$, to be an interference to the PERCA system [Cantrell et al., 1984]. Cantrell's model suggested that PAN would decompose in the reactor to form NO_2 and peroxyacetyl (PA) radicals. The NO_2 formed would appear in the background signal, and the PA radical would have a chain length of 1.5 and appear as a minor interference during the chain reaction cycle. To test out Cantrell's model, PAN was introduced into the PERCA system and its effects on the instrument observed.

To conduct the experiment, the PERCA instrument was first calibrated for NO_2 and then exposed to PAN through an exponential decay flask. The concentrations of PAN and NO_2 were monitored through a PAN/NO_2 chromatographic detector recently developed by our group and total NO_x was monitored by a Thermoelectron NO_x detector (model 14B/E NO, NO_2, NO_x analyzer). Mark Burkhardt supplied the PAN and operated the PAN/NO_2 and NO_x detectors.

Surprisingly, PAN appeared only in the background signal. PAN did not decompose as originally modelled and failed to produce a signal in the CO cycle. PAN, however, induced a non-linear response from the luminol instrument.

Figure 46 shows the response for PAN can be twice the response for NO_2.

Since the experiments were conducted at room temperature (23° C) in the laboratory, further studies of PAN at higher temperatures may show different results. At higher temperatures, PAN is very unstable, and may dissociate as originally modelled. At room temperature, it has shown to be fairly stable and only contributes to the background signal of the PERCA instrument.

PERCA response to PAN

PERCA response relative to NO2
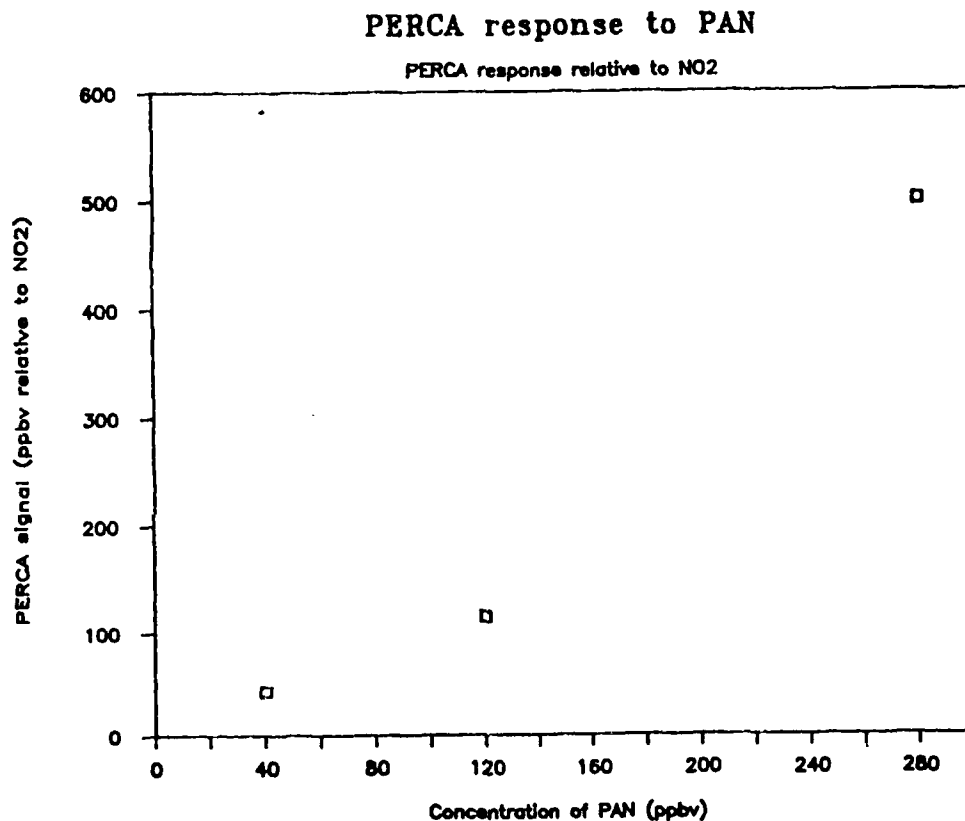
Figure 46.   PERCA response to PAN.   PAN, a
suspected interference in the PERCA system
appeared only in the background signal of the
PERCA instrument.   The response of the PERCA
instrument to PAN was non-linear and was up to
two time more sensitive to PAN than NO_2.

Chapter VIII

SO$_2$ As An Alternate Chain Carrier Reagent

CO, the chain carrier gas, is a colorless, odorless, flammable, and poisonous gas. Substituting CO with another safer reagent would enhance the overall appeal of the PERCA method. In the present scheme, CO oxidized by a hydroxyl radical initiates a chain reaction generating hydroperoxy and hydroxyl radicals. Another reagent that could react as quickly with OH as carbon monoxide to produce hydroperoxy radicals should also work, provided the produced reaction did not interfere with the other reactions in the PERCA method. Buhr [1986] tested formaldehyde, propane, and cis-2-butene, finding them all lacking in one respect or another. In this attempt, SO$_2$ was studied as a possible substitute for CO.

Although SO$_2$ is also a colorless and poisonous gas, it has the distinct advantage of having a very noxious odor which is easily detectable in trace amounts. Due to its easily detectable smell, SO$_2$ is a much safer gas than CO. The reported rate constant for SO$_2$ + OH -> SO$_3$ + H·, 9 x 10^{-13} cm^3 molecule^{-1} second^{-1} [Atkinson and Lloyd, 1984], is faster by two orders of magnitude than OH + CO and makes it a good candidate as a substitute gas.

The first attempts at substituting CO with SO$_2$ from a lecture bottle of pure liquid SO$_2$ (Matheson) failed. The

pure SO_2 was diluted into a stream of N_2 (200 ml/min) through a stainless steel frit (1 ml/min). The setup was abandoned because the SO_2 concentration proved too large. The SO_2 changed the pH of the luminol solution and killed all signals.

Attempts to substitute CO with SO_2 were tried again by diluting 442ppmv SO_2 (Linde) in N_2. The luminol flow through the instrument was increased to 1 ml/min to prevent pH changes in the luminol solution. The 442ppmv SO_2 was further diluted into N_2 by a series of Tylan flow controllers and different concentrations of SO_2 and NO were tried to maximize the radical signal. SO_2 was capable of carrying the chain reaction. Figure 47 shows the optimum NO_2 signal to occur at SO_2 concentrations of 13ppmv. The optimum NO concentration was 1ppmv. The SO_2, however did not work as well as CO.

The 442ppm SO_2 was successful in carrying the chain, but was not a suitable substitute for carbon monoxide. SO_2 produced one-third of the signal given by CO for the same radical density. SO_2 also showed a time lag and abnormal zero-modulation. Figure 48 shows the slow rise of the SO_2 signal and the abnormal zero-modulation. The slow response and the negative zero-modulation (negative zero-modulation also seen when the activated charcoal/ iodine trap for CO is put in backwards) makes SO_2 a poor substitute for CO.

Percent Radical Signal vs. [SO2]
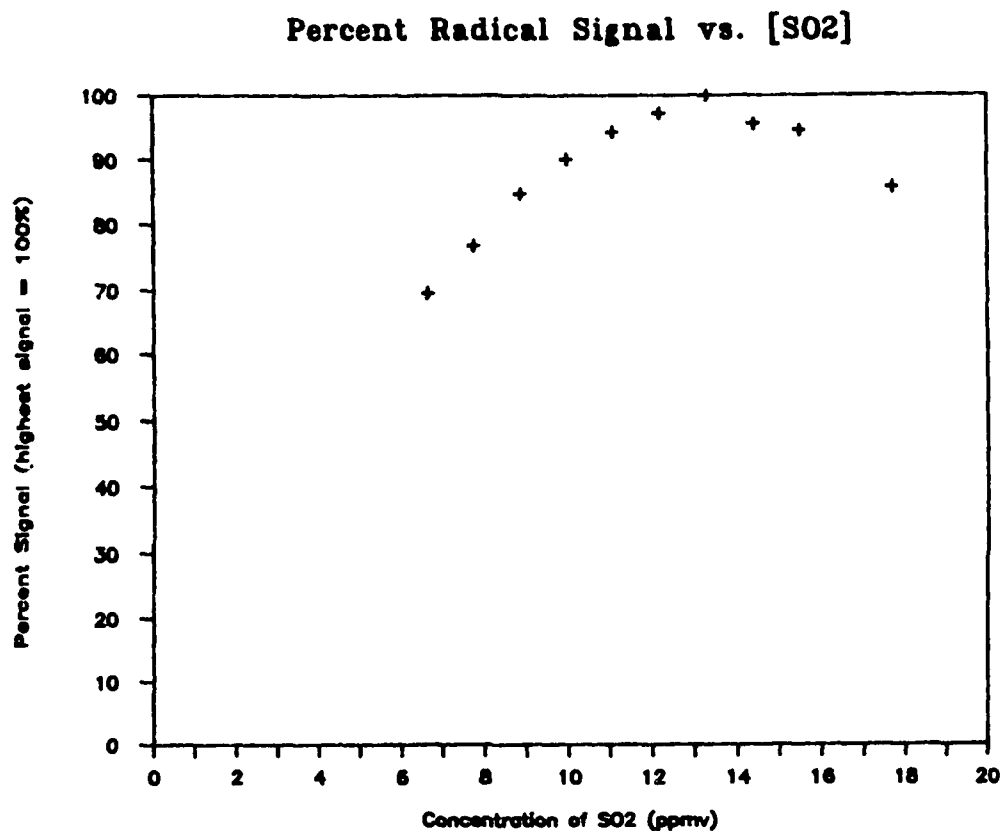
Figure 47.   Radical signal vs. [SO_2] at 1ppm
[NO]. SO_2 was found to carry the PERCA chain
reaction.   The optimum signal was gained at
13ppmv, but only provide 30% of the signal
produced by CO chain propagation.
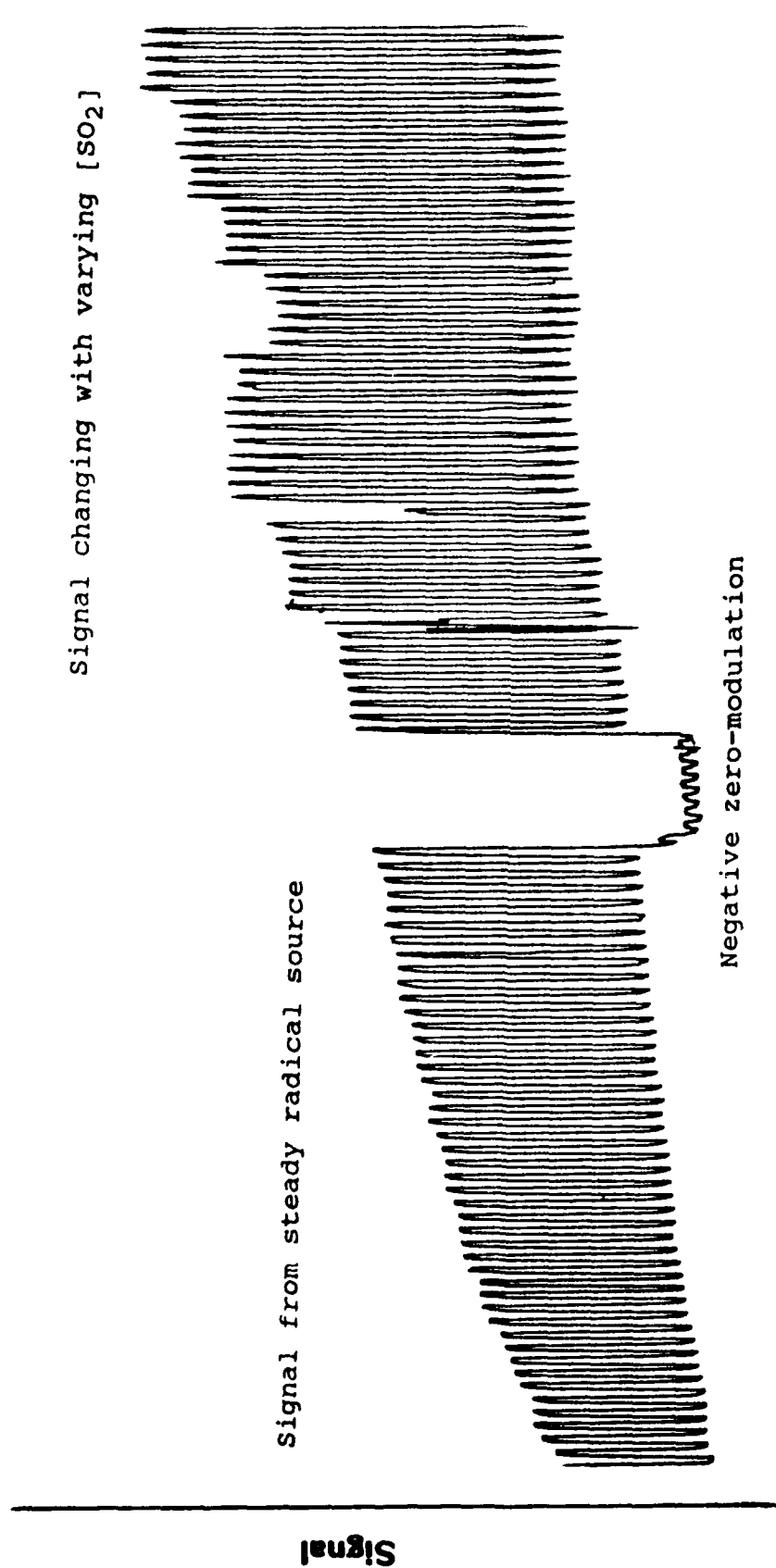
Figure 48. Actual signal produced by SO_2 chain propagation. The SO_2 reaction shows a slowly stabilizing response to a steady radical source. Turning the black light lamps shows that SO_2 does carry the chain, but the zero-modulation is negative.

108

Chapter IX

Conclusion

The PERCA instrument was designed to meet the goal of a simple, compact, and inexpensive instrument to measure ambient free radicals. Cantrell began the investigation and modelled the PERCA method. Although his chain length model was too simplistic, it served as a guide for instrument development. Buhr took the guide and developed the instrument. He designed the latest PERCA instrument and began attempts to calibrate the instrument. We have continued the instrument development and successfully calibrated the PERCA instrument using the formaldehyde photolysis decay method. This instrument is continually being improved and will eventually meet the goal set for it.

Optimizing the Instrument

The derived chain lengths model by Cantrell is too simplistic (Figure 4). Our studies have shown that the whole chain reaction takes place in less than 0.2 seconds, and increasing the reactor volume will not improve chain lengths. We have found chain lengths can be improved by reducing wall reactions. Coating the reaction chamber with halocarbon wax has improved the chain length by 300%. The effects of NO concentrations were more closely studied and the NO concentration which yields the highest chain length

is higher than the NO concentration which yields the highest signal. This effect is due to the luminol instrument's changing sensitivity to NO_2 with added NO. Using the instrument at the optimum NO concentration of 5ppmv will result in the highest chain lengths, and also depress the background signal reducing the interference from zero-modulation.

Wall cleanliness is an area of concern. Calibrations have shown chain lengths decrease with time, and it is necessary to recoat the reactor chamber to regain performance. The effect of wall contamination under various conditions should be studied to set guidelines for recoating the reaction chamber.

Interferences

The major interferences for this instrument are pernitric acid formation, humidity, and zero-modulation. The most serious interference is the formation of pernitric acid. In clean air, the assumption that HONO formation is the limiting reaction remains valid, but as the NO_2 concentration rises, the formation rate of HO_2NO_2 increases until pernitric acid formation is the primary sink for HO_2 molecules in the PERCA reactor chamber. Pernitric acid formation may also prevent an accurate calibration of the PERCA method by prematurely inhibiting the chain reaction due to the build up of NO_2 in the reaction chamber. It may

even be the cause of zero-modulation, or false positive signal, which shows a dependence on the background signal.

Pernitric acid formation could severely limit the scope of the PERCA method. Its actual effect on the PERCA system should be investigated by a-complishing chain length calibrations using the formaldehyde decay method with varying amounts of NO_2 inside the teflon bag. Through the calibrations, a threshold level of NO_2 can be deduced.

Humidity also presents a problem for the PERCA system. The presence of water enhances many reactions present in the PERCA system. The reaction $H\cdot + O_2 + M \rightarrow HO_2 + M$ is enhanced as well as the recombination of HO_2 with itself and pernitric acid formation. The exact reason for the PERCA instrument's degradation in high humidity is uncertain, but surface chemistry and pernitric acid formation may provide an answer. Further investigation into the effect of humidity on the various reactions critical to the PERCA system may reveal insight to the humidity interference.

PAN does not behave as modelled by Cantrell, and is not an interference at room temperature. PAN elicits a non-linear response only in the background signal of the PERCA instrument. PAN can elicit twice the response relative to NO_2 in the instrument and should be checked for its effect on zero-modulation. Also since PAN is unstable, its affect on the PERCA instrument should be investigated at higher

temperatures. At higher temperatures, PAN may be an interference.

All the interferences currently suffered by the PERCA method may be reduced by injecting clean dry air or N_2 with the reagent gases to dilute the sampled air. This will maintain low NO_2 levels in the reaction chamber inhibiting pernitric acid formation, reduce the effect of humidity, and lower the background signal to reduce zero-modulation. Adding clean dry air, or N_2 to dilute the sampled air would be a simple, but highly effective modification to reduce the interferences in the PERCA system. The disadvantage would be the lower concentrations of ambient free radicals drawn into the reaction chamber, but the higher concentrations of free radicals expected in dirty air may offset the reduction.

Calibration

The formaldehyde photolysis decay method is currently the best calibration method for the PERCA instrument. The method has shown consistent and believable results in the laboratory, and although bulky, the method can be adapted for field use. Portland State University already has a formaldehyde decay calibration source operating in the field with their FAGE equipment. The method can be further defined by quantifying the formaldehyde used in the calibration bag, and possibly using paraformaldehyde as a cleaner source of formaldehyde. The formaldehyde decay

method holds great promise in accurately calibrating the PERCA instrument.

The dynamic chlorine photolysis flow tube method of calibration shows potential. Redesigning the flow tube to safely handle higher pressures of H_2 and O_2 may remove the interferences currently plaguing the system. If perfected, the system could validate the formaldehyde decay method and become an excellent laboratory calibration source.

Field Measurements

Although the field studies did not produce useable data, they did point out areas of concern. The instrument as currently configured can measure atmospheric free radicals in a clean, dry environment. Claremont and the Oregon coast presented areas that need to be investigated before attempting further ambient measurements with the PERCA system. They are the following:

1. A temperature compensator circuit to counteract the temperature dependence of the luminol solution's sensitivity to NO_2.

2. A portable calibration source to gauge the effects of ambient humidity and wall contamination through sampling ambient air.

3. The threshold level important to pernitric acid formation, and if NO_2 levels are expected to exceed the safe limit, add clean dry air, or N_2 in addition to the reagent gases in the reactor to dilute the sampled air.

If the above areas are addressed, the PERCA instrument will become a more viable instrument under different conditions, and insure a successful field study.

Reagent Gas Substitute For CO

We are still looking for a substitute reagent for carbon monoxide in the PERCA system. SO_2 has shown to propagate the chain, but it does not perform as well as CO. SO_2 provides only 30% of the signal possible with CO, and does not respond as quickly. It also causes negative zero-modulation. Other reagents will have to be investigated.

Appendix A

Computer Program to Collect Data

```
program colair;
(This program uses the lab tender to accumulate 7 channels
of data.  Channel 14 is used to collect modulated data. The
modulation is controlled by port A pin 1.  When the solenoid
is off, the data read on channel 14 is the background zero
signal.  When it is on, the data sample signal is calculated
from the difference between the data on presently on channel
14 and the background zero signal.  The program begins by
asking the operator what parameters he wishes to use.  The
solenoid valve frequency is the time for the solenoid being
on plus off.  The integration time is the time between
saving data on the disk.  The time between file closures
determines the amount of data stored in each file.  As the
program stores the modulation data it also samples channels
8 through 13 and stores this data on the disk as well.
Written by Bob Lynch.)

type
  str1     = string[1];
  str8     = string[8];
  str10    = string[10];
  str14    = string[14];
  inarry   = array[0..8] of real;

var
  intime   : real;            disk      : text;
  time     : real;            calval    : real;
  sample   : real;            volts     : real;
  hour     : integer;         zero      : real;
  min      : integer;         limit     : real;
  sec      : integer;         channel   : integer;
  gainset  : real;            fivesum   : real;
  fiveave  : real;            fivecnt   : integer;
  flag     : boolean;         hourpnt   : integer;
  fivetime : real;            oldgain   : real;
  hlt      : boolean;         oldzero   : real;
  basesum  : real;            basecnt   : integer;
  baseline : real;            inp       : inarry;
  filename : str14;           x         : integer;
  cal      : inarry;          response  : str1;
  colpos   : integer;         abvtime   : str8;
  indic    : integer;         avetime   : integer;
  testhour : integer;         uptime    : integer;
```

```
{***********************************************************}
   FUNCTION AND PROCEDURE DECLARATION
{***********************************************************}
function adin(channel:integer):real;
(This  function  returns  the  voltage  present  on  channel
CHANNEL in ADIN.}
var
 temp:real;
begin
 port[816]:=channel*2+1;
 repeat
 until port[816]>127;
 temp:=port[817];
 adin:=temp/255*10;
end;


{***********************************************************}

function datestr:str10;
(datestr will contain the current date}
var
 month    : integer;              monthst : string[2];
 day      : integer;              dayst   : string[2];
begin
 month:=port[$2c7];
 month:=(10*(month div 16) + (month mod 16));
 str(month:2,monthst);
 if copy(monthst,1,1)=' ' then begin
  delete(monthst,1,1);
  insert('0',monthst,1);
  end;
 day:=port[$2c6];
 day:=(10*(day div 16) + (day mod 16));
 str(day:2,dayst);
 if copy(dayst,1,1)=' 'then begin
  delete(dayst,1,1);
  insert('0',dayst,1);
  end;
 datestr:=monthst+'-'+dayst+'-1987';
end;


{***********************************************************}

function timestr:str8;
(timestr will contain the current time}
var
 hour : integer;              hourst : string[2];
 min  : integer;              minst  : string[2];
 sec  : integer;              secst  : string[2];

begin
 sec:=port[$2c2];
```

```
 sec:=(10*(sec div 16) + (sec mod 16));
 str(sec:2,secst);
 if copy(secst,1,1)=' ' then begin
  delete(secst,1,1);
  insert('0',secst,1);
  end;
 min:=port[$2c3];
 min:=(10*(min div 16) + (min mod 16));
 str(min:2,minst);
 if copy(minst,1,1)=' ' then begin
  delete(minst,1,1);
  insert('0',minst,1);
  end;
 hour:=port[$2c4];
 hour:=(10*(hour div 16) + (hour mod 16));
 str(hour:2,hourst);
 if copy(hourst,1,1)=' ' then begin
  delete(hourst,1,1);
  insert('0',hourst,1);
  end;
 timestr:=hourst + minst + secst;
end;


(******************************************************)

function keystrk:boolean;
{This function sets keystrk=true if key has been depressed}
begin
 if memw[0000:1050] <> memw[0000:1052] then
  keystrk:=true
 else keystrk:=false;
end;


(******************************************************)

function key: char;
{This function will set key equal to the character struck,
or wait until
 a key is struck.}
var
 temp : char;
begin
 repeat
 until keystrk;
 read(kbd,temp);
 key:=temp;
end;


(******************************************************)

function brk:boolean;
{This function sets brk=true if X was last key depressed.}
```

```
var
 temp : char;
begin
 if keystrk then begin
  read(kbd,temp);
  if temp='X' then brk:=true
  else brk:=false;
 end
 else brk:=false;
end;


(***********************************************************)

procedure solenoid(state:integer);
{This procedure turns on and off digital output port A}
begin
 port[831]:=128;
 port[828]:=state;
end;


(***********************************************************)

procedure timeval(var hour,min,sec:integer);
{timeval returns current hours,minutes, and seconds.}
begin
 sec:=port[$2c2];
 sec:=(10*(sec div 16) + (sec mod 16));
 min:=port[$2c3];
 min:=(10*(min div 16) + (min mod 16));
 hour:=port[$2c4];
 hour:=(10*(hour div 16) + (hour mod 16));
end;


(***********************************************************)

procedure wait(time:real;var hlt:boolean);
{This procedure waits TIME amount of time from HOUR,MIN,SEC
and returns. }
var
 hour  : integer;          initmin : integer;
 min   : integer;          initsec : integer;
 sec   : integer;          minelaps: real;
 inithour:integer;         day     : integer;
 initday:integer;
begin
 timeval(hour,min,sec);
 initday:=port[$2c6];
 initday:=(10*(initday div 16) + (initday mod 16));
 inithour:=hour;
 initmin:=min;
 initsec:=sec;
 repeat
```

```
  timeval(hour,min,sec);
  day:=port[$2c6];
  day:=(10*(day div 16) + (day mod 16));
  gotoxy(68,2);write(timestr);
  minelaps:=(day-initday)*440+(day-initday)*500+
(day-initday)*500+
             (hour-inithour)*60+
             (min-initmin)+(sec-initsec)/60;
  if brk then hlt:=true;
 until (minelaps>=time) or (hlt);
end;

(*********************************************************)

procedure  voltave(limit:real;channel:integer;var
volts:real;var hlt:boolean);
(This procedure averages the voltages until 20% of timer
interval has elapsed. )
var
 minelaps : real;              nowmin   : real;
 voltsum : real;               init     : real;
 voltcnt : integer;            xit      : boolean;
begin
 timeval(hour,min,sec);
 init:=hour*60+min+sec/60;
 voltsum:=0;
 voltcnt:=0;
 xit:=false;
 repeat
  gotoxy(68,2);write(timestr);
  if brk then xit:= true;
  voltsum:=voltsum+adin(channel);
  if brk then xit:=true;
  voltcnt:=voltcnt+1;
  timeval(hour,min,sec);
  nowmin:=hour*60+min+sec/60;
  if brk then xit:=true;
  minelaps:=nowmin-init;
  if minelaps<0 then minelaps:=minelaps+1440;
 until (minelaps>=limit) or (xit);
 volts:=voltsum/voltcnt;
end;

(*********************************************************)

procedure initfile(var disk:text;calval:real;cal:inarry);
(This procedure sets up a data file and puts heading
information into it.)
var
 x : integer;
begin
```

```
filename:='b:'+(copy(datestr,1,2))+(copy(datestr,4,2))+
          (copy(timestr,1,2))+(copy(timestr,3,2))+'.PRN';
assign(disk,filename);
rewrite(disk);
writeln(disk,'"This is data from Pomona California"');
writeln(disk,datestr,'"   TIME = "',timestr);
writeln(disk,'"Gain setting used to calculate DIFF"');
writeln(disk);
writeln(disk,'"Calfactors-"');
writeln(disk,'" DIFF and"','" BASE "','"= "',calval:7:3,'"
nA per ppt"');
 for x:=1 to 7 do
  writeln(disk,'"  CH"',x,'"  =  "',cal[x]:7:3,'" volts  per
ppb"');
 writeln(disk);
 writeln(disk,'"TIME"','"DIFF"','"CH1"','"CH2"','"CH3"',
'"CH4"','"CH5"','"CH6"','"CH7"','"ZERO"');
 writeln(disk,'"HHMMSS"','"uAmps"','"V"','"V"','"V"','"V"',
'"V"','"V"','"V"','"uAmps"');
writeln(disk,'"======================================"');
end;


(**********************************************************)

procedure   five(var   fivetime:real;var
flag:boolean;avetime:integer);
(This procedure calculates if it is time for a five minute
(or  x  minute)  average  calculation  and  set   flag
accordingly.)
var
 hour  : integer;                    nowtime : real;
 min   : integer;
 sec   : integer;
begin
 timeval(hour,min,sec);
 nowtime:=hour*60+min+sec/60;
 if nowtime <= fivetime then nowtime:=nowtime+1440;
 if nowtime >= fivetime + avetime then begin
  flag:=true;
  timeval(hour,min,sec);
  fivetime:=hour*60+min+sec/60;
 end
 else flag:=false;
end;


(**********************************************************)

(begin MAIN program)

begin
intime:=1;
avetime:=5;
```

```
uptime:=1;
for x:=1 to 7 do cal[x]:=1;
repeat {for scale changes loop}
 hlt:=false;
 clrscr;
 channel:=14;
 colpos:=0;
 indic:=0;
 writeln;
 intime:=intime*60;
 write('What  is  the  frequency  of  the  solenoid  valve  in
seconds?');
 write(' (',intime:5:0,') ');
 readln(intime);
 intime:=intime/60;
 writeln;
 write('What is the integration time in minutes');
 write(' (',avetime,') ');
 readln(avetime);
 writeln;
 write('What is the time between file closures in hours');
 write(' (',uptime,') ');
 readln(uptime);
 writeln;
 write('What is the gain setting of the luminol instrument
in uA per volt?');
 if gainset<>0 then write(' (',gainset:7:4,')');
 readln(gainset);
 writeln;
 write('What is the cal factor in nA per ppt?');
 if calval<>0 then write(' (',calval:7:3,')');
 readln(calval);
 for x:=1 to 6 do begin
  writeln;
  write('What is the cal factor for channel ',x+7,' in volts
per ppb?');
  write(' (',cal[x]:7:3,')');
  readln(cal[x]);
 end;
 initfile(disk,calval,cal);
 timeval(hour,min,sec);
 hourpnt:=hour;
{begin taking data.}
clrscr;
gotoxy(1,25);write('To exit or change parameters press X');
gotoxy(1,2);write('STATUS =');
gotoxy(60,2);write('TIME');
timeval(hour,min,sec);
fivetime:=hour*60+min+sec/60;
oldzero:=0;
fivesum:=0;
fivecnt:=0;
```

```
basesum:=0;
basecnt:=0;
 repeat     (for data collection loop)
  limit:=intime/4;
  time:=intime/4;
  gotoxy(15,2);write('ON ');
  solenoid(1);
  wait(time,hlt);
  voltave(limit,channel,volts,hlt);
  sample:=volts;
  gotoxy(15,2);write('OFF');
  solenoid(0);
  wait(time,hlt);
  voltave(limit,channel,volts,hlt);
  zero:=volts;
  if oldzero=0 then oldzero:=zero;
  fivesum:=fivesum+(sample-(zero+oldzero)/2);
  fivecnt:=fivecnt+1;
  basesum:=basesum+zero;
  basecnt:=basecnt+1;
  oldzero:=zero;
  five(fivetime,flag,avetime);
  if flag then begin
   fiveave:=fivesum/fivecnt*gainset;
   baseline:=basesum/basecnt*gainset;
   for x:=1 to 6 do inp[x]:=adin(x+7);
   writeln(disk,timestr,'   ',fiveave:9,'    ',inp[1]:9,'
',inp[2]:9,' ',inp[3]:9,' ',inp[4]:9,' ',inp[5]:9,' ',
inp[6]:9,' ',baseline:9);
   fiveave:=(fiveave/calval*1E+3);
   baseline:=(baseline/calval*1E+3);
   for x:=1 to 6 do inp[x]:=inp[x]/cal[x];
   abvtime:=copy(timestr,1,4);
   gotoxy(15+indic,4);write('    ');
   gotoxy(15+colpos,4);write('****');
   gotoxy(3,5);write('TIME');   gotoxy(15+colpos,5);
write(abvtime);
   gotoxy(3,7);write('HO2ppt');   gotoxy(15+colpos,7);
write(fiveave:5:2);
   gotoxy(3,9);write('CH  8  pb');   gotoxy(15+colpos,9);
write(inp[1]:5:2);
   gotoxy(3,11);write('CH  9  ppb');   gotoxy(15+colpos,11);
write(inp[2]:5:2);
   gotoxy(3,13);write('CH10  ppb');   gotoxy(15+colpos,13);
write(inp[3]:5:2);
   gotoxy(3,15);write('CH11ppb');   gotoxy(15+colpos,15);
write(inp[4]:5:2);
   gotoxy(3,17);write('CH12  ppb');   gotoxy(15+colpos,17);
write(inp[5]:5:2);
   gotoxy(3,19);write('CH13  ppb');   gotoxy(15+colpos,19);
write(inp[6]:5:2);
```

```
      gotoxy(3,23);write('zero  ppb');  gotoxy(15+colpos,23);
write(baseline:5:2);
    indic:=colpos;
    colpos:=colpos+9;
    if colpos>60 then colpos:=0;
    fivesum:=0;
    fivecnt:=0;
    basesum:=0;
    basecnt:=0;
    timeval(hour,min,sec);
    testhour:=hour-hourpnt;
    if testhour < 0 then testhour:=testhour+24;
    if testhour > uptime-1 then begin
     hourpnt:=hour;
     close(disk);
     initfile(disk,calval,cal);
    end
   end
  until (brk) or (hlt);    {end of data collection loop}
  close(disk);
  writeln;
  write('Do you wish to change parameters?');
  readln(response);
  until response='n';    {end of scale changes loop}
  clrscr;
  writeln('exiting calair program.');
  end.
```

Appendix B

Determination of formaldehyde concentration

To quantify the amount of formaldehyde introduced in to the bag, the UV absorbance at 280nm of the original 37.7% solution was accomplished by a Beckman DU-50 spectrophotometer (Figure 49). A known amount of the formaldehyde solution and container were weighed, and 96.3 liters of air were bubbled through the solution at a flow of 9.73ml/min. The solution was reweighed, and the absorbance spectrum was repeated (Figure 50). The concentration of formaldehyde removed from the solution could not be determined. It is likely the formaldehyde solution began polymerizing. This interfered with the ability to measure the formaldehyde concentration, since the polymer has an even larger absorption coefficient than the initial formaldehyde.

BECKMAN

DU 50 SPECTROPHOTOMETER

ABSORBANCE

Scan Speed: 500 nm/min
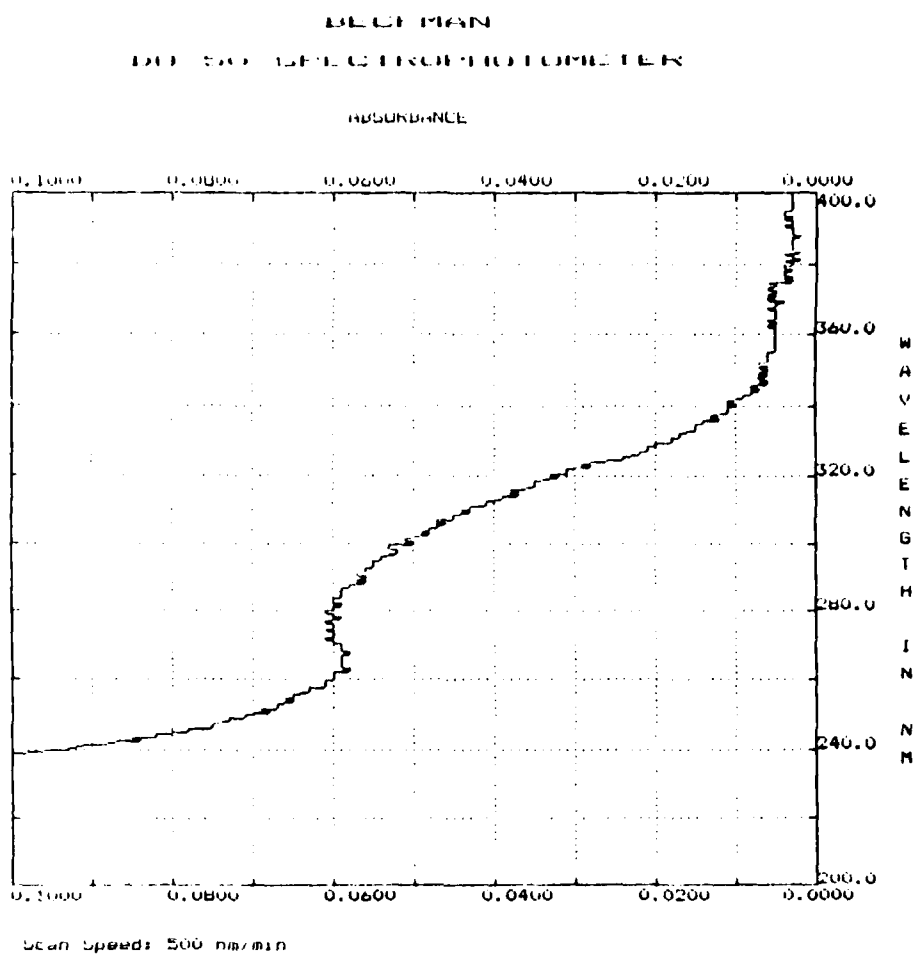
Figure 49. UV absorption spectrum on 37.7% formaldehyde in water with 10% methanol as a preservative.

BECKMAN

DU-50 SPECTROPHOTOMETER

ABSORBANCE

Scan Speed: 500 nm/min
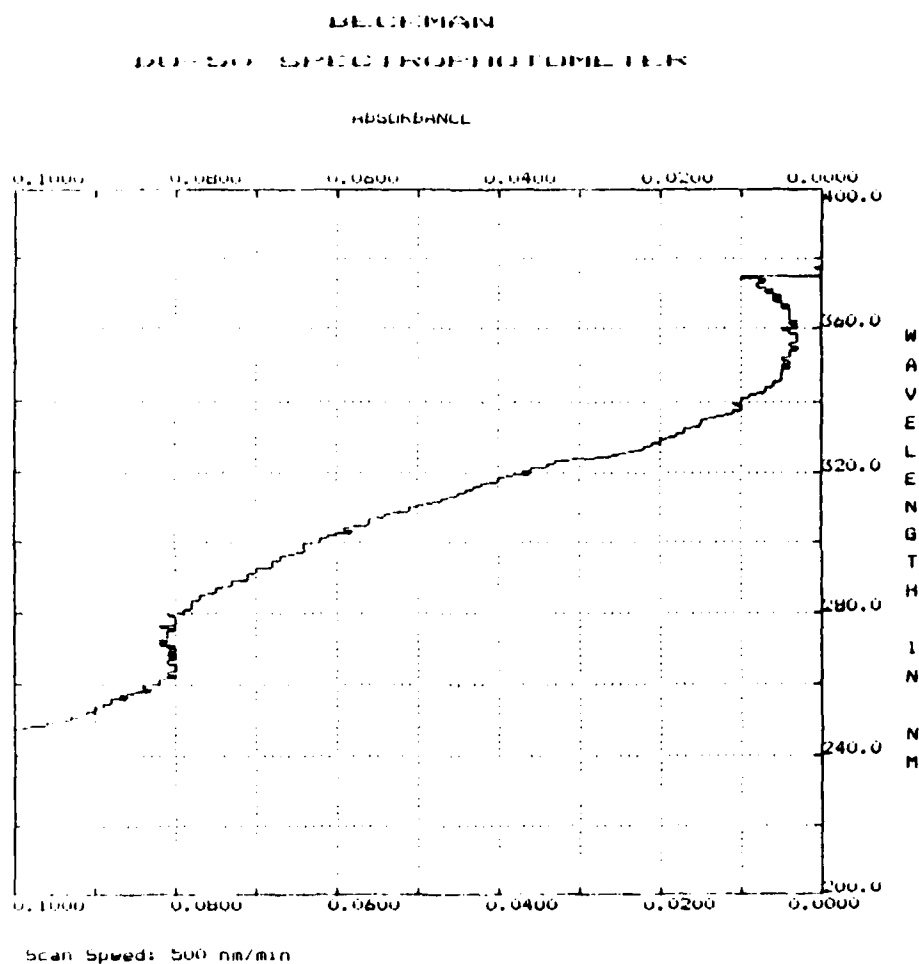
Figure 50. UV absorption spectrum on formadehyde solution after passing 96.3 liters of air through it. Polymerization of the solution is suspected yielding a higher absorbance than is expected.

Appendix C

Hydrocarbon Study of Chlorine Photolysis
Flow Tube Calibration System

Hydrocarbon Study

Signal from Chlorine Photolysis

Figure 51. Hydrocarbon Study. Different hydrocarbons were tried in place of hydrogen in the chlorine photolysis flow tube calibration system with the resulting signals.

References

Anderson, J.G., The Absolute Concentration of OH in the Earth's Stratosphere, _Geophysical Research Letters,_ 3, 165-168, 1976.

Anderson, J.G., H.J. Grassl, R.E. Shetter, and J.J. Margitan, HO_2 in the Stratosphere: Three in situ Observations, _Geophys. Res. Lett.,_ 8, 289-292, 1981.
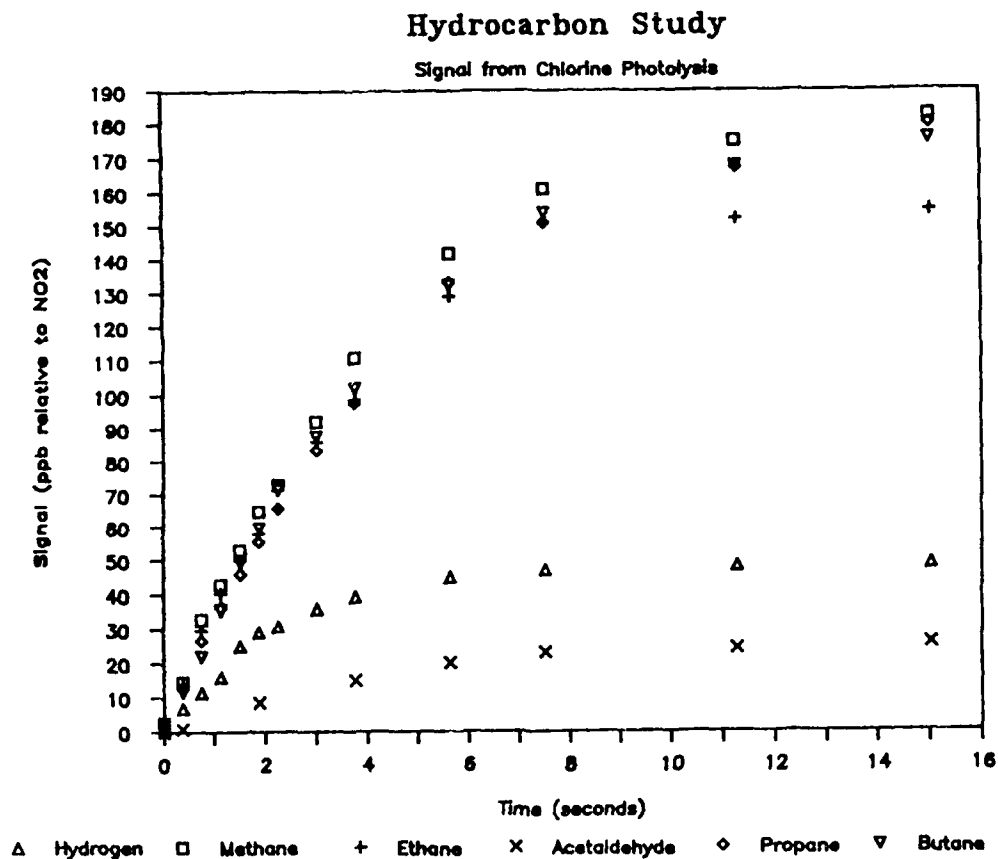
Atkinson, R. and A.C. Lloyd, Evaluation of Kinetic and Mechanistic Data for Modelling of Photochemical Smog, _J. Phys. Chem. Ref. Data,_ 13, 315, 1984.

Bradshaw, J.D., M.O. Rodgers, and D.D. Davis, Sequential Two-Photon Laser-Induced Fluorescence: A New Technique for Detecting Hydroxyl Radicals, _Appl. Opt.,_ 23, 2134-2145, 1984.

Beck, S.M., R.J. Bendura, D.S. McKougal, J.M. Hoell, Jr., G.L. Gregory, H.J. Curfman, Jr., D.D. Davis, J. Bradshaw, M.O. Rodgers, C.C. Wang, L.I. Davis, M.J. Campbell, A.L. Torres, M.A. Carroll, B.A. Ridley, G.W. Sachse, G.F. Hill, E.P. Condon, and R.A. Rasmussen, Operational Overview of NASA GTE/CITE 1 Airborne Instrument Intercomparisons: Carbon Monoxide, Nitric Oxide, and Hydroxyl Instrumentation, _Journal of Geophysical Research,_ 92, 1977-1985, 1987.

Buhr, M.P., Development of a Method for the Measurement of Atmospheric Free Radicals, A Master Thesis, University of Denver, 1986.

Burnett, C.R., and E.B. Burnett, Spectroscopic Measurements of the Vertical Column Abundance of Hydroxyl (OH) in the Earth's Atmosphere, _J. Geophys. Res.,_ 86, 5185-5202, 1981.

Burnett, C.R., and E.B. Burnett, Vertical Column Abundance of Atmospheric OH at Solar Maximum form Fritz Peak, Colorado, _Geophys. Res. Lett.,_ 9, 708-711, 1982.

Burnett, C.R., and E.B. Burnett, OH Column Abundance Measurements from Boca Raton, FL, Fritz Peak, CO, and Poker Flat, AK, _Eos Trans. AGU,_ 64, 781, 1983.

Burnett, C.R., and E.B. Burnett, Observational Results on the Vertical Column Abundance of Atmospheric Hydroxyl: Description of Its Seasonal Behavior 1977-1982, _Journal of Geophysical Research,_ 89, 9603-9611, 1984.

Calvert, J.G., J.A. Kerr. K.L. Demerjian, and R.D. McQuiggy. Photolysis of Formaldehyde as a Hydrogen Atom Source in the Lower Atmosphere, Science, 1, 751-752, 1972.

Calvert, J.G., B.G. Heikes, W.R. Stockwell, V.A. Mohnen, and J.A. Kerr, Some Considerations of the Important Chemical Processes in Acid Deposition, in Chemistry of Multiphase Atmospheric Systems, edited by W. Jaeschke, Springer, New York, 615-648, 1984.

Campbell, M.J., J.C. Sheppard, and B.F. Au, Measurement of Hydroxyl Concentration in Boundary Layer Air By Monitoring CO Oxidation, Geophysical Research Letters, 6, 175-178, 1979.

Campbell, M., J. Sheppard, and W. Blankenship, Measurement of Hydroxyl Radical Concentrations in Boundary Layer air in the CHON Photochemistry of the Troposphere, a colloquium. Nat. Centre. Atmos. Res., Boulder, Colorado, 1980.

Cantrell, C.A., and D.H. Stedman, A Possible Technique for Measurement of Atmospheric Peroxy Radicals, Geo. Res. Letters, 9, 846-849, 1982.

Cantrell, C.A., Peroxy Radical Measurement by Chemical Amplification, Doctoral Dissertation, University of Michigan, 1983.

Cantrell, C.A., D.H. Stedman, and G.J. Wendel, Measurement of Atmospheric Peroxy Radicals by Chemical Amplification, Anal. Chem., 56, 1496-1502, 1984.

Cattell, F.C., and R.A. Cox, Pressure Dependence of the Reactions of HO_2 with Cl and ClO, J. Chem. Soc., Faraday Trans. 2, 82, 1413-1426, 1986.

Clark, T.C., M.A.A. Clyne, and D.H. Stedman, Mechanism of Formation of Triatomic Molecules in Atomic Combination Reactions, Transactions of the Faraday Society, 62, 3554-3365, 1966.

Crutzen, P.Q., I.T. Jones, and R.P. Wayne, Calculation of $O(^1D)$ in the Atmosphere Using New Laboratory Data, J. Geophys. Res., 76, 1490-1497, 1971.

Davis, D.D., W. Heaps, D. Philen, and T. McGee, Bondary Layer Measurements of the OH Radical in the Vicinity of an Isolated Power Plant Plume: SO_2 and NO_2 Chemical Conversion Times, Atmospheric Environment, 13, 1197-1203, 1979.

Davis, D.D., W. Heaps, and T. McGee, Direct Measurements of Natural Tropospheric Levels of OH via an Aircraft Borne Tunable Dye Laser, _Geophysical Research Letters,_ 3, 331-333, 1976.

Davis, D.D., D. Philen, M. Rodgers, T. McGee, A. Nelson, and A.J. Moriarty, An air-borne laser induced fluorescence system for measuring OH and other trace gases in the parts-per-quadrillion to parts-per-trillion range, _Rev. Sci. Instrum._ 50, 70-81, 1979.

Davis, D.D., M.O. Rogers, S.D. Fischer, and K. Asai, An Experimental Assessment of the O_3/H_2O Interference Problem in the Detection of Natural Levels of OH via Laser Induced Fluorescence, _Geophys. Res. Lett.,_ 8, 69-72, 1981a.

Davis, D.D., M.O. Rogers, S.D. Fischer, and K. Asai, An Theoretical Assessment of the O_3/H_2O Interference Problem in the Detection of Natural Levels of OH via Laser Induced Fluorescence, _Geophys. Res. Lett.,_ 8, 73-76, 1981b.

Davis, L.I. Jr., C. Guo, J.V. James, P.T. Morris, R. Postiff, and C. C. Wang, An Airborne Lidar Instrument for Detection of OH Using the Technique of Laser-Induced Fluorescence, _J. Geo. Res.,_ 90, 12835-12843, 1985.

Davis, L.I. Jr., J.V. James, C.C. Wang, C. Guo, P.T. Morris, and J. Fishman, OH Measurements Near the Intertropical Convergence Zone in the Pacific, _Journal of Geophysical Research,_ 92, 2020-2024, 1987.

Demore, W.B., J.J. Margitan, M.J. Molina, R.T. Watson, D.M. Golden, R.F. Hampson, M.J. Kurylo, C.J. Howard, and A.R. Ravishankara, Chemical Kinetics and Photochemical Data for Use in Stratospheric Modeling, Jet Propulsion Lab., Pasadena, CA, 1985.

De Zafra, R.L., A. Parrish, P.M. Soloman, and J.W. Barrett, A Measurement of Stratospheric HO_2 by Ground-Based Millimeter-Wave Spectroscopy, _Journal of Geophysical Research,_ 89, 1321-1326, 1984.

Hagele, J., R. Poschke, and R. Zellner, Field Measurements of Tropospheric OH by Long-Path UV Laser Absorption, in _Optical Remote Sensing of Air Pollution,_ edited by P. Camagni and S. Sandroni, pp. 351-361, Elsevier, New York, 1984.

Hard, T.M., R.J. O'Brien, C.Y. Chan, and A. Mehrabzadeh, Tropospheric Free Radical Determination by FAGE, Environmental Sci. and Tech., 18, 768-777, 1984.

Hard, T.M., C.Y. Chan, A.A. Mehrabzadeh, W.H. Pan, and R.J. O'Brien, Diurnal Cycle of Tropospheric OH, Nature, 322, 617-620, 1986.

Heaps, W.S., T.J. McGee, R.D. Hudson, and L.O. Caudill, Stratospheric Ozone and Hydroxyl Radical Measurements by Balloon-borne Lidar, Appl. Opt., 21, 2265-2274, 1982.

Heaps, W.S., and T.J. McGee, Balloon-borne LIDAR Measurements of stratospheric hydroxyl radical, J. Geo. Res., 88, 5281, 1983.

Heaps, W.S., and T.J. McGee, Progress in Stratospheric Hydroxyl Measurement by Balloon-Borne LIDAR, Journal of Geophysical Research, 90, 7913-7921, 1985.

Heicklen, J., C. Westburg, and N. Cohen, Chemical Reactions in Urban Atmospheres, C.S. Tuesday, Ed., Symposium at General Motors Laboratories, Dearborn, MI, 55-58, 1969.

Helten, M., W. Patz, M. Trainer, H. Fark, E. Klein, and D.H. Ehhalt, Measurements of Stratospheric HO_2 and NO_2 by Matrix Isolation and ESR Spectroscopy, Journal of Atmospheric Chemistry, 2, 191-202, 1984.

Hewitt, C.N., and R.M. Harrison, Tropospheric Concentrations of the Hydroxyl Radical-A Review, Atmospheric Environment, 19, 545-554, 1985.

Horowitz, A., F. Su, and J.G. Calvert, Unusual H_2-Forming Chain Reaction in the 3120 Angstrom Photolysis of Formaldehyde-Oxygen Mixtures at 25° C, International Journal of Chemical Kinetics, 10, 1099-1117, 1978.

Hov, O., and I.S.A. Isaksen, Hydroxyl and Peroxy Radicals in Polluted Tropospheric Air, Geophysical Research Letters, 6, 219-222, 1979.

Hubler, G., D. Perner, U. Platt, A. Tonnissen, and D.H. Ehhalt, Groundlevel OH Radical Concentration: New Measurements by Optical Absorption, Journal of Geophysical Research, 89, 1309-1319, 1984.

Hynes, A.J., P.H. Wine, and A.R. Ravishankara, Kinetics of the OH + CO Reaction Under Atmospheric Conditions, Journal of Geophysical Research, 91, 11815-11820, 1986.

Kircher, C.C., and S.P. Sander, Kinetics and Mechanism of HO_2 and DO_2 Disproportionations, J. Phys. Chem., 88, 2082-2091, 1984.

Levy, H. II., Normal Atmosphere: Large Radical and Formaldehyde Concentrations Predicted, Science, 9, 141-143, 1971.

Levy, H., II, Photochemistry of the Lower Troposphere, Planet. Space Sci., 20, 919-935, 1972

Logan, J.A., M.J. Prather, S.C. Wofsy, and M.B. McElroy, Tropospheric Chemistry: A Global Perspective, Journal of Geophysical Research, 86, 7210-7254, 1981.

Mihelcic, D., D.H. Ehhalt, G.F. Kulessa, J. Klomfass, M. Trainer, U. Schmidt, and H. Rohrs, Measurements of Free Radicals in the Atmosphere by Matrix Isolation and Electron Paramagnetic Resonance, Pure Appl. Geophys., 116, 530-536, 1978

Molina, M.J., and F.S. Rowland, Stratospheric Sink for Chlorofluoromethane: Chlorine atom catalysed Destruction of Ozone, Nature, 249, 810-812, 1974.

Ortgies, G., K.H. Gericke, and F.J. Comes, Is UV Laser-induced Fluorescence a Methode to Monitor Tropospheric OH?, Geophys. Res. Lett., 7, 905-908, 1980.

Ortgies, G., K.H. Gericke, and F.J. Comes, Optical Measurements of Tropospheric Hydroxyl with Lasers, Z. Naturforsch, 36a, 177-183, 1981.

Parrish A., R.L. deZafra, P.M. Solomon, J.W. Barrett, and E.R. Carlson, Chlorine Oxide in the Stratospheric Ozone Layer: Ground-Based Detection and Measurement, Science, 211, 1158-1164, 1981.

Perner, D., D.H. Ehhalt, H.W. Patz, U. Platt, E.P. Roth, and A. Voltz, OH Radicals in the Lower Troposphere, Geophys. Res. Lett., 3, 466-468, 1976.

Rodgers, M.O., J.D. Bradshaw, S.T. Sandholm, S. KeShieng, and D.D. Davis, A Laser-Induced Fluorescence Field Instrument for Ground-Based and Airborne Measurements of Atmospheric OH, J. of Geo. Res., 90, 12819-12834, 1985.

Sander, S.P., M. Peterson, and R.T. Watson, Kinetics Studies of the HO_2 + HO_2 and DO_2 + DO_2 Reactions at 298 K, J. Phys. Chem., 86, 1236-1240, 1982.

Sander, S.P., and M.E. Peterson, Kinetics of the Reaction $HO_2 + NO_2 + M \rightarrow HO_2NO_2 + M$, J. Phys. Chem., 88, 1566-1571, 1984.

Schwartz, S.E., Gas- and Aqueous-Phase Chemistry of HO_2 in Liquid Water Clouds, Journal of Geophysical Research, 89, 11589-11598, 1984.

Singh, H.W., Atmospheric Halocarbons: Evidence in Favour of Reduced Average Hydroxyl Radical Concentrations in the Troposphere, Geophys. Res. Lett., 4, 101-104, 1977a.

Singh, H.W., Preliminary Estimation of Average Tropospheric HO Concentrations in the Northern and Southern Hemispheres, Geophys. Res. Lett., 4, 453-456, 1977b.

Thompson, A.M., and R.J. Cicerone, Possible Perturbations to Atmospheric CO, CH_4, and OH, Journal of Geophysical Research, 91, 10853-10864, 1986.

Trainer, M., E.Y. Hsie, S.A. McKeen, R. Tallamraju, D.D. Parrish, F.C. Fehsenfeld, and S.C. Liu, Impact of Natural Hydrocarbons on Hydroxyl and Peroxy Radicals at a Remote Site, Journal of Geophysical Research, 92, 11879-11894, 1987.

Volz, A., D.H. Ehhalt, and R.G. Derwent, Seasonal and latitudinal variations of ^{14}CO and the tropospheric concentration of OH radicals, J. Geophy. Res., 86, 5163-5171, 1981.

Wang, C.C., and L.I. Davis, Jr., Measurement of Hydroxyl Concentrations in Air Using a Tunable UV Laser Beam, Phys. Rev. Lett., 32, 349-352, 1974.

Wang, C.C., L.I. Davis Jr., C.H. Wu, S. Japar, H. Niki, and B. Weinstock, Hydroxyl Radical Concentrations Measured in Ambient Air, Science, 189, 797-800, 1975.

Wang, C.C., L.I. Davis, Jr., P.M. Selzer, and R. Munoz, Improved Airborne Measurements of OH in the Atmosphere Using the Technique of Laser-Induced Fluorescence, J. Geophys. Res., 86, 1181-1186, 1981.

Watanabe, T, M. Yoshida, S. Fujiwara, K. Abe, A. Onoe, M. Hirota, and S. Igarashi, Spin Trapping of Hydroxyl Radical in the Troposphere for Determination by Electron Spin Resonance and Gas Chromatography/Mass Spectrometry, Anal. Chem., 54, 2470-2474, 1982.

Weinstock, B., E. Daby, and H. Niki, Chemical Reactions in Urban Atmospheres, C.S. Tuesday, Ed., Symposium at General Motors Laboratories, Dearborn, MI, 54-55, 1969.

Wendel, G.J., D.H. Stedman, C.A. Cantrell, and L. Damrauer, Luminol-Based Nitrogen Dioxide Detector, _Analytical Chemistry,_ 55, 937-940, 1983.

Wendel, G.J., Novel Applications of a Luminol/NO_2 Detector, Doctoral Dissertation, University of Michigan, 1985.